Heavy Ion Laboratory

ANNUAL REPORT 2020

UNIVERSITY OF WARSAW

HIL
Heavy Ion Laboratory

Heavy Ion Laboratory
University of Warsaw

Annual Report

2020

Warszawa, May 2021

Various information concerning the Laboratory is distributed via the HIL mailing list.
In order to subscribe to the list please visit the page
`http://mail.slcj.uw.edu.pl/mailman`

Annual Report of the
Heavy Ion Laboratory, University of Warsaw
ul. Pasteura 5a, 02-093 Warszawa, Poland
phone (+48)22-8222123, (+48)22-5546000
fax (+48)22-6592714
`http://www.slcj.uw.edu.pl`

Editors:
Nicholas Keeley, Michalina Komorowska, Monika Paluch-Ferszt,
Justyna Samorajczyk-Pyśk, Marzena Wolińska-Cichocka, Katarzyna Wrzosek-Lipska
e-mail: raport@slcj.uw.edu.pl
ISSN 1895-6726

Cover design:
Maja Rynkowska

Contents

Introduction

As for many other institutions, 2020 was an exceptional and very difficult year for our laboratory due to the COVID pandemic. The last experiment with external users was performed in March and was related to a study of the scattering and one-nucleon transfer reactions in the $^{13}C+^{13}C$ system (see contribution C.8). This was the project of a group of Ukrainian physicists, led by Dr. Ponkratenko, from the Institute for Nuclear Research in Kiev. From 25^{th} of March all experimental activity was suspended. Most of the technical staff worked on-call, while scientists were encouraged to work from home. Only the medical company Warsaw Genomics, with its laboratory in our building, worked more intensively, performing COVID tests for patients at Warsaw hospitals.

In July the COVID situation over the whole country became less dramatic and our laboratory could partially resume normal working conditions. Before the summer holiday one experiment was performed, with the participation of local users only. Its purpose was to study the feasibility of ^{117m}Sn production using the α-particle beam from the U - 200P cyclotron. This isotope is a promising radionuclide, with potential uses in medicine (see contributions B.7 and B.8).

Unfortunately, the second peak of the pandemic in the autumn again limited our activities. Planned experiments had to be suspended and in the last months of the year technical staff worked on the upgrade of the U – 200P heavy ion cyclotron, hoping for a resumption of the experimental campaign at the beginning of 2021. Some work was also devoted to an upgrade of the detector arrays. In particular, a modification of the liquid nitrogen cooling system of the EAGLE array was formulated and a new data acquisition system for this array was developed (contribution A.2).

Some work on the production of medical isotopes using a proton beam accelerated by the PETtrace cyclotron was continued. This is a fruitful collaboration with the Institute of Nuclear Chemistry and Technology in Warsaw which has been on-going for some years now.

However, our scientists mainly worked from home, analyzing data taken earlier. The number of contributions to this Report as well as the number of published papers (as many as in 2019) demonstrates their efficiency. Our young colleague, M. Pęgier, defended his PhD thesis at the Faculty of Chemistry of the University of Warsaw. He synthesized materials enabling the separation of scandium from water samples using the solid-phase extraction technique. Despite travel restrictions, Dr. Hasan M. Maridi from the Taiz University in Yemen managed to join us. He was awarded a prestigious grant from the Polish National Agency for Academic Exchange (NAWA) within the Ulam Programme and he will stay with us till 2022. He is a reaction theorist and his contribution to this report may be found under C.5.

Concerning events organized by HIL, all of them were held on-line using internet platforms. Among them, the 3^{rd} edition of the "Global Nuclear Physics Innovation" meeting took place in December (contribution A.6).

In summary, I say goodbye to 2020 without regret; it was a very difficult time for all of us, the only such period in the history of our laboratory. I sincerely hope that we will not see its like again.

Prof. Krzysztof Rusek, Director of HIL

Part A
Laboratory overview and technical developments

A.1 General information

J. Choiński, P.J. Napiorkowski, K. Rusek

Heavy Ion Laboratory, University of Warsaw, Warszawa, Poland

The Heavy Ion Laboratory (HIL) is a unit of the University of Warsaw, the largest university in Poland. HIL was founded jointly by the Ministry of Education, the Polish Academy of Sciences and the Polish Atomic Energy Agency. It is the largest experimental nuclear physics laboratory in the country, equipped with two cyclotrons - a K=160 U-200P heavy-ion cyclotron and a GE PETtrace, K=16.5 commercial cyclotron delivering high intensity proton and deuteron beams.

The first heavy-ion beam was extracted from the U-200P in 1994 and since then HIL has been an effective "user facility", serving up to the present time several hundred scientists from Poland and abroad and has become a recognized element of the European Research Community. From the 1st of March 2016, HIL has been one of ten European laboratories with Transnational Access granted by the European Union via the ENSAR2 (European Nuclear Science and Application Research 2) project within the HORIZON 2020 framework. Beam time is allocated by the Director based on the recommendations of the international Programme Advisory Committee. The only criteria are the scientific merit of the project and its technical feasibility. The research programme is mostly focused on nuclear physics and medical applications including the production of radio-isotopes.

Experimental teams may take advantage of permanent set-ups installed on the beam lines or use their own dedicated equipment. Available apparatus includes IGISOL —a Scandinavian type on-line separator, CUDAC — a PIN-diode array particle detection system, JANOSIK — a multi-detector system consisting of a large NaI(Tl) crystal with passive and active shields and 32-element multiplicity filter and ICARE, a charged particle detector system used for particle identification and energy measurements, moved to HIL from IReS Strasbourg. The most recent experimental tool, still being developed and improved, is the EAGLE array – a multi-detector γ-ray spectrometer, equipped with 16 HP germanium detectors with anti-Compton shields and up to 14 HP germanium detectors from the GAMMAPOOL consortium. It can be easily coupled to ancillary detectors such as internal conversion electron spectrometer built by the University of Lodz, a 4 π charged particle multiplicity filter (Si-ball), a scattering chamber equipped with 100 PIN-diode detectors, a 60-element BaF_2 gamma-ray multiplicity filter, a sectored HPGe polarimeter and a plunger.

Since 2012, the Radiopharmaceuticals Production and Research Centre, focused on the production of and research into Positron Emission Tomography radiopharmaceuticals, has formed an important part of HIL. The production of longer-lived radioisotopes for life-sciences applications is also carried out.

Being a university unit, HIL is in a natural way involved in teaching. On average about 15 students/year (Bachelors, Masters, PhD, ERASMUS) from Poland and abroad work at HIL supervised by its staff members. As part of its broader educational mission, the HIL staff organize an annual one-week workshop on "Acceleration and applications of heavy-ions" for about 20 students from various Polish universities.

A.2 Status of the EAGLE array

M. Palacz, T. Abraham, M. Kisieliński, M. Kowalczyk, W. Okliński, J. Srebrny, for the EAGLE collaboration

Heavy Ion Laboratory, University of Warsaw, Warszawa, Poland

The central European Array for Gamma Levels Evaluations (EAGLE) is an array of High Purity Germanium (HPGe) detectors located at HIL [1], see also [2]. Up to 30 HPGe detectors with anti-compton shields can be installed in the EAGLE frame, and the setup can be augmented with various ancillary devices.

The Heavy Ion Laboratory operates a number of HPGe detectors on loan from the GAMMAPOOL [3]. In 2020 an application to prolong the loan period until December 2022 was submitted to GAMMAPOOL and subsequently accepted. At present, 15 complete setups of a HPGe detector and its anti-compton shield are allocated by GAMMAPOOL to HIL, and an additional 3 HPGe detectors are shared as spares between HIL and the University of Jyväskylä. HIL also owns 19 smaller detectors with anti-compton shields, which may also be installed in the frame of EAGLE. The detectors located at HIL are routinely serviced in house [4]. In 2020 a project for the modification of the liquid nitrogen detector cooling system was formulated (the automation of the filling of the so-called intermediate tank), to be implemented in 2021.

A new data acquisition system for EAGLE has been developed at HIL [5, 6]. Up to 6 digitizer boards can be used to acquire data from up to 24 HPGe detectors. The analysed HPGE signals can be vetoed by logical NIM signals from the compton-shields. Each board is equipped with a Zynq Z-7030 FPGA unit and an embedded ARM CPU running Linux OS. Each detector is served by an independent program realised in the FPGA hardware. The synchronisation is assured by a 10 MHz clock provided by the first board and forwarded to subsequent units. Each board generates a synchronised 160 MHz clock needed by the ADCs and FPGA. For a synchronisation check, an additional signal is sent to all boards approximately 5 times per second and for each input channel the current clock count is added to the data stream. The data collected by the digitizers can also be synchronised and merged with the CAMAC based electronics using a CEFE logic unit [7]. This makes possible the use of the new system in experiments in which ancillary detectors served by CAMAC units are employed. The acquisition is controlled and visualised by a Linux PC running the software named SMAN, which is also used in experiments with the old analogue system. A new version of the event list mode format was developed. The experiment definition as well as various information about the experiment is stored in the data stream together with event-by-event data. The digitizers have been tested with sources and also in-beam, collecting data in parallel to the analogue system. Experiments which rely on the new system are planned in 2021.

A number of proposal assuming use of EAGLE were presented at the PAC meeting in December 2019. Six of the projects were accepted and were supposed to be run in 2020. However, due to the COVID-19 pandemic, all the experiments were postponed.

Bibliography

[1] J. Mierzejewski *et al.*, Nucl. Inst. and Meth. **A659** (2011) 84.
[2] M. Palacz *et al.*, HIL Annual Report 2019, page 12
[3] T. Abraham *et al.*, HIL Annual Report 2016, page 17.
[4] T. Abraham *et al.*, HIL Annual Report 2017, page 14.

[5] M. Kowalczyk, HIL Annual Report 2017, page 16.
[6] T. Abraham *et al.*, HIL Annual Report 2018, page 51.
[7] M. Kowalczyk, HIL Annual Report 2014, page 14.

A.3 Upgrade of the Control System for the Warsaw Cyclotron

J. Miszczak, Z. Kruszyński

Heavy Ion Laboratory, University of Warsaw, Warszawa, Poland

The control system for the Warsaw cyclotron [1] has performed well over the years, but it is becoming more and more evident that a major upgrade is necessary. The version of the QNX operating system used at the cyclotron has become obsolete, so in the case of a hardware failure, it is not possible to install the OS on any new motherboard or use a modern graphics card due to the lack of drivers. The company behind the QNX operating system is still in business, but newer version of the OS will require extensive changes to the application code. For all practical purposes the control application will have to be written from scratch. The next problem is a lack of programmers familiar with QNX. Twenty years ago general purpose operating systems like Linux or Windows were not suitable for control purposes at all, so there was a market for programmers with QNX or VxWorks skills. Now only very niche applications require this knowledge. It was decided to abandon QNX and use Linux instead. Linux lacks the "hard" real time properties of QNX, but multi-core processors with gigahertz clocks alleviate this problem to some extent. In the control system for the cyclotron critical real time functions were offloaded to hardware and/or embedded processors anyway, so it was OK to go with a general purpose, non real time OS.

The new system follows the old one in the following areas:

1. off the shelf PC hardware is used;
2. there are two levels of control software:

- local/low level;
- main/operator console.

Local/low level software is written in C/C++ using GNU tools. Instead of a fixed repetition period (20Hz) used to poll hardware devices (checking for alarms, updating set-points, measuring read-back values etc.) software now uses threads in an event driven fashion. Main console software is written in the Rust programming language to make it less prone to programming errors associated with the C language, at the same time giving the program the high performance of the latter. Unlike the Java language, Rust does not use "garbage collection", so there are no random delays in execution of the program, which is an important factor in a real time like environment. The main difference between the old and the new control system is the use of the MODBUS protocol [2] by the latter. MODBUS is an application-layer messaging protocol, positioned at level 7 of the OSI model. It provides client/server communication between devices connected on different types of buses or networks. It is very important that it supports both RS-232 links and Ethernet at a reserved system port 502 on the TCP/IP stack. An extensive library of MODBUS programs/examples is available on the Internet making the switch to a new protocol relatively easy. So far three low level systems (magnets on beam-lines, beam diagnostics) and the operator console are controlled by the new system. The RF control subsystem is left on the old control system, and will stay that way for the immediate future due to being more "hard" real time oriented than the rest of the control system.

Bibliography

[1] J. Miszczak, J. Choinski, HIL Annual Report 2004, page 10.
[2] https://modbus.org/.

A.4 An external, well cooled, target holder for the PETtrace cyclotron suitable for irradiation of powder targets

J. Choiński, T. Bracha, B. Radomyski, A. Stolarz, Ł. Świątek, R. Tańczyk
Heavy Ion Laboratory, University of Warsaw, Warszawa, Poland

The PETtrace cyclotron installed at the Radiopharmaceutical Production and Research Center is equipped with standard targets for production of ^{18}F, ^{11}C and ^{15}O and a standalone external target system designed for irradiation of both metal and powder targets. This target system is protected by RP patent no 227402. The dual beam proton/deuteron cyclotron is primarily used for commercial production of fluorine, ^{18}F. The Heavy Ion Laboratory team, implementing its research program, carries out the production of other radioisotopes in the intervals between regular production of ^{18}F provided by an external company.

The external target system is connected to the cyclotron via a beam line consisting of: a drift tube of a total length of 3.4 m, two sets of steering magnets made of permanent magnets, one quadrupole doublet and a four-sector collimator, with shielding provided by a concrete wall of thickness 0.25 m (its specific weight is 3300 kg/m^3). This protective wall ensures the safety conditions for the center staff. The beam line with the target station has its own autonomous vacuum system which allows a static vacuum of 4×10^{-7} mbar to be reached.

The beam transport efficiency to the 12 mm target is greater than 96%. A fully remotely controlled robot loads the target into its position from an eight position carousel. It is an integral part of the target system.

After irradiation the target drops into a lead container and is evacuated from the cyclotron vault on a remotely controlled trolley. Last year, a rather particular case due to the COVID-19 pandemic, we performed only a few irradiations of targets for research groups cooperating with us, producing ^{135}La [1], ^{43}Sc, ^{44}Sc and ^{197}Hg [1] isotopes. Based on the experience gained, the GUI of the control system was upgraded making it more transparent and user-friendly.

Bibliography

[1] A. Matuszyńska, E. Górzyńska, R Walczak HIL Annual Report 2020, page 15 .

A.5 The HIL – ICHTJ Collaboration

A. Matuszyńska[1], E. Górzyńska[2], R. Walczak[2]

1) Faculty of Chemistry, University of Warsaw, Warszawa, Poland
2) Institute of Nuclear Chemistry and Technology, Warszawa, Poland

Cyclotron production of ^{135}La

^{135}La was produced on natural $BaCO_3$ targets (28.01.2020, 18.03.2020, 02.12.2020).

After irradiation, the targets were transported to the Institute of Nuclear Chemistry and Technology.

The targets were then dissolved in 1 mL of 1M HCl and alkalized to pH 3 with 5 M NaOH.

Under these conditions, lanthanum radionuclides can be separated from the target material by column chromatography with Chelex 100 chelating resin.

The target material solution (pH 3) was loaded on a column filled with 200 mg of Chelex 100 resin and barium was eluted from the column with 5 mL of 0.005M HCl. The efficiency of barium removal was 79.5±1.5%. Then lanthanum was eluted with 1 M HCl with an efficiency of 65.6±3.6%. The eluate was fractioned (single fraction = 300 μL). Each time 8 fractions were collected. The main activity of ^{135}La was in the third and fourth fractions. These fractions were combined. After that the solution of ^{135}La was evaporated to dryness and dissolved in 1 M of acetate buffer at pH 4.5.

10 MBq of ^{135}La in acetate buffer at pH 4.5 was used for labeling 50 nm of DOTATATE. Labeling was carried out for 30 min I temp. 95°C. Efficiency of labeling was checked by the ITLC method with a citrate buffer at pH 5 as a solvent. Efficiency of labeling was about 100%.

Cyclotron production of ^{197}Hg

^{197}Hg was produced on a natural Au target (15.12.2020).

After irradiation, the target was transported to a measurement laboratory at the Heavy Ion Laboratory facility and placed in an activity measurement set equipped with a HPGe gamma spectrometer. Measurements were carried out for one week to check the production efficiency of ^{197}Hg on a Au target. The efficiency was 2.74 MBq/μAh.

A.6 3rd edition of the Nuclear Physics Innovation of brokerage event — Global Nuclear Physics Innovation

T.J. Krawczyk, M. Paluch-Ferszt, P.J. Napiorkowski, K. Rusek,
the organisers of the workshop

Heavy Ion Laboratory, University of Warsaw, Warszawa, Poland

The University of Warsaw co-organized the 3rd edition of the Nuclear Physics Innovation of brokerage event — "Global Nuclear Physics Innovation" on 2-3 December 2020 in Warsaw, Poland (Digital Edition). The brokerage event at Global Nuclear Physics Innovation (Digital Edition) brought together scientists and companies (buyers as well as suppliers) from all over the world. Meetings took place online and were arranged in advance by means of the website `https://nupinno-2020.b2match.io/` Nuclear physics laboratories had the chance to establish links with international industry and SMEs.

During the workshop, 59 bilateral meetings (brokerage meetings) were organized between researchers and companies in which 69 participants took part (`https://nupinno-2020.b2match.io/`). The purpose of bilateral meetings was to establish initial contacts that may or may not lead to further research cooperation and to intensify the transfer of innovative technologies.

The forum explored a recent achievements and challenges in the following areas:

- COVID-19: virus protein structure analysis (synchrotron).
- Development of Ion Beam Analysis (IBA) Techniques for materials analysis.
- Development of irradiation trials of technological components and biological samples.
- Development of radiation detectors and nuclear instrumentation.
- Radiopharmaceutical production and molecular imaging.
- PET diagnosis.
- Radiobiology.
- Ionizing radiation.
- Scientific instrumentation and medical physics.
- Medical imaging.
- Computation and information technology sciences.
- Data acquisition and analysis of software development.
- Energy and environmental technologies.
- Laser-plasma acceleration.
- Radiation resistance studies of electronic systems.

- Radiation detection.
- Detector electronics development.
- Ion source developments for radioactive ion beam production.
- Monitoring of environmental radioactivity.
- R and D for gamma radiation detectors.
- Big data application (Data Mining, Data Science, Machine Learning, Deep Learning, Neural Networks, Genetic Algorithms).
- Machines (CNC and other technical tools necessary for the exploitation of research facilities).
- CAD/CAM/CAE, FEM software and applications for nuclear research.
- Special engineering construction services for nuclear facilities.
- Research cooperation and transfer of knowledge and technology.

This 3rd edition of the brokerage event was organized in a special time. Among the different areas of research activity an additional subject was added with reference to fighting against the COVID-19 - virus protein structure analysis with the use of synchrotrons.

Part B
Research for medical and biological applications

B.1 Quality control of ^{18}F MISO for small animal PET imaging

M. Cudny[1], K. Kilian[2]

1) Faculty of Physics, Warsaw University of Technology, Warszawa, Poland
2) Heavy Ion Laboratory, University of Warsaw, Warszawa, Poland

A characteristic feature of solid tumors is their hypoxia, which is a biological parameter of the tumor — significant levels of hypoxia are detected in 50 – 60% of all neoplasms, which translates directly into the prognosis and assessment of the stage of the disease. Moreover, hypoxemic cells are more resistant to ionizing radiation in relation to aerobic cells. The radiation resistance of these cells is related to the lack of oxygen, which is responsible for perpetuating the damage caused by irradiation. Knowledge of the level of hypoxia has found application in the treatment aimed at hypoxia, which translated into the benefits of dose escalation in hypoxic areas. Therefore, imaging of the hypoxic state can identify, spatially map and quantify tumor hypoxia before treatment, as well as track changes in hypoxia during treatment, which directly translates into its effectiveness and examines the response to standard treatment regimens (chemotherapy and radiotherapy).

The interest in measuring hypoxia has shifted towards non-invasive techniques such as positron emission tomography (PET), which uses as a marker a wide spectrum of nitroimidazoles labeled with fluorine-18. Hypoxia imaging using [^{18}F] fluoromisonidazole (^{18}FMISO) positron emission tomography has become the gold standard in the assessment of hypoxia over time.

The aim of the study was the synthesis and quality control of ^{18}FMISO based on the requirements of the European Pharmacopoeia and the purification of the final product in order to obtain the best possible radiochemical purity.

The source of the F 18 isotope was the GE PETtrace 840 medical cyclotron located at HIL. The ^{18}O(p,n)^{18}F reaction using a proton beam with an energy of 16.5 MeV was utilised.

In animal experiments, the residual activity (4.0 – 6.0 GBq of fluorine) was used for this study rinsing the target after commercial FDG synthesis. The isotope was transferred to an automated Synthra RNPlus system (Synthra, Germany) where ^{18}FMISO was then synthesized and purified.

^{18}FMISO synthesis is a fully automated radiochemical process involving the nucleophilic fluorination of the NITTP (1- (2'-nitro-1'-imidazolyl) -2-O-tetrahydropyranyl-3-O-toluenesulfonyl-propanediol) precursor. The ^{18}FMISO syntheses that were the subject of research in this work were carried out according to the following protocol:

1. In order to separate fluorine from the target material, the solution was passed through a PS-HCO_3- ion exchange column,

2. Then, fluorine was eluted into the reaction vessel with a mixture of potassium carbonate and Kryptofix.

3. In the next stage of the synthesis, water was removed from the reactor (fluorination takes place in an anhydrous environment, hence the need for drying), in the process of azeotropic distillation with anhydrous acetonitrile,

4. After removal of acetonitrile, precursor was added to the reactor and nucleophilic fluorination of NITTP precursor (5 mg) was performed (10 minutes, 100°C),

5. The reaction mixture obtained was purified on a C18 column, then the fluorinated precursor was eluted with ethanol into the second reactor, where 1.5 ml of 1 mol/l hydrochloric acid was added for hydrolysis (5 minutes, $100°C$),

6. After acid hydrolysis, the solution was purified using an inline chromatographic system on a C18 – RP column (Phenomenex Gemini C18 250 mm x 10 mm x 7 μm).

7. About 1ml of the final product was collected, isolating the fraction with the highest specific activity of the final product.

8. The purified end product was sterilized on a 0.22 μm filter and then dispensed directly into a sterile vial.

The radiochemical purity was determined using a Shimadzu AD20 chromatography system with a radiometric detector. 5 μl samples were separated on a C18 (150 mm x 4.0 mm i.d x 5 μm) column with a 95 : H_2O/ethanol mobile phase at a flow of 1ml/l. The results of the determinations were read directly from the report generated by the synthesizer software. The retention time determined on the radiometric detector was 5 – 5.5 min, and on the detector UV-VIS, 4.8 min.

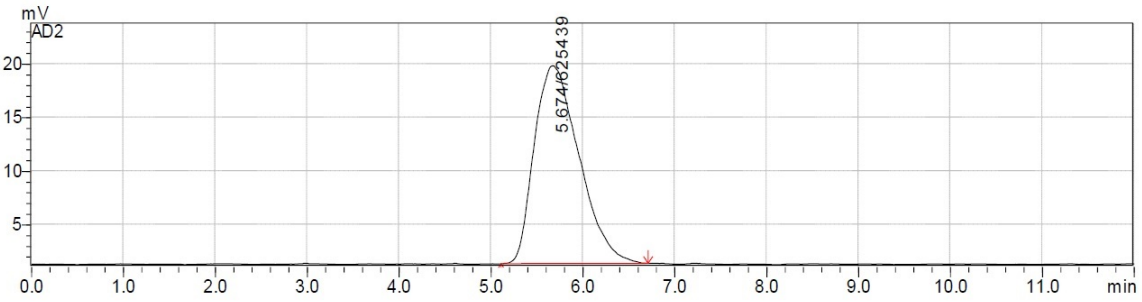

Figure 1: Chromatographic analysis of ^{18}FMISO.

The obtained average radiochemical purity of the final product (after HPLC purification) with n = 3 syntheses was: 99.15 ± 0.39%. The result was radiochemically pure ^{18}FMISO. The synthesized ^{18}FMISO was used in further preclinical studies on small animals as a reliable tool for imaging hypoxia.

The following results were obtained:

- The obtained radiochemically pure [F18] FMISO (purity at the level of 99.15 ± 0.39%) meets the requirements of the European Pharmacopoeia.
- As a result of the purification of the radiopharmaceutical a several percent increase in radiochemical purity and a significant increase in specific activity were obtained.
- An effective and reproducible method of synthesis and quality control [F18] of FMISO was developed.

B.2 Synthesis of ^{18}FHBG on a Synthra RN unit

A. Lenartowicz[1], K. Kilian[2]

1) Faculty of Physics, Warsaw University of Technology, Warszawa, Poland
2) Heavy Ion Laboratory, University of Warsaw, Warszawa, Poland

Radiopharmaceuticals based on guanine derivatives are a group of tracers with a high degree of effectiveness for gene therapy imaging. The target in this case is the herpes simplex virus type 1 thymidine kinase protein (HSV1-tk). Mouse cells are modified with a retroviral vector with altered DNA that contains the virus thymidine kinase gene. By administering ^{18}FHBG to a patient the treatment progress can be observed because ^{18}FHBG undergoes the same processes as penciclovir (phosphorylation to triphosphate), as a result of which the radioactive compound accumulates in the cells.

An automatic Synthra RN synthesizer was used for the production of labeled compounds with fluorine-18 by nucleophilic substitution. The synthesizer has all the necessary components to carry out all stages of the production of radiopharmaceuticals, i.e. preparation, labeling and purification along with the final formulation of the product. Monitoring and control of the synthesis steps were performed with the SynthraView software.

After transferring the radioisotope to the hot cell, the first step was the separation of fluorine-18 on an ion exchange column. Fluorine was then eluted with a mixture of Kryptofix 2.2.2 and acetonitrile to the first reactor. FHBG precursor (tosyl-FHBG, 6H-Purin-6-one) in anhydrous acetonitrile was added. The radiolabelling reaction was carried out at $100°C$ for 10 min. The reactor was then cooled to $50°C$ to condense acetonitrile which was then evaporated under reduced pressure at a temperature of 70 - $90°C$. Deionized water was added successively to dissolve the residue. The resulting solution was separated on a C18 column and the ^{18}FHBG was then transported to the second reactor, where hydrochloric acid was added and the acid hydrolysis reaction of the labeled product was carried out for 5 minutes at $95°C$.

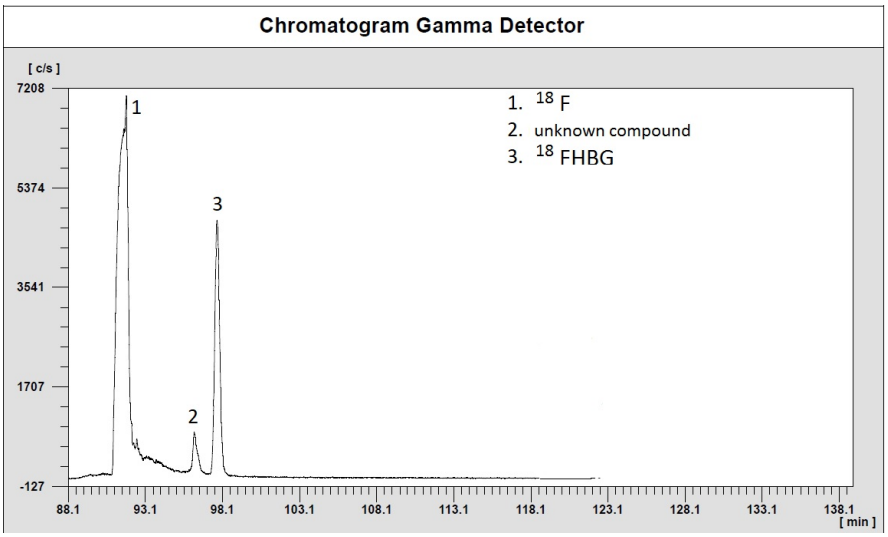

Figure 1: Radiochromatogram of the crude synthesis mixture.

After the hydrolysis step, the mobile phase to dilute and buffer were added to the sample. The mixture was then purified on a C18-RP HPLC column (Phenomenex Gemini C18 250 mm × 10 mm × 7 microns, ethanol to water in a ratio of 8:92), with a final radiochemical purity of >99%.

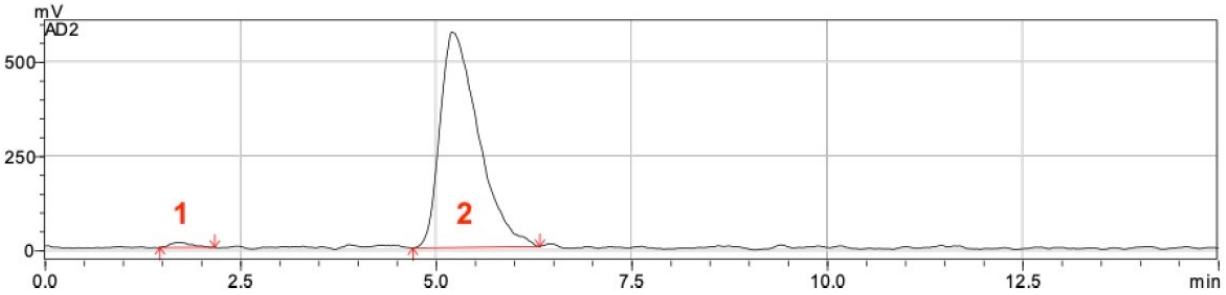

Figure 2: Radiochromatogram of 18FHBG after final purification. 1-^{18}F, 2-^{18}FHBG.

B.3 Study of the stability of selenomethionine depending on the method of sample storage for the example of selenized green tea

A. Sentkowska[1], K. Pyrzyńska[2]

1) Heavy Ion Laboratory, University of Warsaw, Warszawa, Poland
2) Faculty of Chemistry, University of Warsaw, Warszawa, Poland

Selenomethionine (SeMet) is a predominant selenium species in products of plant origin, e.g. green tea, Brazil nuts, cereals. However, the compound is not stable. Conversion of SeMet to selenomethionine oxide (SeMetO) has been observed in Se-enriched yeast, onion extract and wheat grain [1–3]. In our case, this conversion was observed in Ziyang green tea samples. The aim of the research was to check how the method of sample storage influences the conversion of SeMet to its oxide. For this purpose, the tea infusion was prepared and then stored for 28 days at room temperature (exposed to light and in the dark) as well as at low temperature (fridge and freezer). The concentration of SeMet and SeMetO was determined just after sample preparation and then every 7 days for 4 weeks. The results obtained for water samples of tea are presented in Fig 1.

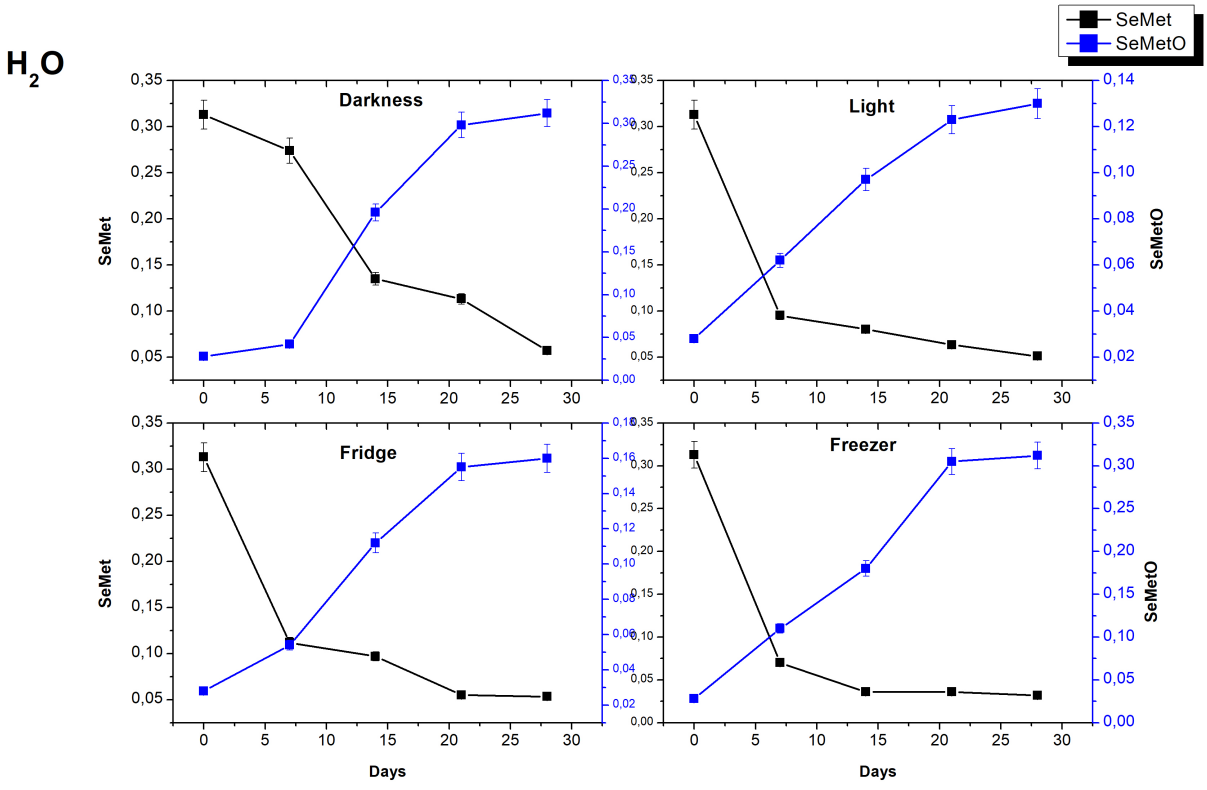

Figure 1: Changes in the concentrations of SeMet and SeMetO depending on the storage method, determined for a water extract of tea.

It turned out that regardless of the sample storage conditions, conversion of SeMet still occurs. The greatest decrease in SeMet concentration was observed in the first 7 days after

sample preparation. The highest concentrations of SeMet after 28 days were determined in a sample stored in a dark room and a freezer. These are valuable insights from the point of view of selenium speciation analysis. If we want to determine reliable SeMet content, the analysis should be performed in the shortest possible time from the moment of sample preparation. The literature offers suggestions for sample additives to prevent oxidation of SeMet, e.g. DTT. However, such additives as well as other substances present in the sample have an influence on the speciation of selenium and any interference in the composition of such a sample may significantly change its composition. Our experience shows that the addition of DTT to an aqueous tea extract does not completely inhibit SeMet oxidation, but only reduces it by approx. 10%. The described results come from the initial stage of research on the stability of various speciation forms of selenium in various types of extracts.

Bibliography

[1] Z. Pedrero *et al.*, J. Anal. Atom. Spec. **22** (2007) 1061.
[2] M. Michalsa-Kacymirow *et al.*, Anal. Bioanal. Chem. **406** (2014) 3717.
[3] F. Cubadda *et al.*, J. Agric. Food Chem. **58** (2010) 2295.

B.4 Comparison of the antioxidant capacity of selenium nanoparticles obtained with different synthesis methods

A. Sentkowska[1], K. Pyrzyńska[2]

1) Heavy Ion Laboratory, University of Warsaw, Warszawa, Poland
2) Faculty of Chemistry, University of Warsaw, Warszawa, Poland

In recent years there has been growing interest in selenium owing its important role in overall human health [1]. Selenium is known for its anti-cancer properties, hence the interest in selenium nanoparticles (SeNPs) as they can be used in cancer therapy. Similar to other nanoparticles, SeNPs possesses significant physical, chemical and biological properties which differ from the properties of the corresponding bulk materials. These properties as well as the morphology and size depend on several parameters, including the method of synthesis, use of surfactants or additives, reaction temperature and time [2].

The most commonly used method for preparation of SeNPs is chemical reduction of inorganic selenium forms as the precursors. In this study, ascorbic acid and cysteine were used as reducing agents. Additionally, synthesis with ascorbic acid was performed both without and in the presence of polyvinyl alcohol (pVA) as a stabilizing agent to prevent aggregation of nanoparticles. After the nanoparticles were obtained and purified, their antioxidant capacity was tested using the method with DPPH radical. The antioxidant abilities of selenium nanoparticles may be an additional advantage when used in cancer therapy. It turned out that pVA as a stabilizing agent does not affect the ability of the synthesized nanoparticles. The values of antioxidant activity obtained for the SeNPs from the synthesis with ascorbic acid with and without pVA were 42.0 $\pm$ 0.11 and 41.9 $\pm$ 0.20 μmolTr/L respectively. This is a valuable insight as pVA is expected to prevent nanoparticle aggregation, which reduces the antioxidant capacity. In this case, aggregation does not take place, or it occurs to a very small extent, because the use of pVA did not affect the values obtained for the antioxidant capacity of the nanoparticles. For selenium nanoparticles obtained by the method using cysteine as a reducing agent, the highest value of antioxidant capacity was obtained, equal to 47.1 μmolTr/L.

It seems that selenium nanoparticles have great potential as anti-cancer drugs, but in order fully to utilise their properties it is necessary to understand and optimize the process of their synthesis. The described research was designed to answer the question whether and how the method of nanoparticle synthesis affects their antioxidant properties.

Bibliography

[1] M.P. Rayman, N. Aslam, Hormones **19** (2020) 9.
[2] C. Kim *et al.*, Polymers **11** (2019) 1052.

B.5 Setting up a new Laboratory for Radiobiology at HIL

M. Paluch-Ferszt, U. Kaźmierczak, Z. Szefliński

Heavy Ion Laboratory, University of Warsaw, Warszawa, Poland

All radiobiological experiments with heavy ions designed and constructed at the Heavy Ion Laboratory in Warsaw University have so far been carried out without the facilities of a radiobiology laboratory [1–4]. All biological samples were prepared and tested in the Laboratory of Cytogenetics and Genotoxicology (Head: Anna Lankoff) of the Institute of Nuclear Chemistry and Technology.

In 2018 a group dedicated to experiments in the field of radiobiology at HIL obtained funding for a research program involving the research group at JINR and research centers in Poland. As part of the funds obtained in 2018-2020, the equipment necessary to equip a radiobiological laboratory at HIL was purchased.

The following equipment was bought:

- A flat alpha source — for irradiating biological samples [5]. A schematic view of the irradiation device for biological samples is shown in Fig. 1.
- Laminar airflow chamber — necessary for a clean work bench and sterile sample preparation.
- Inverted microscope — for observation of adherent cells.
- CO_2 incubator — providing optimum conditions for the cultivation of biological samples.

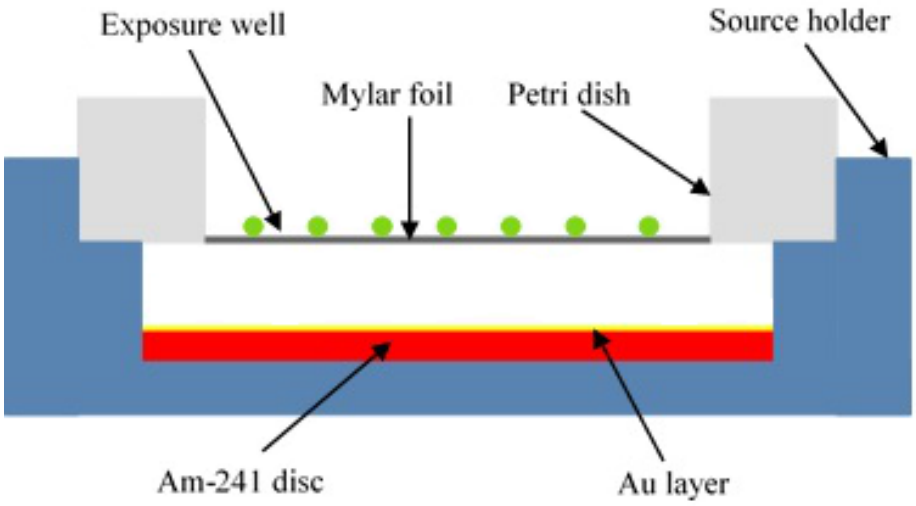

Figure 1: Schematic view of the irradiation device. The lower surface of the Petri made of Mylar foil is located 5mm from the source surface. The distance between the source and Petri dish can be changed [5].

In the following years further expansion of the radiobiology laboratory is planned.

Bibliography

[1] J. Czub *et al.*, HIL Annual Report (2007) 48-50.
[2] U. Kaźmierczak *et al.*, HIL Annual Report (2010) 57-58.
[3] U. Kaźmierczak *et al.*, HIL Annual Report (2013) 49-50.
[4] U. Kaźmierczak *et al.*, HIL Annual Report (2014) 52-53.
[5] Z. Szefliński *et al.*, RAP Conf. Proc. **4** (2019) 7-9.

B.6 Investigation of scandium sorption onto magnetic nanoparticles modified with morin

M. Pęgier[1,2], K. Kilian[1], K. Pyrzyńska[2]

1) Heavy Ion Laboratory, University of Warsaw, Warszawa, Poland
2) Faculty of Chemistry, University of Warsaw, Warszawa, Poland

Sorbents with magnetic properties can be utilized in solid phase extraction. Magnetic nanoparticles (MNPs), with their large surface area and dispersibility, are excellent candidates for this purpose [1]. MNPs for solid phase extraction of metal ions are generally materials with core-shell structure. The magnetic core, which can consist of magnetite (Fe_3O_4), maghemite (γ-Fe_2O_3) or metallic iron can interact with an external magnetic field. Surface modification of the core provides the desired properties of the material, such as selectivity for the analyte of interest or the chemical stability of the sorbent. One of the groups of compounds used for surface modification of nanoparticles are flavonoids, compounds of plant origin, that have the ability to form complexes with metal ions, including scandium. Scandium is an emerging element that can be utilized not only in the high-tech industry but also in nuclear medicine as both a therapeutic agent (^{47}Sc) and a positron emitter($^{43,\ 44,\ 44m}$Sc) for positron emission tomography (PET) diagnostics [2].

The aim of the study was to investigate sorption of scandium onto carbon encapsulated magnetic iron nanoparticles (CEMN) modified with morin. CEMN nanoparticles were obtained using the carbon arc plasma route [3]. Raw MNPs were further oxidized using HNO_3 to produce surface acidic carboxylic groups [4]. The oxidized material (CEMN-COOH) was treated with $SOCl_2$ to obtain CEMN-COCl. In the final step a morin molecule was covalently attached through an ester bond resulting in CEMN-COO-morin nanoparticles.

The results for sorption capacity (sorption isotherm) were obtained for an initial metal concentration range of 1–100 mg/L. The amount of sorbed Sc(III) slowly increased with increasing initial concentration from 1 to 50 mg/L. To describe Sc(III) adsorption behaviour on CEMN-COO-morin sorbent the experimental data were analyzed using two isotherm models.

The Freundlich model describes adsorption on heterogeneous surfaces and is represented by equation 1:

$$q_e = K_F C_e - 1/n \tag{1}$$

where K_F and n are the Freundlich isotherm constants related to adsorption capacity and intensity, respectively.

The Langmuir model, which assumes monolayer coverage is described by equation 2:

$$q_e = q_{max} K_L C_e (1 + K_L C_e) - 1 \tag{2}$$

where q_{max} and K_L are the maximum monolayer adsorption capacity and the adsorption energy related constant, respectively.

The obtained values of the parameters are presented in Table 1.

Table 1: Parameters of the Langmuir and Freundlich models for CEMN-COO-morin.

Adsorption model	Parameters	
Langmuir	q_{max}	8.14
	K_L	0.538
	R^2	0.9954
Freundlich	K_F	1.446
	n	1.996
	R^2	0.9377

The CEMN-COO-morin sorbent shows a much better fit to the Langmuir model (high coefficient of determination R^2) than the Freundlich model. The value of q_{max} obtained from the model is close to the experimental value of 7.53 mg/g, The sorption of scandium onto CEMN-COO-morin is most likely monolayer on the sorbent surface. For further investigation of the mechanism of Sc(III) adsorption kinetic measurements were conducted. Results show that the adsorption rate rapidly increased during the first 10 min and then, as the number of surface sites for sorption reduced, gradually tended to equilibrium. Four different kinetic models were applied to test the experimental data. Equations and parameter values are presented in Table 2, while plots can be found in Fig. 1.

Table 2: Parameters of kinetic models fitted to experimental data.

Kinetic model	Equation	Parameters	
Pseudo-first order kinetic	$ln(q_e - q_t) = lnq_e - k_1 \cdot t$	k_1:	0.035 min^{-1}
		R^2:	0.9576
Pseudo-second order kinetic	$t/q_t = 1/k^2 q_e^2 + (1/q_e) \cdot t$	k_2:	1.63 g mg^{-1} min
		R^2:	0.9981
Elovich equation	$q_t = \beta ln(\alpha\beta) + \beta lnt$	α:	5.46 mg g^{-1} min^{-1}
		β:	26.97 g mg^{-1}
		R^2:	0.9967
Intra-particle diffusion	$q_t = \Theta + k_i \cdot t^{0.5}$	k_i:	0.0229 min^{-1}
		Θ:	0.3930

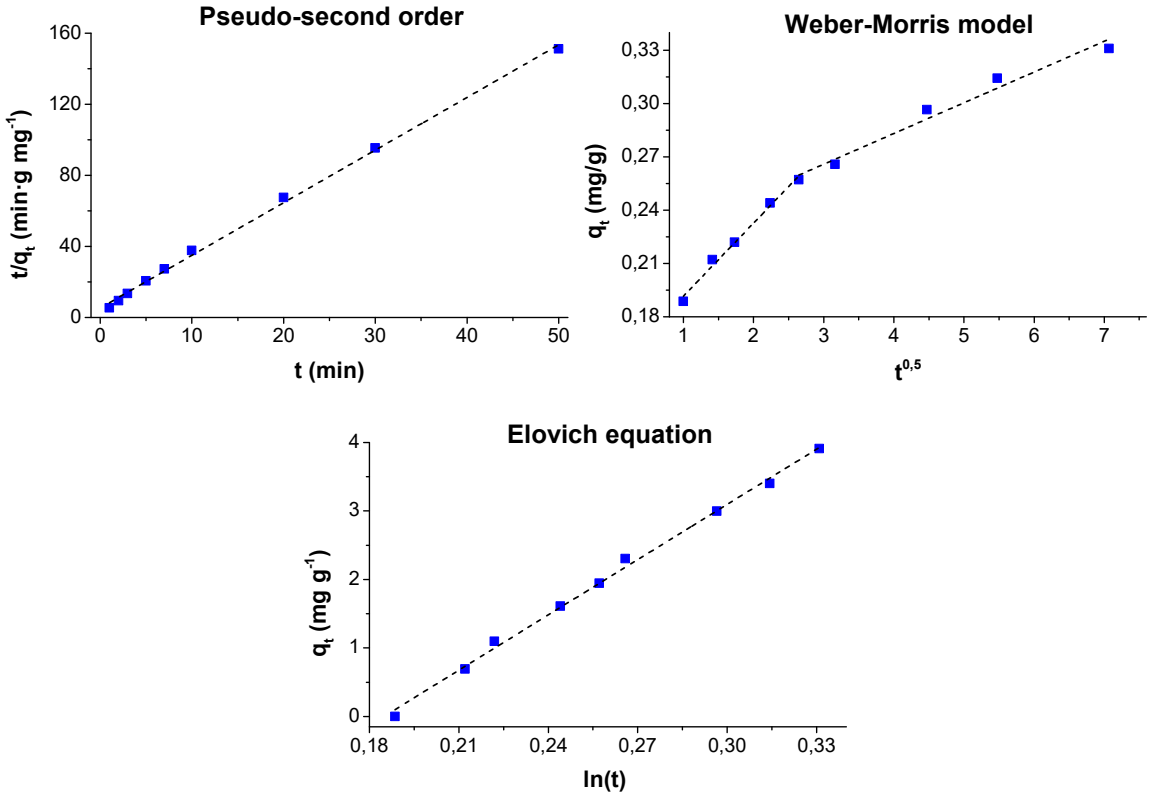

Figure 1: Modeling of Sc adsorption kinetics on CEMN-COO-morin.

The sorption of Sc(III) follows a pseudo-second order kinetic model, but the Elovich equation also shows good agreement with an only slightly lower R^2. This leads to the conclusion that the mechanism of Sc(III) removal might be chemisorption. Furthermore, an intra-particle diffusion model was used to investigate the contribution of intraparticle and film diffusions to adsorption process. The plot of the Weber-Morris model shows two linear ranges with early adsorption step up to 10 min, where the process is generally controlled by intraparticle diffusion and diffusion in thin film near the surface of the sorbent. The subsequent adsorption step, characterized by a lower slope, is probably controlled by the film diffusion (Fig. 1).

Bibliography

[1] M. Hemmati, M. Rajabi, A. Asghari, Microchim. Acta. **185** (2018) 160.
[2] S. Huclier-Markai *et al.*, Cancer Biother Radiopharm. **33** (2018) 316.
[3] M. Bystrzejewski *et al.*, Carbon **47** (2009) 1201.
[4] K. Kilian, K. Pyrzyńska, M. Pęgier, Solvent Extr. Ion Exch. **35** (2017) 450.

B.7 Preliminary experimental results of ^{117m}Sn production cross section for theranostics

L. De Dominicis[1,2,3], F. Barbaro[4,5], L. Canton[5], M.P. Carante[6], A. Colombi[4,6], A. Fontana[6], L. Mou[2], P.J. Napiorkowski[3], G. Pupillo[2], A. Stolarz[3], A. Trzcińska[3].

1) Università degli Studi di Padova, Padova, Italy
2) INFN, Laboratori Nazionali di Legnaro, Legnaro, Italy
3) Heavy Ion Laboratory, University of Warsaw, Warszawa, Poland
4) Università degli studi di Pavia, Pavia, Italy
5) INFN Sezione di Padova, Padova, Italy
6) INFN Sezione di Pavia, Pavia, Italy

^{117m}Sn is a promising theranostic radionuclide due to its γ emissions, suitable for imaging with SPECT cameras, and low energy conversion electrons, able to deliver a highly localized dose of radiation in human body tissues. Different chelators have been developed to realize radiopharmaceuticals, aimed mainly at bone cancer palliation and atherosclerotic plague treatment, which are in the phase of clinical and preclinical tests.

The purpose of this work is to study the feasibility of ^{117m}Sn production with the HIL U-200P cyclotron, bombarding ^{nat}Cd and ^{nat}In targets with the available 30 MeV α beam. Two targets have so for been irradiated. They were assembled following the stacked-foils technique consisting of an alternation of different foils. In both targets a ^{nat}Ti and then two other ^{nat}Cu foils were inserted to evaluate the incoming beam energy. ^{nat}Cu foils also act as a monitor of the cross section calculations, by the use of the nuclear reaction ^{nat}Cu(α,x)^{66}Ga recommended by the IAEA (International Atomic Energy Agency). One thicker ^{nat}Al foil was also added in the middle of each target to degrade the energy of the beam and to obtain more cross section values, at different energies, in one irradiation run. Before and after each Al foil one target foil is placed in which the ^{117m}Sn production cross section is effectively evaluated. In the first irradiation the two target foils were made of metallic ^{nat}Cd while in the second irradiated target there were two ^{nat}In metallic foils.

After the bombardment the target was disassembled and each foil measured with a CANBERRA HPGe detector. γ acquisitions of all the foils were then repeated once per day, up to 5 days after bombardment. The last γ spectra were acquired approximately 25 days after bombardment. In this way the decays of the produced radioisotopes were followed to check the possible presence of interference in γ peaks and decay chains. The number of counts in the γ peaks of each spectrum was used to calculate the cross sections [1]:

$$\sigma_x = \sigma_r \cdot \frac{C_x}{C_r} \frac{n_r \varepsilon_r I_r f_r}{n_x \varepsilon_x I_x f_x}$$

where r refers to the monitor radionuclide and x to the radioisotope of interest. The final cross section value, associated to a specific energy, is calculated as the weighed average of the results obtained for each spectrum. The energy associated with these values is determined through SRIM simulations of the beam energy loss.

The cross sections obtained are presented in Figures 1 and 2 as a function of the beam energy, for ^{nat}Cd and ^{nat}In foils respectively. The results are compared with the literature data available in the EXFOR database [2]. General agreement is noticeable in the investigated energy range (14-22 MeV). The experimental analysis was completed with theoretical cross section estimations obtained using two nuclear reaction codes [3, 4]: TALYS, which relies on a combination of different models, and FLUKA, which is based on Monte Carlo simulations. The experimental results from this work (red points) seem

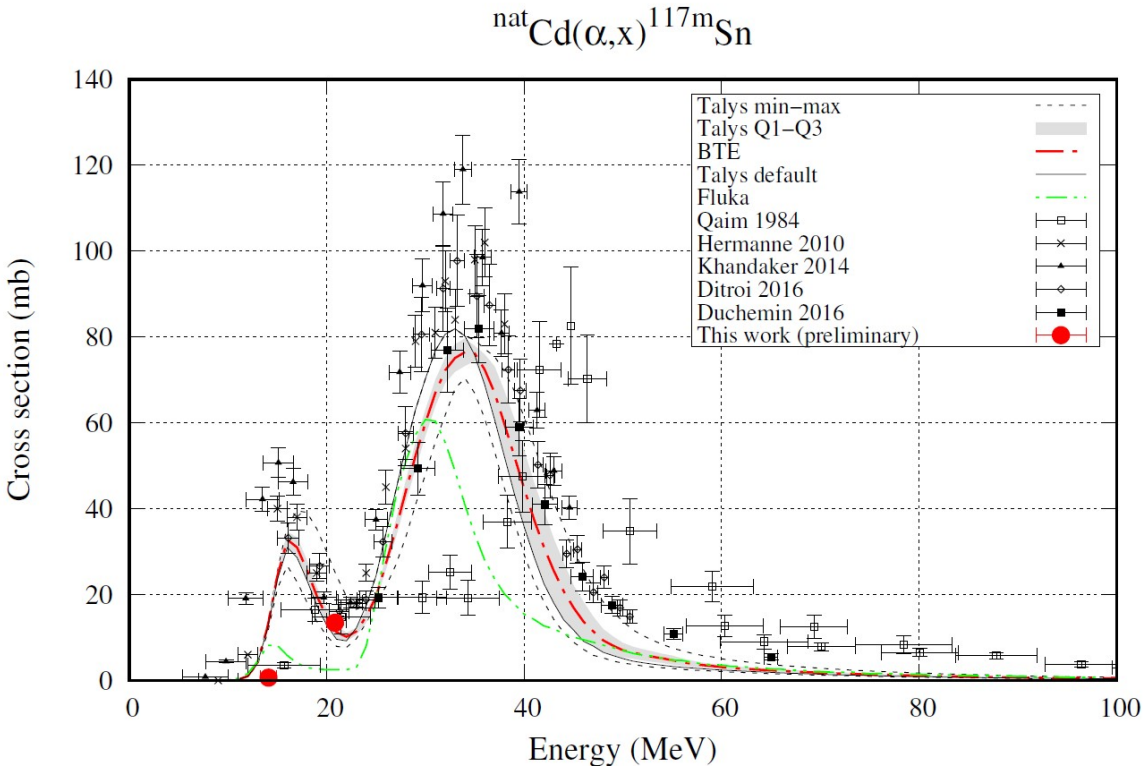

Figure 1: Cross sections for ^{nat}Cd(α,x)^{117m}Sn. Detailed description and discussion of theoretical estimations can be found in [3].

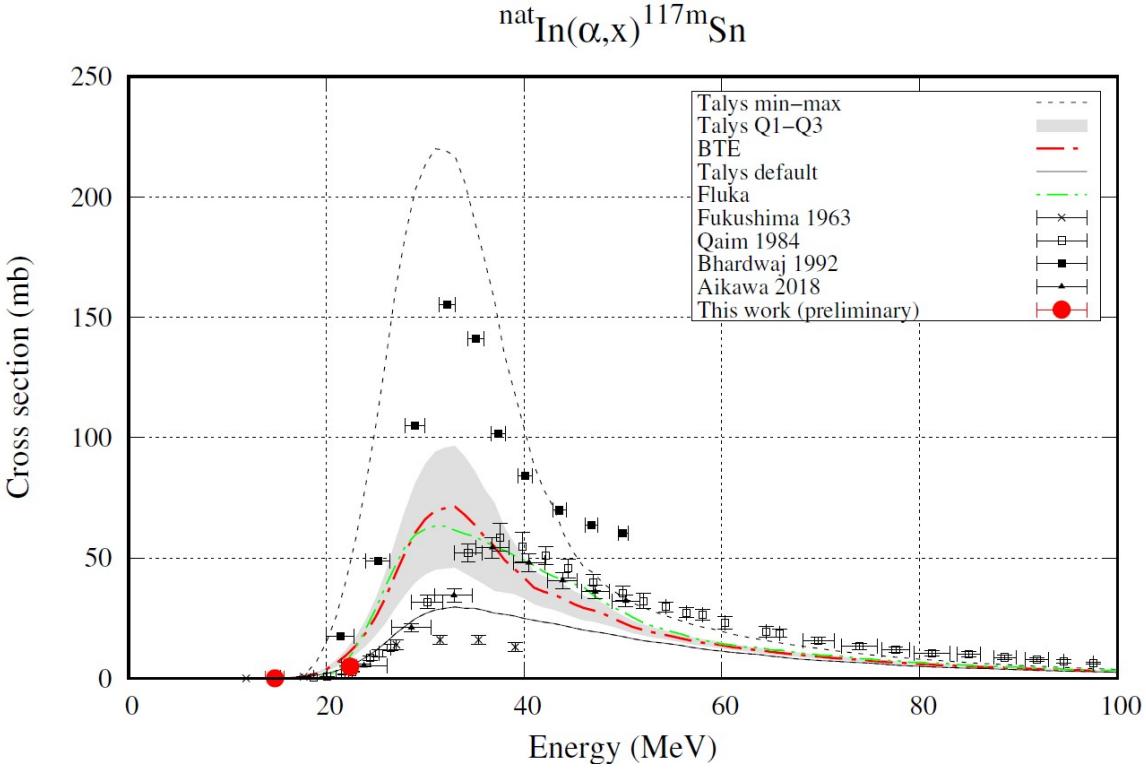

Figure 2: Cross sections for ^{nat}In(α,x)^{117m}Sn. Detailed description and discussion of theoretical estimations can be found in [3].

to agree with the theoretical predictions, except for the value at the lowest energy for the ^{nat}Cd target that differs a little. Future irradiation runs are necessary to confirm the cross section trend between these first two values and to add new points.

Bibliography

[1] N. Otuka *et al.*, Radiat. Phys. Chem. **140** (2017) 502-510.
[2] EXFOR Database, `https://www-nds.iaea.org/exfor/exfor.htm`.
[3] F. Barbaro *et al.*, Il Nuovo Cimento **43 C** (2020) 136.
[4] L. De Dominicis *et al.*, HIL Annual Report (2019) 43-45.

B.8 Targets for production of ^{117m}Sn in reactions induced by α beam

A. Stolarz[1], J. Kowalska[1], J. Choiński[1], L. De Dominicis[1,2,3]

1) Heavy Ion Laboratory, University of Warsaw, Warszawa, Poland
2) Università degli Studi di Padova, Padova, Italy
3) INFN, Laboratori Nazionali di Legnaro, Legnaro, Italy

Test studies of ^{117m}Sn production in reactions induced by α particles: ^{114}Cd$(\alpha,n)^{117m}$Sn + ^{116}Cd$(\alpha,3n)^{117m}$Sn and ^{115}In$(\alpha,x)^{117m}$Sn were performed at HIL [1] using targets made of natural target material. The target stacks were composed of target material (Cd or In), foils acting as beam energy monitors (Ti and Cu) and to evaluate the cross section of the monitor reactions (Cu), and Al foil used as an energy degrader [1]. At the end of the stack a second Al foil was added to stop protons that may possibly get through the whole stack (Fig. 1, right side of the drawing). The 'production' target foils, i.e. Cd and In, were prepared in house using the rolling technique.

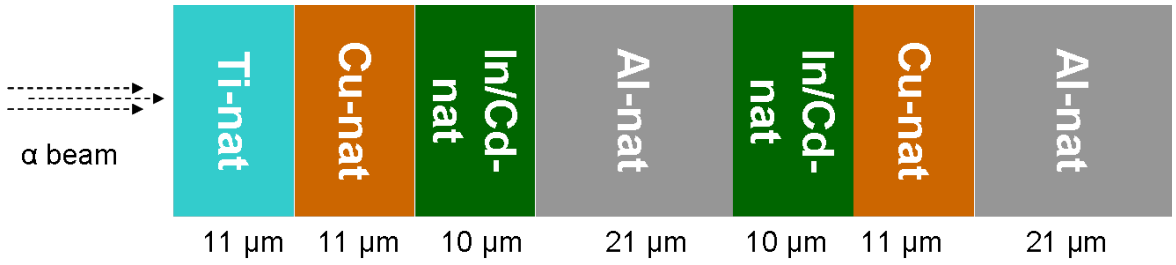

Figure 1: Arrangement of stacked foil targets.

The availability of alpha projectiles from the Warsaw Cyclotron only as an internal beam imposes constraints on the target set-shape. The holder and the target frames should have one side open (frame-less) so as not to lose the beam.

For several years a simple station designed for other purposes than production of medical radioisotopes was used for such irradiations [2–10], but due to poor cooling systems it could not be used for intense beams. Taking into account this and other disadvantages a new station was designed [11] and constructed in house and was used for the first time for studies of the production of ^{117m}Sn in reactions induced by α particles. The new design allows the placement of the target at an angle of 20° with respect to the beam direction.

The foils composing the targets were mounted on an aluminium backing (of 2 mm thickness). A stable position of the foils needed for secure handling of the target during placement in the set-up was ensured by screwing a cover with an appropriate aperture (Fig. 2 left), corresponding to the shape of the aperture in the system head (Fig. 2 right), to the lower backing.

Considering the low melting points of the targets used (Cd, 321°C and In, 156.6°C,) a low beam current was applied for this test irradiation. Taking into account that none of the foils demonstrated damage caused by the elevated temperature it is plannedto use a higher beam intensity in future irradiations of Cd and/or In targets. There were no problems with foil disassembly, required to perform measurements for post irradiation analyses.

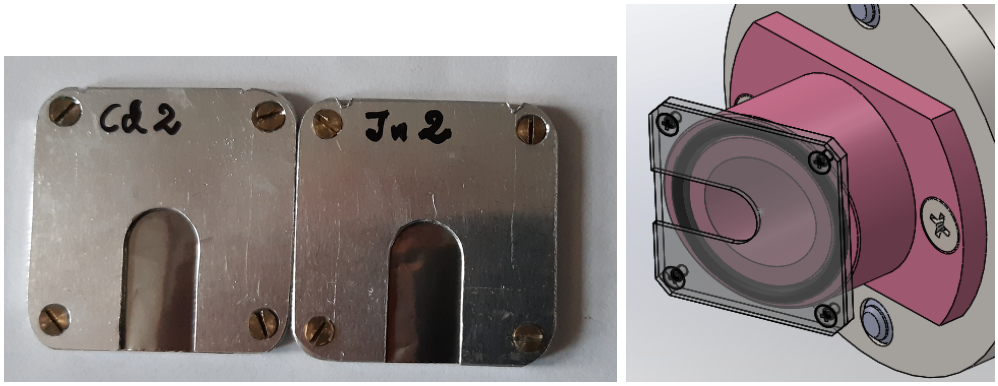

Figure 2: Target foils mounted between aluminium clamping plates (left) and the head of the target holder (right).

Bibliography

[1] L. De Dominicis *et al.*, HIL Annual Report 2020, page 33 .
[2] K. Szkliniarz *et al.*, HIL Annual Report 2013 page 41.
[3] K. Szkliniarz *et al.*, HIL Annual Report 2014 page 27.
[4] J. Jastrzębski *et al.*, HIL Annual Report 2015 page 25.
[5] A. Stolarz *et al.*, HIL Annual Report 2016 page 28.
[6] K. Szkliniarz *et al.*, Acta Phys. Pol. **A127** 5 (2015) 1471.
[7] J. Jastrzębski *et al.*, Radiotherapy and Oncology **118** (2016) S52.
[8] K. Szkliniarz *et al.*, Applied Radiation and Isotopes **118** (2016) 182.
[9] A. Stolarz *et al.*, AIP Conference Proceedings **1962** (2018) 020004.
[10] A. Stolarz *et al.*, European Physical Journal Web of Conferences **229** (2020) 06004.
[11] J. Choiński *et al.*, HIL Annual Report 2017 page 25.

Part C
Nuclear physics

C.1 Barrier distributions studies – influence of transfer reactions

A. Trzcińska[1], G. Colucci[1] E. Piasecki[1], M. Kisieliński[1], M. Kowalczyk[1], C. Bordeanu[2], B. Gnoffo[3,4], H. Jia[5], C. Lin[5], N. S. Martorana[6,4], M. Mutterer[7,8], E. V. Pagano[6], K. Piasecki[9], P. Russotto[6], L. Quatrocchi[3,4], W. H. Trzaska[10], G. Tiurin[10], M. Wolińska-Cichocka[1], R. Wolski[11,12], D. Wójcik[9], H. Zhang[5]

1) Heavy Ion Laboratory, University of Warsaw, Warszawa, Poland
2) Horia Hulubei National Institute of Physics and Nuclear Engineering, Bucharest, Romania
3) INFN Sezione di Catania, Catania, Italy
4) Dip. di fisica e astronomia Università di Catania, Italy
5) China Institute of Atomic Energy, Xinzhen, Fangshan, Beijing, China
6) INFN - LNS, Catania, Italy
7) IKP, Technical University Darmstadt, Darmstadt, Germany
8) GSI Helmholtz Center for Heavy Ion Research, Darmstadt, Germany
9) Faculty of Physics, University of Warsaw, Warszawa, Poland
10) Department of Physics, University of Jyväskylä, Finland
11) Joint Institute for Nuclear Research, Dubna, Russia
12) The H. Niewodniczański Institute of Nuclear Physics PAN, Kraków, Poland

Studies of barrier height distributions (BD) have been a long-standing project of our group. One of the project goals is to identify processes determining the fusion excitation function and the shape of BDs, and therefore influencing the fusion process.

The influence of couplings to collective excitations on the barrier height distribution has been well established experimentally and theoretically. Much less is known about the influence of dissipation caused by transfer reactions and noncollective excitations.

In [1, 2] and references therein the influence of the latter on the barrier distribution shape and fusion cross section was studied. It was shown that for systems where one of the nuclei involved has a high single particle level density, weak but numerous noncollective excitations significantly change the barrier distribution. In particular, the structure in the barrier distribution resulting from collective excitations can be smoothed out.

^{208}Pb is a doubly magic nucleus, so the s.p. level density is low. Therefore, noncollective excitations cannot be responsible for the smooth (Gaussian-like) shape of the barrier distribution for the ^{20}Ne + ^{208}Pb [1] system. On the other hand, in this system the cross sections for transfer reactions are relatively high and thus the transfer reactions probably dominate the modification of the barrier distribution. Unfortunately, except for the simplest cases transfers are very difficult to handle by existing theories. This is among other reasons due to lack of knowledge of the coupling strengths for sequential transitions involving excited states in the intermediate and final channels.

On the other hand, one can check the influence of transfers on barrier distributions using the simple model implemented in a modified version of the CCQEL code [3]. The modification allows the simultaneous inclusion of various transfer channels with different Q-values. Having the experimental Q-value distribution one can determine the "effective" coupling strengths for a given transfer channel and Q-value.

To perform the calculations with this version of the CCQEL code, one needs to determine the Q-value distribution for each transfer process. Such a unique set of spectra can be extracted from the data gathered in experiments measuring the transfer cross sections for this system, see Fig. 1.

From similar data gathered in other measurements of the transfer cross sections for the ^{24}Mg + ^{90,92}Zr systems [4, 5] at barrier energies one can also obtain the Q-value distributions

for transfer reactions in these systems (Fig. 2). This will allow verification of the supposition that for the ^{24}Mg + ^{92}Zr system transfer channels do not influence significantly the BD [2]. The calculations are in progress.

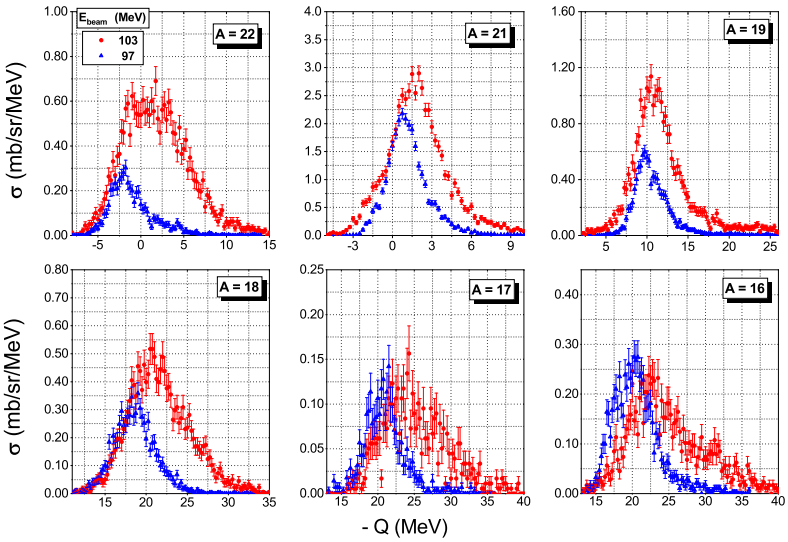

Figure 1: Preliminary results: Q-value distributions for the strongest transfer channels for ^{20}Ne + ^{208}Pb at beam energies 96 MeV and 103 MeV. "A" denotes the mass number of the transfer products.

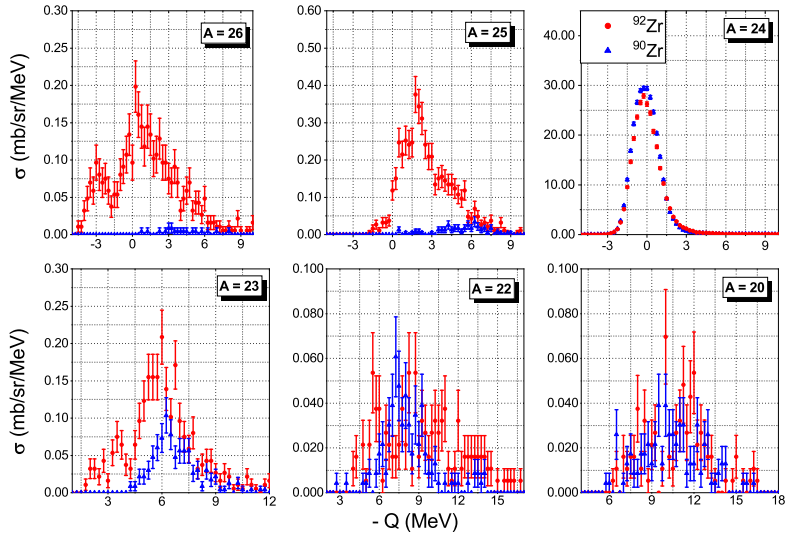

Figure 2: Preliminary results: Q-value distributions for the strongest transfer channels and elastic scattering for ^{24}Mg + ^{90,92}Zr at a beam energy of 76 MeV. "A" denotes the mass number of the reaction products.

Bibliography

[1] E. Piasecki *et al.*, Phys. Rev. C **100**(2019) 014616.
[2] A Trzcińska *et al.*, Phys. Rev. C **102** (2020) 034617.
[3] K. Hagino, P.W. Wen, private communication.
[4] D. Wójcik *et al.*, Acta Phys. Pol. **B49** (2018) 387.
[5] A. Trzcińska *et al.*, in preparation.

C.2 Double Sided Silicon Strip Detector for analysis of ^{146}Nd and ^{148}Sm Coulex experiments

M. Komorowska[1], P.J. Napiorkowski[1], M. Zielińska[2], L. Próchniak[1], W. Korten[2], K. Hadyńska-Klęk[1], K. Wrzosek-Lipska[1]

1) Heavy Ion Laboratory, University of Warsaw, Warszawa, Poland
2) IRFU/SPhN, CEA Saclay, Gif-sur-Yvette, France

For an experiment aimed to investigate the octupole properties of ^{146}Nd and ^{148}Sm [1] a Double Sided Silicon Strip Detector was used [2]. It is colloquially called a CD Detector due to its physical resemblance to a Compact Disc with an inner diameter of 10 mm and outer of 85 mm, covering an angular range of θ= 120 to 160 degrees in the laboratory frame. It has 64 radial-like segments on the front-junction side and 32 annular segments on the back-ohmic side creating 2048 (θ, ϕ) defined positions (see Fig. 1). The segments are connected to the electronics in groups of 16 signals, dividing the detector into 6 parts – two for the rings (odd and even) and four for the radial segments.

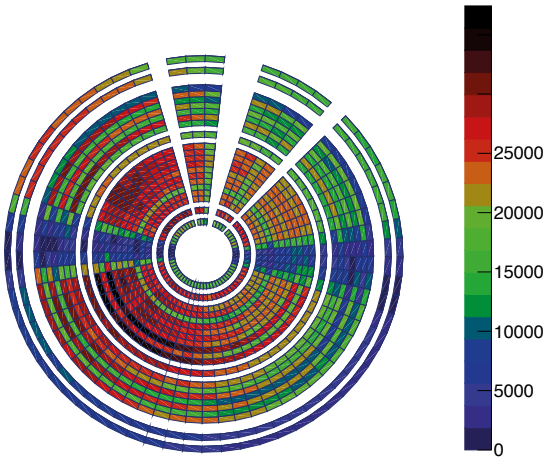

Figure 1: Hit pattern from ^{58}Ni ions scattered from a ^{146}Nd target. The grid shows the detector electronic segmentation – 2048 individual "pixels". Noisy or otherwise broken segments were excluded from the analysis and are marked in white. The detector has an outer diameter of 85 mm and inner diameter of 10 mm and was placed 24.5 mm from the target.

Charged particle detectors coupled with position sensitive gamma detectors allow a Doppler correction procedure to be performed. To get a proper Doppler-corrected gamma-ray energy, information about the angle between the de-exciting scattered nuclei and the emitted gamma ray is necessary. The higher the segmentation of the particle detector the higher the precision in the determination of the kinematics, hence the better the Doppler correction. The procedure strongly depends on an accurate detector geometry.

In the aforementioned experiment the preamplifiers were originally designed for a different detector divided into 8 instead of 6 parts. This in part contributed to the unfortunate mislabeling of the signal read-out from the new DSSSD, resulting in incorrect phi angles that were fed into the sorting code. After a thorough investigation the proper angles were determined. The 3D histogram displayed on Fig. 2 shows ^{146}Nd excited with ^{58}Ni zoomed on the first 2^+. It clearly demonstrates the alignment after Doppler correction. The y axis is gamma energy and the colour scale is a visual representation of the number of counts.

The x axis of the histogram represents the radial (ϕ angle) segments of the DSSSD detector after relabeling.

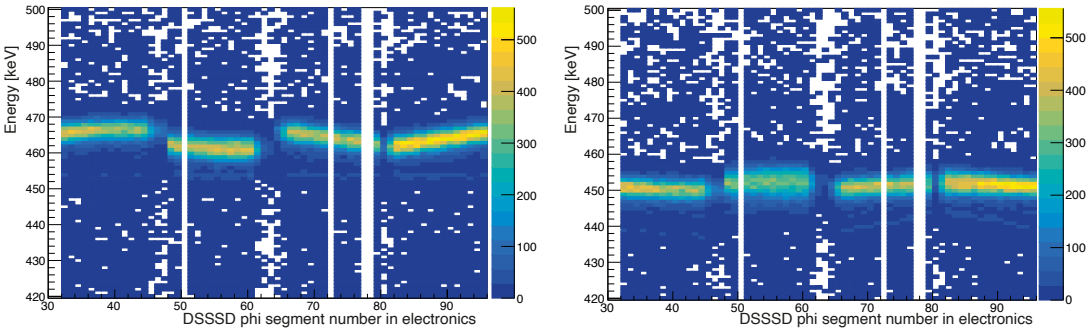

Figure 2: An example energy spectrum of ^{146}Nd excited by ^{58}Ni energy spectrum from one germanium detector response in coincidence with the ohmic (ϕ angle) part of the DSSSD detector before (left) and after Doppler correction.

Bibliography

[1] M .Komorowska *et al.*, Acta Phys. Pol. B **47**, (2016), 923.
[2] M .Komorowska *et al.*, HIL Annual Report 2015, page 66.

C.3 Position sensitivity of FATIMA $LaBr_3$ timing an with analog ORTEC-935 CFD

E. Grodner[1], M. Kowalczyk[2] A. Nałęcz-Jawecki[1]

1) National Centre for Nuclear Research, Poland
2) Heavy Ion Laboratory, University of Warsaw, Poland

$LaBr_3$ crystals have found applications in a variety of fast-timing nuclear spectroscopy techniques in view of their relatively good energy resolution. These techniques are mostly used for lifetime measurements of nuclear excited states from nanoseconds down to picoseconds. In the latter case a correction of timing walk versus energy of the registered gamma quanta is required in order to reduce possible systematic errors. The walk curve can be determined based on a limited set of Full Energy Peaks (FEPs) from radiation sources where gamma quanta are absorbed in $LaBr_3$ crystals. Therefore, it is highly recommended to develop new methods for walk curve determination which are based on a continuous Compton background instead of a small set of FEPs.

As shown in Fig. 10 of Ref. [1], the walk curve obtained from Compton events differs from the corresponding curve obtained from the set of FEPs. The reason for this difference may be twofold:
i) the time response of the $LaBr_3$ detector at energy E_C left in the crystal as a result of a Compton event differs from the time response at the absorbed energy E_{FEP} even for $E_C = E_{FEP}$, hence both events happen at different depths inside the crystal resulting in different times of light propagation from the points of scintillation to the PMT cathode.
ii) the pulse shapes generated by the $LaBr_3$ as a response to Compton events differ from the corresponding pulse shapes from FEPs, affecting the timing logic based on an analog CFD.

It is important to verify which cause is behind the observed difference since in case i) time corrections for gamma interaction depth and light propagation within the crystal can be calculated. For this purpose we used a ^{60}Co source and a dedicated setup of 8 $LaBr_3$ detectors (4 pairs of facing detectors shown in fig. 1) that guarantees sterile measurement conditions eliminating unwanted gamma scatterings on close mechanical construction elements or other unrelated objects. A gamma quantum of energy E may traverse some path λ_E in the crystal before interacting either as a Compton scattering or photoabsorption event with the atoms inside. The timing in turn depends on both the interaction depth and the energy deposited in the crystal. In order to study the registration timing as a function of depth only, the same deposited energy for different interaction depths within the crystal was selected by gating on 214 keV - 1119 keV coincidences representing two types of events in the facing detector pair, here Labr 1 and Labr 5:
a) two gamma quanta emitted from the Co source hit the two detectors in a pair and both undergo Compton scattering. The 1173 keV gamma scatters forward at an angle of 26° in the LaBr 1 detector leaving 214 keV deposited in the crystal. The 1332 keV gamma scatters backward in the LaBr 5 detector almost at angle of 180°, leaving 1119 keV energy deposited in the crystal. In this type of event the backscattered gamma quantum closely misses the LaBr 1 detector and the backscattering is not registered;
b) only the 1332 keV quantum interacts with the detectors while the 1173 keV one escapes and is not observed. The 1332 keV gamma hits LaBr 5 and is backscattered towards LaBr 1 leaving 1119 keV energy deposited. The backscattered 214 keV gamma hits LaBr 1 and is absorbed.

In both types of event the LaBr 5 detector registers almost the same component scattering with 1119 keV energy deposited at nearly the same mean interaction depth marked as λ_{1332}. So the timing characteristic in both types of events is assumed to be the same for the LaBr 5 detector which is necessary for these characteristics to vanish in the final results. Also, the 214 keV energy deposited within the LaBr 1 crystal is the same in both events while the depth of this deposit differs significantly as required by the proposed method. For the events of type a) the 1173 keV gamma traverses a mean depth marked as λ_{1173} in the LaBr 1 detector to deposit 214 keV in the crystal while for events of type b) the 214 keV gamma traverses a shorter depth marked as λ_{214} within the LaBr 1 detector before depositing its entire 214 keV energy as a result of a photoabsorption event

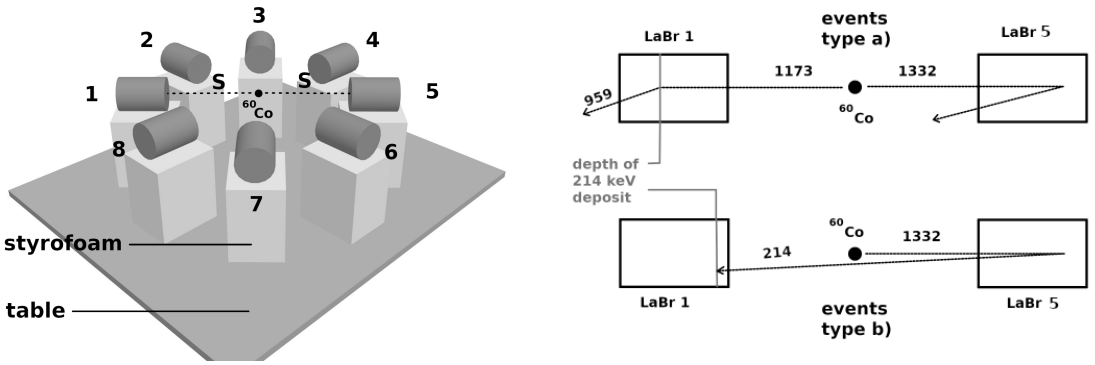

Figure 1: Left: the experimental setup. Right: 214 keV - 1119 keV coincidences. Coincidences of type a) giving 214 keV deposited deep in the LaBr 1 crystal as a result of forward Compton scattering. The energy deposit of 214 keV in LaBr 1 occurs at a shallower depth in events of type b).

Coincidences of type a) and type b) are separated in the timing spectrum according to the equation:

$$t^b - t^a = 2t(S) + 2t(\lambda_{1332}) + t(\lambda_{214}) - t(\lambda_{1173}) + T^1_{214/214} - T^1_{214/1173} \quad (1)$$

where $t(S)$ denotes the time required for a gamma quantum to propagate through distance S between the source and detector front window while $t(\lambda)$ corresponds to the time required for the gamma to traverse a depth λ within the crystals. The last factor, $T^1_{214/214} - T^1_{214/1173}$, describes the timing difference of the LaBr 1 detector for the 214 keV deposit at two distinct depths. This factor should be the same for 8 tested detectors if the differences in timing response for 214 keV Compton events and 214 keV FEP comes from scintillations happening at two different depths, as assumed in reason i) described above. By keeping the same distance S between facing detectors in each pair variations of $T_{214/214} - T_{214/1173}$ on the level of 200ps are observed through variation of $t^b - t^a$ for all detector pairs (1,5),(2,6)...(8,4). This shows that the difference between the FEP and the Compton walk curve is a result of the specific detection setup based on an analog CFD (reason ii) rather than physical processes related to interaction depths and light propagation times.

Bibliography

[1] E. R. Gamba et al., Nuclear Inst. and Methods in Physics Research, A 928 (2019)

C.4 Collective properties of neutron deficient even-even Sm isotopes

L. Próchniak
Heavy Ion Laboratory, University of Warsaw, Warszawa, Poland

For several years the unstable ^{140}Sm isotope has been extensively investigated using various experimental methods, see [1, 2], and various theoretical models have been applied to interpret the low-energy properties of the nucleus [1, 2]. Generally speaking, low-energy collective excitations are well described but some questions remain, for example the existence of an almost degenerate doublet of spin 0 levels, at 1559 and 1629 keV, which is not predicted by any theoretical model so far.

In this report I present theoretical results concerning low-energy spectra and $B(E2)$ transition probabilities for the chain of even Sm isotopes on the neutron deficient side, namely $^{130\text{-}142}$Sm. All these nuclei are unstable with half-lives ranging from 72.49 min (^{142}Sm) to 4.0 s (^{132}Sm). Experimental information for the lighter isotopes, $A < 136$, is rather scarce but some ot the lowest levels are known. The main theoretical tool which I use here is a collective Hamiltonian acting in a full quadrupole space, commonly called the General Bohr Hamiltonian (GBH) [3]. To determine a specific form of the Hamiltonian one needs seven functions depending on the deformation variables (β, γ), six so-called inertial parameters (including three moments of inertia) and a potential energy. An important feature of the employed approach is that all these seven functions are calculated from microscopic mean-field configurations using the Adiabatic Time Dependent HFB theory. In consequence, no parameters of the model are fitted to spectroscopic data. In the mean-field part of the calculations I use the well known and broadly used SLy4 variant of the Skyrme nucleon-nucleon effective interaction augmented with the seniority-type pairing interaction in the particle-particle channel. The strengths of the pairing interaction were fixed through comparison of minimum quasi-particle energies with odd-even mass differences in the considered region of Sm isotopes. The same parameters were used in recent calculations for the ^{140}Sm case [2].

Looking at the calculated potential energies one can see a systematic evolution from a weakly deformed and almost γ independent form to a range of strongly deformed shapes according to decreasing mass number, i.e. moving away from a closed neutron shell. For illustration, in Fig.1 I show plots of the potential energy for two isotopes, close to the limits of the considered chain.

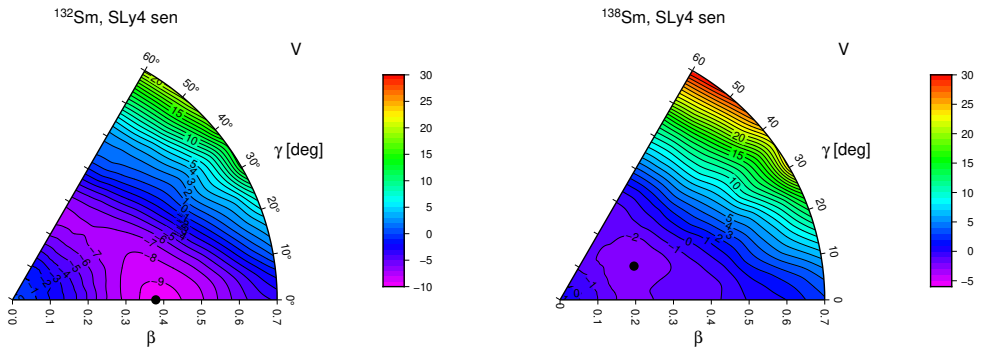

Figure 1: Plots of the potential energy for ^{132}Sm (left panel) and ^{138}Sm (right panel).

Once the collective (GBH) Hamiltonian is fully determined one calculates its eigenvalues and eigenfunctions. The eigenvalues can be directly compared with experimental level energies and such a comparison, for selected important levels, is made in Fig. 2. One can see very good agreement, in particular for the yrast levels. One can also note some discrepancies for $A = 142$, $(N = 80)$, as could be expected due to the vicinity of the closed shell for neutrons.

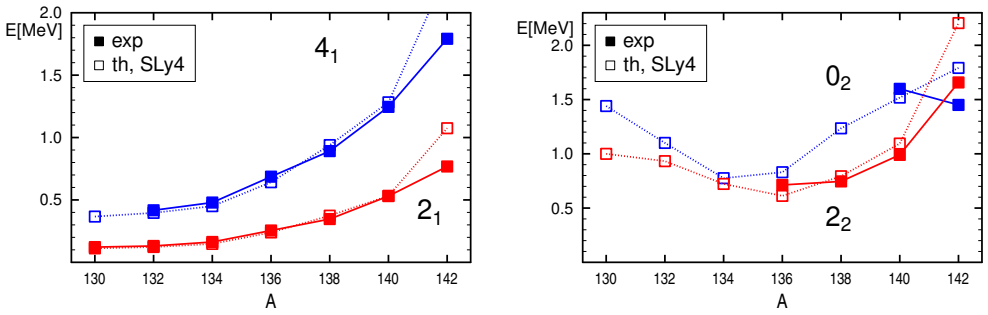

Figure 2: Experimental [4] and theoretical energies of the 2_1^+, 4_1^+, 2_2^+ and 0_2^+ levels for the chain of $^{130\text{-}142}$Sm isotopes.

Other important observables, such as reduced electromagnetic transition probabilities, can be calculated using the obtained collective eigenfunctions. Collective EM transition operators are also determined from the microscopic theory so there is no needs to introduce the so-called effective charge. Experimental data on EM transition for the considered chain are not rich, but nevertheless Fig. 3 shows very good agreement between theory and experiment for the case of the $2_1^+ \to 0_{\text{g.s.}}^+$ transition.

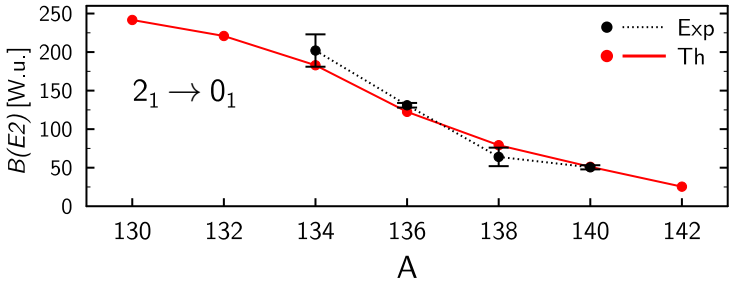

Figure 3: $B(E2)$ reduced probabilities (in W.u.) for the $2^+ \to 0_{\text{g.s}}^+$ transition in the chain of $^{130\text{-}142}$Sm isotopes. Experimental data are taken from [4].

In conclusion, it appears that the collective properties of the neutron-deficient even-even Sm isotopes, including those that are short lived, are very well described by the General Bohr Hamiltonian based on the SLy4 variant of the mean-field.

Bibliography

[1] F. L. Bello Garrote *et al.*, Phys. Rev. C **92** (2015) 024317; M. Klintefjord *et al.*, Phys. Rev. C **93** (2016) 054303; J. Samorajczyk *et al.*, Phys. Rev. C **92** (2015) 044322.
[2] J. Samorajczyk *et al.*, to be published.
[3] L. Próchniak, S.G. Rohoziński, J. Phys. G: Nucl. Phys. **36** (2009) 123101
[4] Data from the NNDC database, revision as of December 2020.

C.5 Coulomb dipole polarization potential for ^{6}He+^{208}Pb

H.M. Maridi[1], K. Rusek[1], N. Keeley[2],

1) Heavy Ion Laboratory, University of Warsaw, Warszawa, Poland
2) National Centre for Nuclear Research, Otwock, Poland

The procedure of Borowska *et al.* [1, 2] was used to derive the Coulomb dipole polarization potential (CDPP) for the ^{6}He+^{208}Pb system. As in Refs. [1, 2] the Schroedinger equation, with the Coulomb potential only, was solved using the adiabatic approximation and the resulting complex CDPP was expressed in terms of the regular and irregular Coulomb functions.

This potential was compared with the similar potential obtained from continuum-discretized coupled channels (CDCC) calculations by means of the trivially equivalent method [3]. Only dipole (E1) couplings to the continuum were included in the calculations. In Fig. 1, the CDCC potential is plotted as short-dashed curves while the CDPP potential is denoted by solid curves. The real part of the CDPP coincides very well with the real part of the CDCC potential at projectile-target separations larger than 20 fm whereas the imaginary part is more absorptive. This means that the dipole polarizability of ^{6}He should be correctly represented by the CDPP, while the Coulomb breakup cross section calculated using the CDPP will be larger than that calculated by the CDCC method.

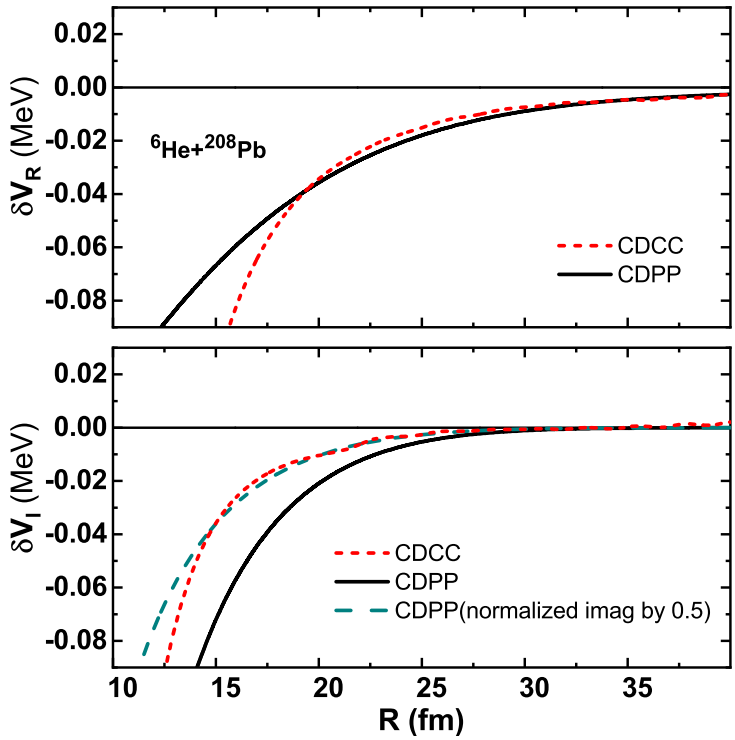

Figure 1: Comparison of the dynamical dipol a polarization potentials derived in this work (CDPP) and obtained from CDCC calculations (CDCC). The imaginary part of the CDPP reduced by a factor 0.5 is also plotted.

This problem is well illustrated when the model calculations are compared with the data for ^{6}He+^{208}Pb elastic scattering at an energy well below the Coulomb barrier [4]. In Fig. 2

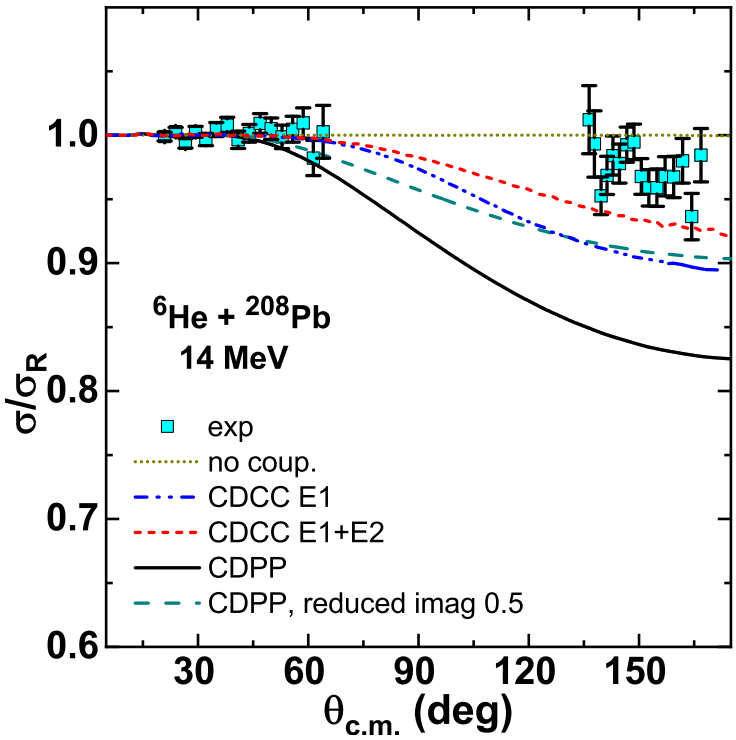

Figure 2: Angular distribution for ^{6}He+^{208}Pb elastic scattering at 14 MeV. The data set is from [4]. The optical model calculations with the CDPP are plotted as the solid black and (with reduced imaginary part) by the dashed green curves. The results of CDCC calculations including only dipole couplings (E1) and dipole+quadrupole couplings (E1+E2) are plotted as the dot-dashed blue and dashed red curves, respectively. The dotted line shows the Rutherford cross section.

optical model calculations where the potential consisted of a central Coulomb potential plus the CDPP, are plotted with the solid curve. They underpredict the measured cross section at backward angles more than the CDCC result (dot-dashed curve). The difference between the CDPP and CDCC results is reduced when the imaginary part of the CDPP is reduced by a half (in this case their imaginary parts are simillar, see Fig. 1). In the case of the CDCC calculations the underprediction could be partly accounted for by inclusion of quadrupole couplings (curve E1+E2). Thus, the too large absorption of the CDPP is partly due to the omission of the E2 couplings.

This study is the first part of a larger programme devoted to the study of the electric dipole polarizability of weakly bound, neutron rich light nuclei.

This work was funded by the Polish National Agency for Academic Exchange (NAWA) within the Ulam Programme under grant agreement No. PPN/ULM/2019/1/00189/U/00001.

Bibliography

[1] L. Borowska, K. Terenetsky, V. Verbitsky, S. Fritzsche, Phys. Rev. C **76** (2007) 034606.
[2] L. Borowska, K. Terenetsky, V. Verbitsky, S. Fritzsche, Phys. Rev. C **79** (2009) 044605.
[3] M.A. Franey, P.J. Ellis, Phys. Rev. **23** (1981) 787 .
[4] A. M. Sánchez-Benítez *et al.*, Nucl. Phys. A **803** (2008) 30.

C.6 Experimentlal setup alignment at ACCULINNA-2

B Zalewski[1], M.C. Golovkov[2], K. Rusek[1],

1) Heavy Ion Laboratory, University of Warsaw, Warszawa, Poland

2) Joint Institute for Nuclear Research, Dubna, Russia

In 2018 an investigation of ^{6}He + ^{2}H reactions at 26 MeV/n was performed at the ACCULINNA-2 fragment separator in the Flerov Laboratory of Nuclear Reactions of the Joint Institute for Nuclear Research in Dubna [1]. It was the first physical experiment at the new fragment separator. The data collected enable the determination of the differential cross sections for both elastic and inelastic scattering the one nucleon transfers ^{6}He(^{2}H,^{3}H)^{5}He and ^{6}He(^{2}H,^{1}H)^{7}He as well as a measurement of the excited states of ^{6}He.

The experimental setup consisted of a Time of Flight detector (ToF), two Multi-wire Proportional Chambers (MWPC), two telescopes for reaction product detection and the target. MWPCs were used for beam tracking along the X and Y axes, where the Z-axis was set by the ion guide. The telescopes consisted of a Double Side Silicon Strip Detector (DSSSD) and a CsI detector. The DSSSD was used for energy loss measurement and tracking and the CsI detectors for the full energy measurement. Deuterated polyethylene foil was used as a target. Measurements were performed in three runs, each with different geometry. For each geometry the angle of the telescope on the left side of the beam was changed. The schematic of the experimental setup is presented in Fig. 1.

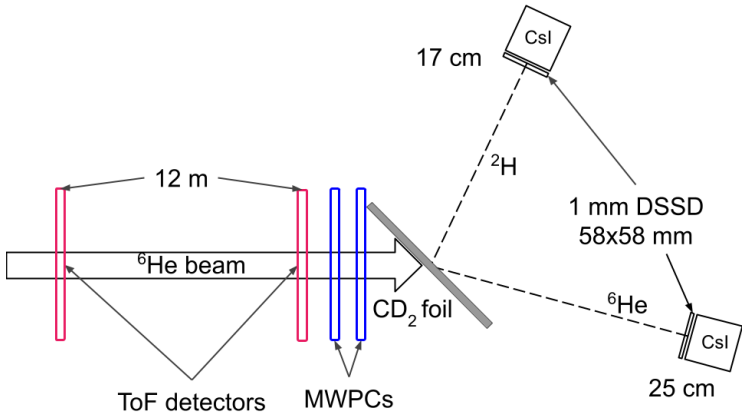

Figure 1: Schematic of the experimental setup for investigations of ^{6}He reactions with a ^{2}H target .

It was discovered only during data analysis that some elements of the experimental setup, such as the target and detectors, were misaligned. In order to find the real positions of the target and detectors in the lab system, optimization methods were used. As the method of choice, the Minuit [2] package within the ROOT environment [3] in the C++ programming language was used. The Minuit package finds the minimum of a given function by a procedure of changing the function input parameters. As a function to minimize, the goodness of fit of the angle-angle relation of the elastic scattering of ^{6}He from ^{1,2}H was used. Goodness of fit was defined as the squared difference between the expected and obtained data points for both processes. Altogether nine input parameters were chosen, shift of each axis of MWPC: MWPC 1 X, MWPC 1 Y, MWPC 2 X and MWPC 2 Y, shift of angle of the Left Telescope in each geometry: Left Angle 1 and Left Angle 2, 3, as well

Table 1: Nominal, input and fitted parameters for the optimization macro.

Parameter	MWPC 1 X	MWPC 1 Y	MWPC 2 X	MWPC 2 Y	Target Shift	Left Angle 1	Left Angle 2,3	Right Angle 1	Right Angle 2,3
Unit	[mm]	[mm]	[mm]	[mm]	[mm]	[deg]	[deg]	[deg]	[deg]
Nominal value	-1.0	-2.1375	0.2	-1.125	5.0	65.0	50.0, 35.0	15.0	15.0
Starting point	-5.0	-5.0	-5.0	-5.0	5.0	-5.0	-5.0	-3.0	-3.0
Obtained shift	-1.0	0.0	-2.1375	0.0	10.0	0.0	0.536	-0.192	0.275

as the shift of the Right Detector Angle in each geometry: Right Angle 1 and Right Angle 2, 3. Additionally, in order to increase the flexibility of the model of the experimental setup reconstruction, the shift in position along the Z axis of the target was included: Target Shift. Obtained corrections for the parameters are presented in Table 1. The Minuit package finds a local minimum with the target situated 10 mm further down the beam line than expected. This might have been a real misalignment during the experiment. The rest of the parameters are only slightly changed.

The angle-angle relation for the elastic scattering of ^{6}He from protons and deuterons with and without correction, (target shift) is presented in Fig. 2. One can see that the match of the data points and calculated points is not perfect. This is caused by Minuit getting stuck in a local minimum of the goodness of fit function instead of finding the global minimum. As an alternative, a program that includes mechanisms preventing this kind of drawback will be used. For example, a more advanced program following the steepest descent or one of the many optimization packages included in the Tensorflow library [4]. The obtained corrections will increase the accuracy of future results and will be a crucial element of the data analysis process.

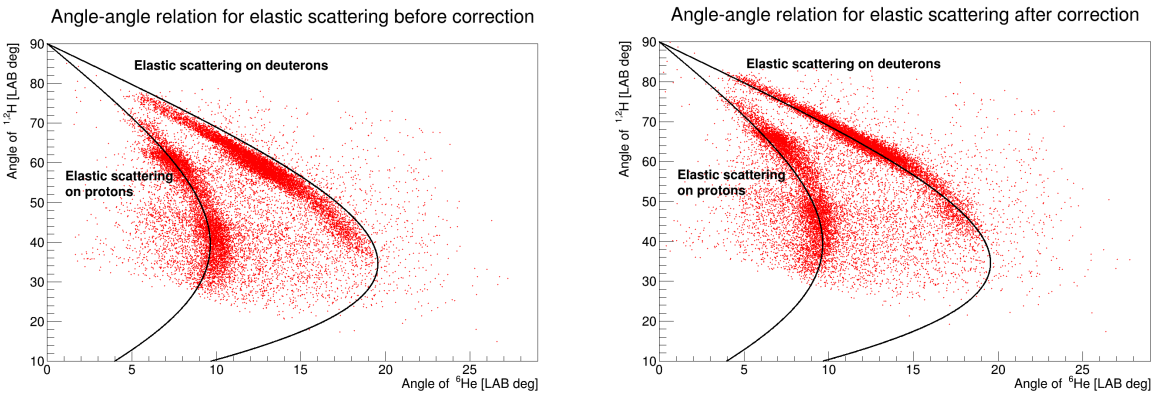

Figure 2: Angle-angle relation for elastic scattering of ^{6}He from ^{1,2}H. On the left is the plot without correction and on the right the plot with corrections.

Bibliography

[1] S.E. Arnell *et al.*, Nucl. Inst. and Meth. **A300** (1991) 303.
[2] F. James, M. Roos, Comp. Phys. Comm. **vol 10, issue 6** (1975) 343-367.
[3] R. Brun, F. Rademakers, Nucl. Inst. and Meth. in Phys. Res. A **389** (1997) 81-86.
[4] `https://www.tensorflow.org/`

C.7 γ–γ angular correlation analysis of the $2^-\rightarrow 2^+\rightarrow 0^+$ cascade

L. Próchniak[1], J. Samorajczyk-Pyśk[1], Ch. Droste[2], J. Srebrny[1]

1) Heavy Ion Laboratory, University of Warsaw, Warszawa, Poland
2) Faculty of Physics, University of Warsaw, Warszawa, Poland

We report here some results concerning angular correlations for the $2^-\rightarrow 2^+\rightarrow 0^+$ cascade when the upper transition radiation ($2^- \rightarrow 2^+$) is composed of three multipolarities $E1$, $M2$ and $E3$. Such transitions are rare but there are at least four well documented cases (^{174}Gd, ^{176}Hf, ^{182}W, ^{184}W) [1]. Our motivation for this study was the puzzle of an almost degenerate doublet of spin 0 levels, at 1559 and 1629 keV in ^{140}Sm [2, 3]. While the spin and parity of the 1559 keV level are firmly established, the same cannot be said about the 1629 keV level. The typical argument for assigning a positive parity to the 1629 keV state, i.e. the value of the $\log ft$ for the β^+/EC decay from the 1^+ g.s. in the parent nucleus ^{140}Eu, is not fully convincing here because for the 1629 keV level $\log ft = 6.1$, which is only slightly above the commonly accepted limit (5.9) for decays that preserve parity. However, if one accepts a positive parity for this level, the data from angular correlation measurements of the $0\rightarrow 2^+\rightarrow 0^+_{\text{g.s.}}$ cascade unambiguously show that the spin should be 0 [3]. However, in the case of a much less probable, but still not fully excluded, negative parity for this state one should consider the $2^-\rightarrow 2^+\rightarrow 0^+_{\text{g.s.}}$, $1^-\rightarrow 2^+\rightarrow 0^+_{\text{g.s.}}$ and $3^-\rightarrow 2^+\rightarrow 0^+_{\text{g.s.}}$ cascades, but the last case can be excluded for ^{140}Sm because for the first forbidden unique β^+/EC decay ($1^+ \stackrel{\beta^+/EC}{\longrightarrow} 3^-$), $\log ft$ should be larger than 8.5.

Transitions in the upper parts of the cascades can now contain three multipolarities: $E1$, $M2$ and $E3$. To calculate the angular correlation coefficient $A_{kk} = A_k(\text{upper transition}) \times A_k(\text{lower transition})$ we need a formula for A_k in the presence of three multipolarities which reads (assuming a nonzero $M2$ component) [4]:

$$A_k = \frac{\delta_{12}^2 f_k(1,1) + f_k(2,2) + \delta_{32}^2 f_k(3,3) - 2\delta_{12} f_k(1,2) - 2\delta_{32} f_k(2,3) + 2\delta_{32}\delta_{12} f_k(1,3)}{\delta_{12}^2 + 1 + \delta_{32}^2} \quad (1)$$

where $\delta_{12} = \delta_{E1/M2}$ and $\delta_{32} = \delta_{E3/M2}$ are the mixing parameters and f_k being abbreviated notation, $f_k(L_1, L_2) = F_k(J_f, J_i, L_1, L_2)$, for the standard coefficients F_k, see e.g. [5].

The coefficients A_{22} and A_{44} now depend on two mixing ratios, δ_{12} and δ_{32}, but if we assume that we know the fraction, say η, of the total transition intensity coming from the $E1$ radiation we can express δ_{12} through η and δ_{32}:

$$\delta_{12} = \pm\sqrt{\frac{\eta}{1-\eta}(\delta_{32}^2 + 1)} \quad (2)$$

In consequence, A_{22} and A_{44} are functions of η and δ_{32}. We choose such a representation because the known cases, mentioned above, can give us some hints on the size of the $E1$ fraction. We then want to investigate if it is possible to get, for some range of δ_{32}, values of A_{22} and A_{44} that are close to those for the $0\rightarrow 2^+\rightarrow 0$ cascade. We have checked that for the $3^-\rightarrow 2^+\rightarrow 0$ cascade the A_{22} and A_{44} coefficients are far away from those of the $0\rightarrow 2^+\rightarrow 0$ cascade for all values of η and δ_{32}, see also the comment above, while for the $1^-\rightarrow 2^+\rightarrow 0$ cascade $A_{44} \equiv 0$, Therefore, we present below the analysis of the $2^-\rightarrow 2^+\rightarrow 0$ case only.

For a fixed η, equations (1,2) give a curve on the A_{22}, A_{44} plane parametrized by δ_{32}, similarly to the ellipses occurring in the angular coefficient theory in the case of two mixed

multipolarities. In Fig. 1 we show such curves for the $2^- \rightarrow 2^+ \rightarrow 0$ cascade, now more complicated than ellipses, for η equal to 0 (the case of an $M2/E3$ transition), 0.1, 0.5 and 0.8. The black dot in the figure corresponds to the $0 \rightarrow 2 \rightarrow 0$ cascade.

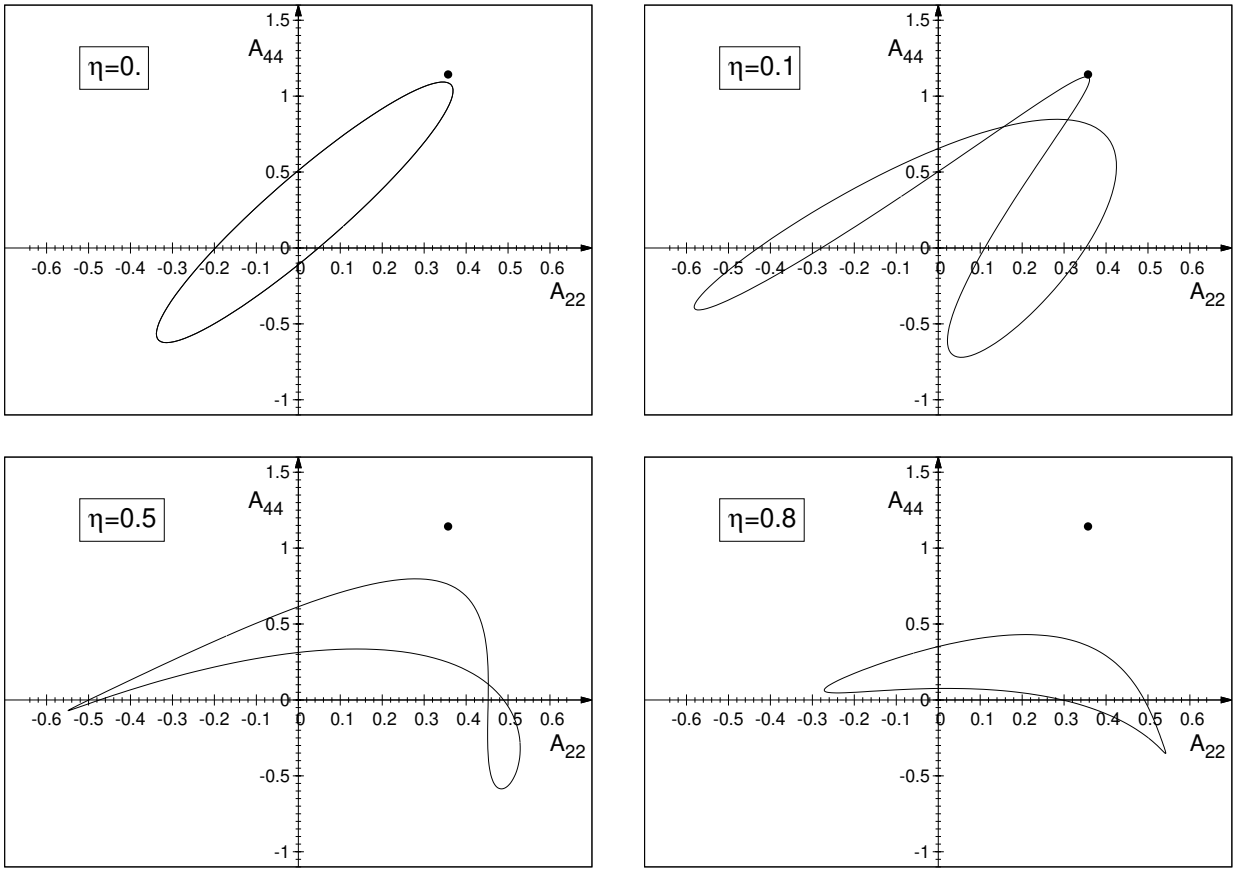

Figure 1: $2^- \rightarrow 2^+ \rightarrow 0^+$ cascade. Plots of angular correlation coefficients for $\eta = 0.0, 0.1, 0.5, 0.8$. The black dot corresponds to the $0 \rightarrow 2 \rightarrow 0$ cascade.

An inspection of Fig. 1 suggests that for $\eta > 0.5$ the A_{22} and A_{44} coefficients for the $2^- \rightarrow 2^+ \rightarrow 0^+$ cascade are 'sufficiently' distant from those of the $0^+ \rightarrow 2^+ \rightarrow 0^+$ one, however, a more quantitative assessment can only be done by using equations (1,2). Of course, when analysing experimental data one should also take into account experimental uncertainties.

The estimates of the η fraction for known cases are as follows: ^{174}Yb, $\eta = 0.96$; ^{176}Hf, $\eta = 0.71$; ^{182}W, $\eta = 0.60$ (here the initial state is a 1.2 ns isomer); ^{184}W, $\eta = 0.99$. From these systematics one may draw the conclusion that the hypothesis of 2^- assignment for the 1629 keV level is very improbable, however, in order to reach the final verdict some other experiments are needed, e.g. with measurement of conversion electrons (including the $E0$ transition).

Bibliography

[1] Data from the NNDC database, revision as of December 2020.
[2] F. L. Bello Garrote *et al.*, Phys. Rev. C **92** (2015) 024317; M. Klintefjord *et al.*, Phys. Rev. C **93** (2016) 054303; J. Samorajczyk *et al.*, Phys. Rev. C **92** (2015) 044322.
[3] J. Smorajczyk-Pyśk *et al.*, to be published.
[4] A. G. Schmidt *et al.*, Phys. Rev. C **9** (1974) 2346.
[5] M. Ferentz and N. Rosenzweig, in *Alpha- Beta- and Gamma-Ray Spectroscopy*, vol. 2, ed. K. Siegbahn, North-Holland (Amsterdam), 1965, p. 1687.

C.8 Scattering and one-nucleon transfers in ^{13}C+^{13}C collisions at an energy of 97 MeV

O.A. Ponkratenko[1], K. Rusek[2], V.V. Uleshchenko[1], O.O. Chepurnov[1], J. Choiński[2], G. Colucci[2], P. Gmaj[2], K.W. Kemper[3], M. Kisieliński[2], E.I. Koschy[4], M. Kowalczyk[2], O.E. Kutsyk[1], S.Yu. Mezhevych[1], E. Piasecki[2], A.A. Rudchik[1], A.T. Rudchik[1], Yu.O. Shyrma[1], Yu.M. Stepanenko[1], A. Stolarz[2], A. Trzcińska[2], M. Wolińska-Cichocka[2]

1) Institute for Nuclear Research, The National Academy of Sciences of Ukraine, Kyiv, Ukraine
2) Heavy Ion Laboratory, University of Warsaw, Warszawa, Poland
3) Physics Department, Florida State University, Tallahassee, USA
4) Cyclotron Institute, Texas A&M University, College Station, USA

At the present time there is still no complete theory of nuclear forces. The most often used phenomenological approach in analyses of nucleus-nucleus collisions is based on the optical potential. Parameters of the potential are determined by analyzing the experimental elastic scattering data. Sometimes there are no experimental data for the considered pair of nuclei at the considered energy, so, one has to estimate the proper parameters of the potential. Therefore, the energy and mass dependencies of the optical potential are of great interest (see for instance [1]).

In order to find such dependencies one needs to analyze large sets of scattering data over broad ranges of collision energy and mass of the interacting nuclei. However, quite often data are present within a narrow energy range only. This is the case for the ^{13}C + ^{13}C interaction where there are no data at energies higher than E_{LAB} = 50 MeV. New data for the ^{13}C + ^{13}C scattering at a substantially higher energy would be very helpful for understanding the energy dependence of the ^{13}C + ^{13}C interaction.

In our experiment a beam of 97 MeV ^{13}C ions was delivered by the U-200P cyclotron. A self-supporting 400 μg/cm^2 ^{13}C target was installed in the ICARE chamber. The $\Delta E - E$ - technique was used for the identification of the reaction products. All E-detectors were 300 μm silicon detectors while the ΔE-detectors were either silicon detectors of thickness around 40 μm or gas detectors. Examples of a two-dimentional $\Delta E - E$ spectrum as well as a ^{13}C energy spectrum are presented in the left and right panels of Fig. 1 respectively.

As one can see the technique used alloved for charge separation of the reaction products as well as for mass separation of different isotopes. For instance, in the three $Z = 6$ loci one can easily see three nearby peaks corresponding to the elastic scattering and the one neutron transfer reactions. A clear peak of ^{12}B corresponding to the proton transfer reaction is visible in the $Z = 5$, $A = 12$ locus. Figure 1a shows that the elastic scattering peak is well fitted by simple Gaussian shape. The average statistical uncertainty was found to be $\sim$ 1 % ($\sim$ 0.6 % of which is related to the energy spread of the beam). Next to the elastic peak one can also see a peak corresponding to inelastic scattering with excitation of the 3.09 MeV $\left(\frac{1}{2}\right)^+$, 3.68 MeV $\left(\frac{3}{2}\right)^-$ and 3.85 MeV $\left(\frac{5}{2}\right)^+$ states of the ^{13}C nucleus.

Measured differential cross sections for the ^{13}C(^{13}C,^{12}C)^{14}C neutron-transfer and ^{13}C(^{13}C,^{14}N)^{12}B proton-transfer reactions provide the possibility to evaluate the nucleon spectroscopic factors for the ^{13,14}C nuclei and ^{14}N nuclei by means of coupled reaction channels analyses. Information about the interaction of the radioactive nuclei ^{14}C or ^{12}B can also be extracted by a careful CRC analysis [2].

The first step in the theoretical analysis of all the new data must be a description of the elastic scattering. The newly obtained differential cross section data for the ^{13}C elastic scattering from ^{13}C at an energy E_{LAB} (^{13}C) = 97 MeV are presented in Fig.2. The solid

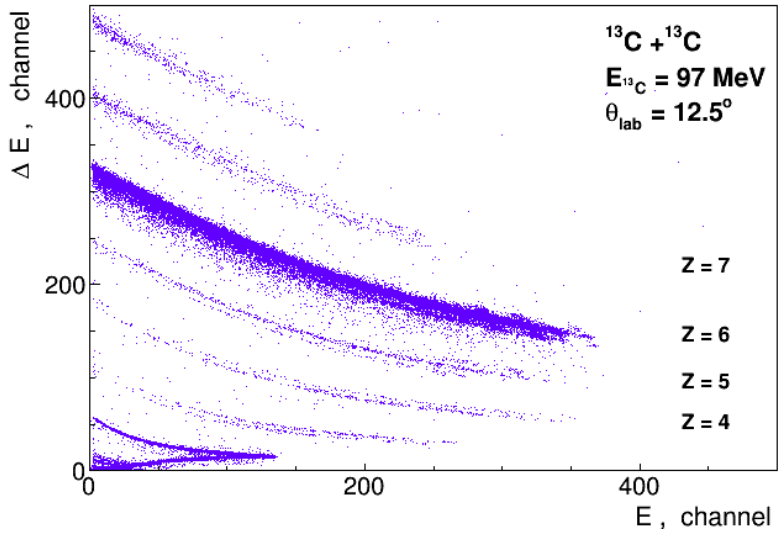

(a) Fig. 1a

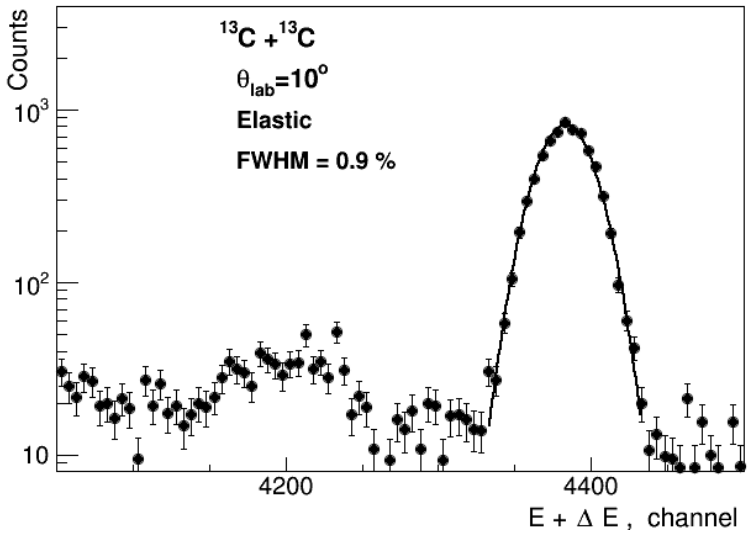

(b) Fig. 1b

Figure 1: Typical $\Delta E - E$(Fig. 1a) and energy spectra (Fig. 1b) of the registered reaction products. The solid line in the right panel represents a Gaussian fit to the elastic scattering peak.

curve shows an OM-calculation with the potential adjusted to the new data. The parameters of the ^{13}C + ^{13}C Woods-Saxon optical potential are: V= 93 MeV, r_V= 1.083 fm, a_V = 1.069 fm, W = 830 MeV, r_W= 0.768 fm, a_W = 0.489 fm.

To study the mass dependence of the ^{13}C interaction it is very interesting to compare the new ^{13}C + ^{13}C data to similar data for ^{13}C scattering from other targets at nearby energies. The ^{13}C + ^{12}C scattering cross section at E_{LAB} (^{13}C) = 102 MeV is the presented by an optical model curve (dashed) for easier comparison of the positions of the diffractive peaks which are expected to be close [3]. The cirve fits the corresponding ^{13}C + ^{12}C data fairly well. Indeed, one can see very close patterns of the ^{13}C diffractive scattering ^{13}C and from ^{12}C, as expected.

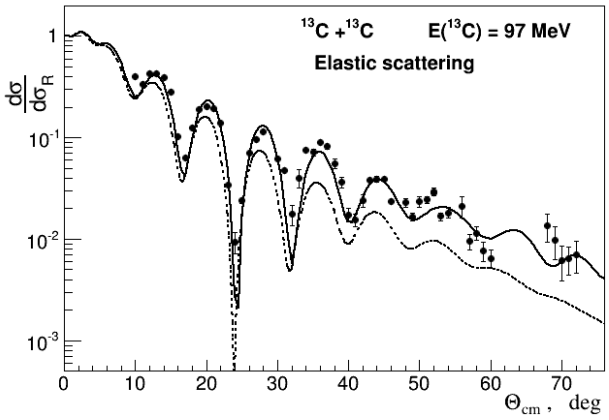

Figure 2: Angular distribution of the differential cross section of the ^{13}C + ^{13}C elastic scattering normalized to the Rutherford cross section. The dashed curve represents the ^{13}C + ^{12}C cross section at E_{LAB} (^{13}C) = 102 MeV for comparison (see details in the text).

Bibliography

[1] Yongli Xu *et al.*, Phys. Rev. C **99** (2019) 034618.
[2] S.Yu. Mezhevych *et al.*, Acta Phys. Pol. **B51** (2020) 1949.
[3] O.A. Ponkratenko *et al.*, Acta Phys. Pol. **B49** (2018) 31.

C.9 Use of the mass separator of the Warsaw IGISOL as an ion implantor for construction of ion implanted silicon detectors

A.J. Kordyasz[1], S. Lewandowski[2], A. Wojtasiewicz[1], A. Bednarek[1], M. Kisieliński[1],

1) Heavy Ion Laboratory, University of Warsaw, Warszawa, Poland

2) Institute of Experimental Physics, University of Warsaw, Warszawa, Poland

The mass separator of the Warsaw IGISOL was produced at the Institute for Nuclear Research in Świerk. Before using the separator at the Heavy Ion Laboratory of Warsaw University for separation of products obtained from heavy-ion reactions, it was initially used for pure implantation of B^+ and P^+ ions to obtain p^+-n-n^+ junctions in X-Y position sensitive silicon detectors [1]. This was done at the Institute for Nuclear Research in Świerk. Position sensitive detectors produced in this Institute X-Y were used for "Precise determination of size and uniformity of a fissionable source" [2] and for "Angular distributions of light charged particles from ^{252}Cf in the ranges 0-46° and 134-180°" [3]. We now plan to make B^+ implantation at the Heavy Ion Laboratory of Warsaw University to produce n-p^+ junctions in a "Silicon epitaxial 20 μm thick double sided strip test detector with read-out of induced signals on the back detector strips" [4]. Preliminary tests producing argon ions using a duoplasmatron ion source and the mass separator of the Warsaw IGISOL were performed with success. A device for directing the ion beam to achieve a homogeneous ion implantation distribuion into the surface of the silicon is being constructed and tested.

Bibliography

[1] S. Kalbitzer *et al.*, Nucl. Inst. and Meth. **54** (1967) 323.
[2] A. Kordyasz *et al.*, Nucl. Inst. and Meth. **154** (1978) 405.
[3] A.J. Kordyasz *et al.*, Nucl. Phys. A **439** (1985) 28.
[4] A.J. Kordyasz, Ł. Kordyasz, HIL Annual Report 2019, page 76.

Part D
Experiments using external facilities

D.1 AGATA-NEDA-DIAMANT data analysis

M. Palacz[1], G. Jaworski[1], D. Wójcik[1,2] and the NEDA and N=Z Collaborations

1) Heavy Ion Laboratory, University of Warsaw, Warszawa, Poland
2) Faculty of Physics, University of Warsaw, Warszawa, Poland

In this contribution we report on the analysis of data collected in an experiment performed in May 2018 at GANIL, France, which aimed at studies of excited states in ^{102,103}Sn to deduce two-body neutron interactions, single-particle energies and $N = Z = 50$ core excitations. The experimient E703, was realised as one of 5 experiments in which the NEutron Detector Array (NEDA) was employed for the first time, together with the 1Π AGATA γ-ray spectrometer [1] and the DIAMANT charged particle detector [2]. The data analysis is in progress in Warsaw, Stockholm and Uppsala. Selected aspects of the work pursued in Warsaw are briefly described below. First results of another experiment from the same series have already been published [3]. Participation of the Warsaw group in the construction of NEDA was covered in contributions to previous HIL annual reports [4–7]. The NEDA project has been described in more detail in several regular papers, see [8, 9] and references therein.

In the E703 experiment the ^{102,103}Sn nuclei were expected to be produced with very small cross sections, namely 0.2 μb and 0.5 μb respectively. Events of interest have to be selected out of the background of other fusion-evaporation channels, with a total fusion cross section of about 0.5 barn. Random target radioactivity events and Coulomb excitation of the target and projectile nuclei also contribute significantly to the background, so do products of reactions on target contaminants (^{12}C and ^{16}O). Selection is made using data from the charged particle and neutron detectors, and its quality as well as efficiency are crucial.

Protons and α particles detected in the DIAMANT detectors are discriminated using 3 parameters: the energy deposited in the detector, the so-called particle-id (PID) and the detection time with respect to the cyclotron RF signal. The PID parameter reflects the shape of the signal, which depends on the type of the detected particle. In Figure 1 an example of gates used for one of the detectors is shown.

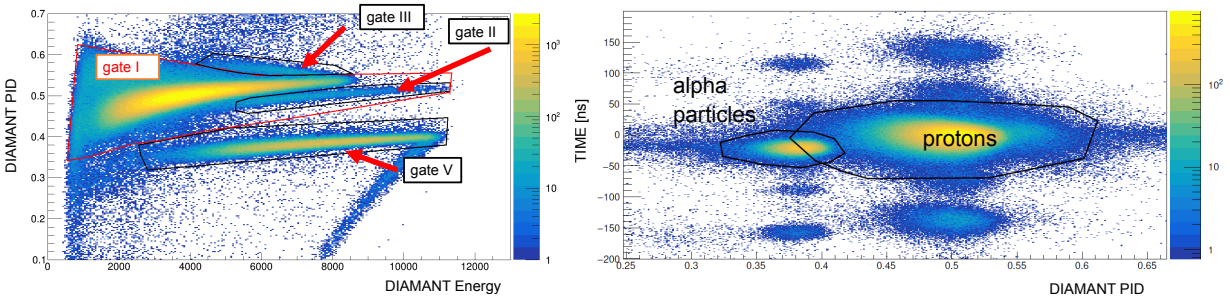

Figure 1: DIAMANT spectra: particle-id vs. energy (left) and time vs. particle-id (right). The following 2-dimensional structures were identified in the particle-id vs. energy spectra: gate I — at least 1 proton, gate II – two protons, gate III – protons from reactions on target contaminants, gate V – α particles. The discrimination is improved by setting gates on α-particle and proton distributions in the time vs. particle-id plot.

Neutrons detected in the neutron detectors have to be distinguished from γ rays. This is done by setting gates on the detection time, the shape of the signal, and the amount of

light produced in the scintillator detector. In addition to the neutron–γ-ray discrimination, care has to be taken for the proper determination of the multiplicity of neutrons detected in the array of neutron detectors. This is due to the fact that neutrons tend to scatter between multiple detectors, which results in one neutron generating a signal in more than one detector [11].

A very high quality of gating both on charged particles and neutrons has been achieved, and this is illustrated in Fig. 2.

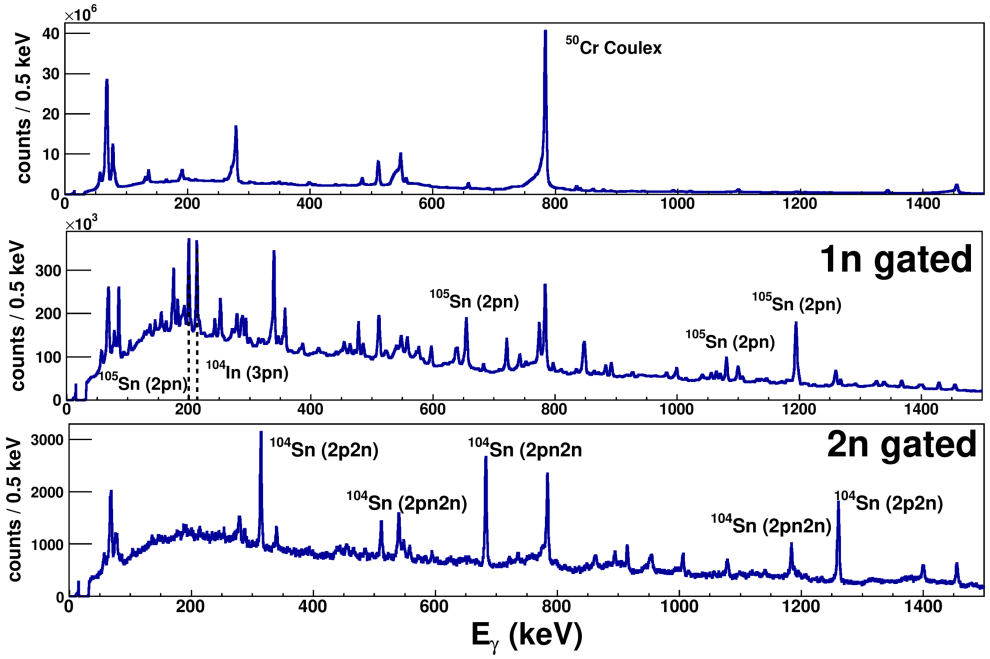

Figure 2: Gamma spectra from the E703 experiment with: no off-line condition on the detected neutrons (top), gated on 1 (middle) and 2 (bottom) neutrons. Gamma rays from the reaction channels which include the emission of 1 or 2 neutrons are labelled in the plots, as well as lines originating from Coulomb excitation of the target and beam.

Work on the data analysis is in progress.

Acknowledgement: the Polish contribution to NEDA and related investigations of rare proton-rich isotopes are supported by the Polish National Science Centre (grants nos. 2017/25/B/ST2/01569, 2016/22/M/ST2/00269, and 2014/14/M/ST2/00738), COPIN-IN2P3, COPIGAL, and POLITA projects.

Bibliography

[1] E. Clément *et al.*, Nucl. Inst. and Meth. **A855** (2017) 1.
[2] J.N. Scheurer *et al.*, Nucl. Inst. and Meth. **A385** (1997) 501.
[3] B. Cederwall *et al.*, Phys. Rev. Lett. **124** (2020) 062501
[4] M. Palacz *et al.*, HIL Annual Report 2016, page 79.
[5] M. Palacz *et al.*, HIL Annual Report 2017, page 70.
[6] M. Palacz *et al.*, HIL Annual Report 2018, page 77.
[7] G. Jaworski *et al.*, HIL Annual Report 2019, page 87.
[8] J.J. Valiente-Dobon *et al.*, Nucl. Inst. and Meth. **A673** (2012) 64.
[9] G. Jaworski *et al.*, Acta Phys. Pol. **B50** (2019) 585.
[10] Ö. Skeppstedt *et al.*, Nucl. Inst. and Meth. **A421** (1999) 531
[11] J. Ljungvall, M. Palacz, J. Nyberg, Nucl. Inst. and Meth. **A528** (2004) 741

D.2 Detection of fast neutrons employing digital Pulse Shape Analysis

A.M. Quỳnh[1], W. Poklepa[2], T.M.N. Le[1], A. Bezbakh[1], G. Jaworski[3], G. Kamiński[1,3], P.J. Napiorkowski[3]

1) Joint Institute for Nuclear Research, Dubna, Russia
2) Faculty of Chemistry, University of Warsaw, Warszawa, Poland
3) Heavy Ion Laboratory, University of Warsaw, Warszawa, Poland

Fast neutrons detectors are used in numberous fields of science and industry: they are employed in border security, to investigate the radiation-hardness of electronics for use in aeroplanes and space, utilized in radiopharmaceutical production and in basic nuclear physics research. Within this contribution we report on the result of the digital readout of two state-of-the-art detectors: a stilbene crystal employed in an experimental setup placed after the ACCULINNA-2 separator [1] for tagging reaction channels and exploring the neutron drip-line of light elements; and one unit of the NEDA detector array [2] used as a neutron multiplicity filter in the investigations of neutron-deficient nuclei along the N=Z line.

The stilbene crystal was cylindrical with a diameter of 80 mm and height of 50 mm, the NEDA dectector had the shape of a uniform hexagonal prism of height 20 cm and volume ∼3.15 liter. Both detectors, shown in Fig. 1, were readout by a CAEN V1725B 250 MS/s 14-bit digitizer. The Pulse Shape Analysis (PSA) of signals was performed online inside the FPGA employing CAEN's PSA firmware, and the results are shown in Fig. 2. The PSD parameter represents the ratio between light collected in two time gates (Charge Comparison method [3]).

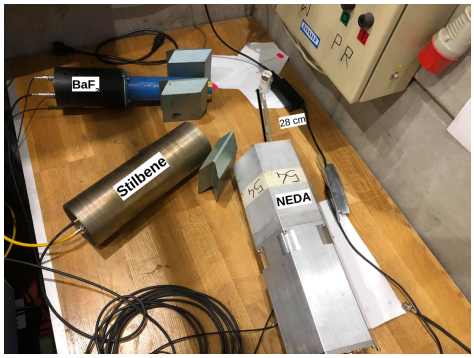

Figure 1: The experimental setup with the stilbene and NEDA detectors placed at the same distance from the Cm-C neutron source.

Having the detectors at the same distance from the source resulted in obtaining less counts for stilbene than for NEDA. The signal size was 380 mV and 2.5 V per MeVee for stilbene and NEDA, respectively. Both effects, the detector size and signal height, are visible in Fig. 2. The parameters of the Charge Comparison method employed in the FPGA of the digitizer were optimized for each detector. The light yield of the detectors was calibrated using ^{241}Am, ^{137}Cs and ^{60}Co γ-ray sources.

A commonly-used quantity which is utilized to show the quality of PSA is called the Figure-Of-Merit (FOM). It is calculated as FOM= $\frac{C_n - C_\gamma}{FWHM_n + FWHM_\gamma}$, where C_n and C_γ are the positions of the centroids of the neutron and gamma peaks, respectively; while $FWHM_n$ and $FWHM_\gamma$ are the widths of the corresponding distributions. In Fig. 3 FOM

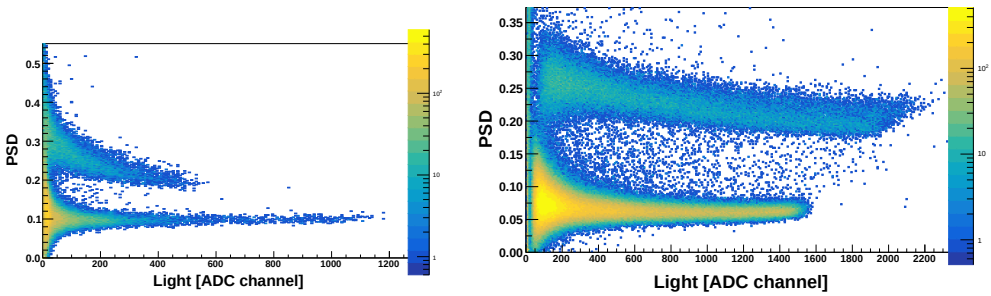

Figure 2: Neutron-gamma discrimination obtained directly from the FPGAs of a Caen V1725B digtizer for stilbene (left) and NEDA (right) detectors. See text for details and discussion.

is shown as a function of the light output for the stilbene and NEDA detectors. Different ranges of the data come from different signal sizes and effectively different dynamic range coverage. In both cases an increase will be noted for the FOM with increasing light output. In the case of the stilbene the growth is reaches in saturation value, while for NEDA there is a drop down at the highest light point. This is due to large signals which exceed the Vpp range of the digitizer leading to a fallacious PSD value. This effect is not present for stilbene, as it gives much smaller signals.

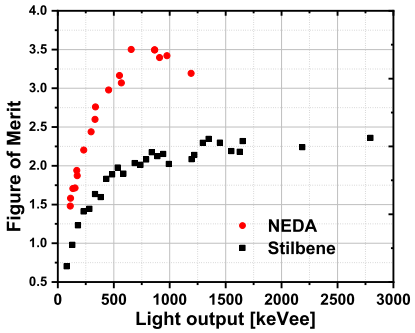

Figure 3: Figure-of-Merit as a function of the light yield for stilbene (black) and NEDA (red) detectors. See text for details and discussion.

Stilbene is known to have excellent neutron-γ discrimination (NGD) capabilities, exceeding those of the EJ301/BC501 liquid scintillator filling NEDA. The results presented here suggest that the dynamic range of the digitizer should be adjusted to the smaller signals of the stilbene detector. Nevertheless, the NGD for both detectors was satisfying. Additionally, the risetime was 5 and 7 ns for the stilbene and NEDA detectors, respectively, and the question arises whether 250 MS/s probing is fast enough for the stilbene detector. These effects will be further addressed in up-coming measurements.

Acknowledgement: This project is partially supported by a grant of the Plenipotentiary Representative of Poland at JINR, Dubna, Russia and by the Polish National Science Centre (grant no. 2017/25/B/ST2/01569).

Bibliography

[1] A.S. Fomichev *et al.*, Eur. Phys. J. **A 54** (2018) 97.
[2] J. Valiente *et al.*, Nucl. Inst. and Meth. **A927** (2019) 81.
[3] F.D. Brooks, Nucl. Inst. and Meth. **4** (1959) 151.

Part E
Appendices

E.1 List of experiments performed at HIL in 2020

A list of the experiments performed in 2020 is presented in the following pages. The following acronyms of institution names are used in the list:

- HIL — Heavy Ion Laboratory, University of Warsaw, Warszawa, Poland;
- CI TA&MU Texas — Cyclotron Institute, Texas A&M University, College Station, USA;
- INFN Padova — INFN Sezione di Padova, Padova, Italy;
- INFN LNL — INFN, Laboratori Nazionali di Legnaro, Legnaro, Italy;
- INFN Pavia — INFN Sezione di Pavia, Pavia, Italy;
- INR NANU Kiev —Institute for Nuclear Research, The National Academy of Sciences of Ukraine, Kyiv, Ukraine;
- NRCKI Moscow — National Research Center "Kurchatov Institute", Moscow, Russia;

For each experiment the following information is provided: ion, energy, setup/beam line information, date, proposal number, subject, spokespersons and institutions.

^{13}C — 78-104 MeV — ICARE 13.01 – 24.01

HIL081 — Scattering and transfer reactions in collisions of ^{13}C ions with light nuclei at an energy of 100 MeV

(O.Ponkratenko, K. Rusek)

INR NANU Kiev, CI TA&MU Texas, NRCKI Moscow, HIL

17.02 - 21.02

HIL000 — Beam development (P. Gmaj)

HIL

24.02 - 28.02

HIL000 — Beam development (P. Gmaj)

HIL

2.03 - 6.03

HIL000 — Beam development (P. Gmaj)

HIL

^{13}C — 78-104 MeV — ICARE 9.03 – 18.03

HIL081 — Scattering and transfer reactions in collisions of ^{13}C ions with light nuclei at an energy of 100 MeV

(O.Ponkratenko, K. Rusek)

INR NANU Kiev, HIL, CI TA&MU Texas

19.03 - 27.03

HIL000 — Beam development (P. Gmaj)

HIL

^{4}He — 30 MeV — Internal beam 10.07 – 13.07

HIL091 — Cross-section measurements of ^{117m}Sn and its contaminants produced by alpha particles on natural Cadmium and natural Indium targets.

(L. De Dominicis, G. Pupillo)

HIL, INFN LNL, INFN Padova, INFN Pavia

E.2 Degrees and theses completed in 2020 or in progress

E.2.1 PhD theses of students affiliated to HIL, of HIL staff members, and supervised by HIL staff

Mateusz Pęgier, Faculty of Chemistry, University of Warsaw
Wykorzystanie techniki ekstrakcji do fazy stałej do wydzielania i zatężania jonów skandu
Application of solid phase extraction for separation and preconcetration of scandium ions
Supervisor: prof. dr hab. K. Pyrzyńska. Thesis completed in October 2020.

Michalina Komorowska, Faculty of Physics, University of Warsaw
Korelacje oktupolowe w jądrach atomowych z obszaru $N \sim 88$
Pear-shaped Nuclei in the $N \sim 88$ *region*
Supervisors: dr hab. L. Próchniak, dr P. Napiorkowski, dr W. Korten, dr M. Zielińska. (program cotutelle) Expected completion time: 2022.

Olga Saeed Mohamed Nassar, Faculty of Physics, Warsaw University of Technology
Optyka jonowa w centrum cyklotronu U-200P
Ion trajectories in the central region of the U-200P cyclotron
Supervisors: dr hab. M. Palacz, dr I. Ivanenko. Expected completion time: 2023.

Łukasz Standyło, National Centre for Nuclear Research, Świerk
Badanie mechanizmu wychwytu i termalizacji strumieni jonów i atomów wprowadzonych do plazmy wytwarzanej metodą elektronowego rezonansu cyklotronowego
Investigation of capture and thermalization mechanism of ion and atomic beams injected into plasma produced by the electron cyclotron resonance
Supervisor: prof. dr hab. K. Rusek, dr K. Sudlitz. Expected completion time: 2023.

Bogumił Zalewski, Faculty of Physics, University of Warsaw
Badanie oddziaływania $^{6}He+d$
Study of the $^{6}He+d$ interaction
Supervisors: prof. dr hab. K. Rusek. Expected completion time: 2023.

E.2.2 Other PhD theses based on experiments performed at HIL

Sunil Dutt, Aligarh Muslim University, Aligarh, (U.P.) India
Supervisor: prof. A. Rizvii. Thesis completed in October 2020.

Feruzjon Ergashev, Institute of Nuclear Physics, Academy of Sciences of the Republic of Uzbekistan, Tashkent, Uzbekistan
Study of nucleon transfer reactions in $^{10}B+^{16}O$ ***at energies near the Coulomb barrier for nuclear astrophysics***
Supervisors: prof. S. Artemov. Expected completion time: 2021.

Bakytbek Mauey, L.N. Gumilyov Eurasian National University, Astana, Kazakhstan
Investigation of the elastic scattering of ^{15}N ions on 1p-shell nuclei at energies near the Coulomb barrier
Supervisors: prof. A. Morzabayev. Expected completion time: 2021.

Maulen Nassurlla, Al-Farabi Kazakh National University, Almaty, Kazakhstan
Effects of cluster structure of stable boron and lithium isotopes on the products of nuclear reactions with deuterium and helium isotopes
Supervisors: prof. N. Burtebayev. Expected completion time: 2021.

Maria Pęgier, Faculty of Chemistry, University of Warsaw
Macrocyclic compounds labeled with metallic isotopes for applications in positron emission tomography
Supervisors: prof. dr hab. K. Pyrzyńska, dr hab. K. Kilian. Expected completion time: 2023.

Daniel Andrzej Piętak, Faculty of Electronics and Information Technology, Warsaw University of Technology
Metoda oceny jakości wyników z eksperymentów wzbudzeń kulombowskich z wykorzystaniem algorytmu genetycznego
Evaluation method based on a genetic algorithm for results of Coulomb excitation experiments
Supervisors: dr hab. inż. P. Bilski. Submitted in December 2020.

Auganbek Sabidolda, Al-Farabi Kazakh National University, Almaty, Kazakhstan
Study of nucleon transfer reactions in $^{10}B+^{12}C$ at energies near the Coulomb barrier for nuclear astrophysics
Supervisors: prof. N. Burtebayev. Expected completion time: 2022.

Dominika Wójcik, Faculty of Physics, University of Warsaw
Supervisors: dr hab. M. Palacz. Expected completion time: 2023.

Oleksandr Kutsyk, Institute for Nuclear Research, National Academy of Sciences of Ukraine
Nuclear reactions in the interaction with ^{15}N ions by ^{12}C and ^{13}C nuclei
Supervisor: prof. A.T. Rudchik. Expected completion time: 2023.

Oleksandr Chepurnov, Institute for Nuclear Research, National Academy of Sciences of Ukraine
Nuclear reactions in the interaction with ^{15}N and ^{10}B ions by ^{6}Li nuclei
Supervisor: prof. A.T. Rudchik. Expected completion time: 2023.

E.2.3 MSc and BSc theses supervised by HIL staff members

Michał Cudny, Faculty of Physics, University of Warsaw
Kontrola jakości 18FMISO zsyntezowanego do badań przedklinicznych na małych zwierzętach
Quality control of [18F]FMISO for small animal PET imaging

Supervisors: dr hab. K. Kilian, dr P. Suffczyński. Thesis completed in October 2020.

Karolina Milewska, Faculty of Physics, University of Warsaw
Synteza radiofarmaceutyku 18FHBG
9-(4-fluoro-3-hydroxymethylbutyl)guanine ([18F]FHBG) radiosynthesis
Supervisors: dr hab. K. Kilian. Thesis completed in September 2020.

Vladyslav Kheilo, Taras Shevchenko National University of Kyiv
Mechanism of the $^{12}C(^{15}N, ^{14}N)^{13}C$ reaction at E_{lab} = 81 MeV and nuclear structure
Supervisor: prof. A.T. Rudchik. Thesis completed in June 2020.

Michał Smolarek, Jakub Krauz, Jakub Łaguna, Krzysztof Witczyński, Faculty of Mathematics, Informatics and Mechanics, University of Warsaw
System sterowania warszawskim cyklotronem
Control system for the Warsaw Cyclotron
Supervisors: mgr G. Grudziński, mgr inż. J. Miszczak. Expected completion time: 2021.

Kinga Kitlińska, Faculty of Chemistry, University of Warsaw
Extraction of selenium species from samples of various matrices
Supervisors: prof. dr hab. K. Pyrzyńska, dr A. Sentkowska. Expected completion time: 2021

E.3 Publications

N. Amangeldi, N. Burtebayev, S.B. Sakuta, M. Nassurlla, J. Burtebayeva, M. Nassurlla, G. Yergaliuly, A. Sabidolda, K. Rusek, A. Trzcińska, M. Wolińska-Cichocka, B. Mauyey. *Study of Elastic Scattering of ^{10}B ions on ^{12}C Nuclei at the Energy of 17.5 MeV.* Acta Phys. Pol. B **51**, 757(2020).

F. Barbaro, L. de Dominicis, L. Canton, M.P Carante, A. Colombi, A. Fontana, A. Stolarz. *Theoretical study for a ^{117m}Sn production experiment with a 30 MeV a-beam cyclotron.* Nuovo Cimento C **43**, 136(2020).

S. Barlini, M. Bini, A. Buccola, A. Camaiani, G. Casini, C. Ciampi, C. Frosin, P. Ottanelli, G. Pasquali, S. Piantelli, G. Poggi, A.A Stefanini, S. Valdré, E. Bonnet, B. Borderie, R. Bougault, A. Chibli, M. Cicerchia, M. Cinausero, J.A. Duenas, D. Fabris, J. Frankland, D. Gruyer, M. Henri, A. Kordyasz, T. Kozik, N. Leneindre, I. Lombardo, O. Lopez, G. Mantovani, T. Marchi, J. Quicray, S. Upadhyaya, G. Verde, E. Vient, M. Vigilante. *FAZIA: A new performing detector for charged particles.* J. Phys.: Conf. Ser. **1561**, 012003(2020).

A.A.Bezbakh, S.G. Belogurov, D. Biare, V. Chudoba, A.S. Fomichev, E.M. Gazeeva, M.S. Golovkov, A.V. Gorshkov, G. Kamiński, S.A. Krupko, B. Mauyey, I.A. Muzalevskii, E.Y. Nikolskii, Y.L. Parfenova, W. Piątek, A.M. Quynh, A. Serikov, S.I. Sidorchuk, P.G. Sharov, R.S. Slepnev, S.V. Stepantsov, A. Swiercz, P. Szymkiewicz, G.M. Ter-Akopian, R. Wolski, B. Zalewski. *Study of ^{10}Li Low Energy Spectrum in the $^{2}H(^{9}Li, p)$ Reaction.* Bull. Russ. Acad. Sci.: Phys. **84**, 491(2020).

A.A. Bezbakh, V. Chudoba, S.A. Krupko, G. Belogurov, D. Biare, A.S. Fomichev, E.M. Gazeeva, A.V. Gorshkov, L.V. Grigorenko, G. Kamiński, O.A. Kiselev, D.A. Kostyleva, M.Yu. Kozlov, B. Mauyey, I. Mukha, I.A. Muzalevskii, E.Yu. Nikolskii, Yu.L. Parfenova, W. Piątek, A.M. Quynh, V.N. Schetinin, A. Serikov, S.I. Sidorchuk, P.G. Sharov, R.S. Slepnev, S.V. Stepantsov, A. Swiercz, P. Szymkiewicz, G.M. Ter-Akopian, R. Wolski, B. Zalewski, M.V. Zhukov. *Evidence for the First Excited State of ^{7}H.* Phys. Rev. Lett. **124**, 022502(2020).

J. Bradbury, D. Testov, S. Bakes, A. Goasduff, D. Mengoni, J.J. Valiente-Dobon, G. de Angelis, D. Bazzacco, C. Boiano, A. Boso, B. Cederwall, M. Cicerchia, G. Colucci, P. Colovic, F. Didierjean, M. Doncel, J. A. Duenas, F. Galtarossa, A. Gozzelino, K. Hadyńska-Klęk, G. Jaworski, P.R. John, H. Liu, S. Lenzi, S. Lunardi, R. Menegazzo, A. Mentana, C. Mueller-Gatermann, D.R. Napoli, G. Pasqualato, F. Recchia, M. Rocchini, S. Riccetto, B. Saygi, M. Siciliano, Yu Sobolev, S. Szilner. *Lifetime measurements using a plunger device and the EUCLIDES Si array at the GALILEO gamma-ray spectrometer.* Nucl. Instrum. Methods Phys. Res. A**979**,164345(2020).

P.A. Butler, L.P. Gaffney, P. Spagnoletti, K. Abrahams, M. Bowry, J. Cederkall, G. de Angelis, H. De Witte, P.E. Garrett, A. Goldkuhle, C. Henrich, A. Illana, K. Johnston, D.T. Joss, J.M. Keatings, N.A. Kelly, M. Komorowska, J. Konki, T. Kroell, M. Lozano, B.S. Nara Singh, D. O'Donnell, J. Ojala, R.D. Page, L.G. Pedersen, C. Raison, P. Reiter, J.A. Rodriguez, D. Rosiak, S. Rothe, M. Scheck, M. Seidlitz, T.M. Shneidman, B. Siebeck, J. Sinclair, J.F. Smith, M. Stryjczyk, P. Van Duppen, S. Vinals, V. Virtanen, N. Warr, K. Wrzosek-Lipska, M.Zielińska. *Evolution of Octupole Deformation in Radium Nuclei*

from Coulomb Excitation of Radioactive ^{222}Ra and ^{228}Ra Beams. Phys. Rev. Lett.**124**, 042503(2020).

P.A. Butler, L.P. Gaffney, P. Spagnoletti, J. Konki, M. Scheck, J.F. Smith, K. Abrahams, M. Bowry, J. Cederkäll, T. Chupp, G. de Angelis, H. De Witte, P.E. Garrett, A. Goldkuhle, C. Henrich, A. Illana, K. Johnston, D.T. Joss, J.M. Keatings, N.A. Kelly, M. Komorowska, T. Kröll, M. Lozano, B.S.N. Singh, D. O'Donnell, J. Ojala, R.D. Page, L.G. Pedersen, C. Raison, P. Reiter, J.A. Rodriguez, D. Rosiak, S. Rothe, T.M. Shneidman, B. Siebeck, M. Seidlitz, J. Sinclair, M. Stryjczyk, P. Van Duppen, S. Vinals, V. Virtanen, N. Warr, K. Wrzosek-Lipska, M. Zielińska. *Addendum: The observation of vibrating pear-shapes in radon nuclei.* Nat. Commun.**11**, 3560(2020).

P.A. Butler, L.P. Gaffney, P. Spagnoletti, J. Konki, M. Scheck, J.F. Smith, K. Abrahams, M. Bowry, J. Cederkäll, T. Chupp, G. de Angelis, H. De Witte, P.E. Garrett, A. Goldkuhle, C. Henrich, A. Illana, K. Johnston, D.T. Joss, J.M. Keatings, N.A. Kelly, M. Komorowska, T. Kröll, M. Lozano, B.S.N. Singh, D. O'Donnell, J. Ojala, R.D. Page, L.G. Pedersen, C. Raison, P. Reiter, J.A. Rodriguez, D. Rosiak, S. Rothe, T.M. Shneidman, B. Siebeck, M. Seidlitz, J. Sinclair, M. Stryjczyk, P. Van Duppen, S. Vinals, V. Virtanen, N. Warr, K. Wrzosek-Lipska, M. Zielińska. *Publisher Correction: The observation of vibrating pear-shapes in radon nuclei (Nature Communications, (2019), 10, 1, (2473), 10.1038/s41467-019-10494-5).* Nat. Commun.**11**, 5185(2020).

B. Cederwall, X. Liu, O. Aktas, A. Ertoprak, W. Zhang, C. Qi, E. Clement, G. de France, D. Ralet, A. Gadea, A. Goasduff, G. Jaworski, I. Kuti, B. M. Nyako, J. Nyberg, M. Palacz, R. Wadsworth, J.J. Valiente-Dobon, H. Al-Azri, A. Atac Nyberg, T. Back, G. de Angelis, M. Doncel, J. Dudouet, A. Gottardo, M. Jurado, J. Ljungvall, D. Mengoni, D.R. Napoli, C.M. Petrache, D. Sohler, J. Timar, D. Barrientos, P. Bednarczyk, G. Benzoni, B. Birkenbach, A.J. Boston, H.C. Boston, I. Burrows, L. Charles, M. Ciemała, F.C.L. Crespi, D.M. Cullen, P. Desesquelles, C. Domingo-Pardo, J. Eberth, N. Erduran, S. Erturk, V. Gonzalez, J. Goupil, H. Hess, T. Huyuk, A. Jungclaus, W. Korten, A. Lemasson, S. Leoni, A. Maj, R. Menegazzo, B. Million, R.M. Perez-Vidal, Zs. Podolyak, A. Pullia, F. Recchia, P. Reiter, F. Saillant, M. D. Salsac, E. Sanchis, J. Simpson, O. Stezowski, Ch. Theisen, M. Zielińska. *Isospin Properties of Nuclear Pair Correlations from the Level Structure of the Self-Conjugate Nucleus ^{88}Ru.* Phys. Rev. Lett.**124**, 062501(2020).

M. Ciemała, S. Ziliani, F.C.L. Crespi, S. Leoni, B. Fornal, A. Maj, P. Bednarczyk, G. Benzoni, A. Bracco, C. Boiano , S. Bottoni, S. Brambilla, M. Bast, M. Beckers, T. Braunroth, F. Camera, N. Cieplicka-Oryńczak, E. Clement, S. Coelli, O. Dorvaux, S. Erturk, G. de France, C. Fransen, A. Goldkuhle, J. Grębosz, M.N. Harakeh, L.W. Iskra, B. Jacquot, A. Karpov, M. Kicińska-Habior, Y. Kim, M. Kmiecik, A. Lemasson, S.M. Lenzi, M. Lewitowicz, H. Li, I. Matea, K. Mazurek, C. Michelagnoli, M. Matejska-Minda, B. Million, C. Mueller-Gatermann, V. Nanal, P. Napiorkowski, D.R. Napoli, R. Palit, M. Rejmund, Ch. Schmitt, M. Stanoiu, I. Stefan, E. Vardaci, B. Wasilewska, O. Wieland, M. Zięblíński, M. Zielińska, A. Atac, D. Barrientos, B. Birkenbach, A.J. Boston, B. Cederwall, L. Charles, J. Collado, D.M. Cullen, P. Desesquelles, C. Domingo-Pardo, J. Dudouet, J. Eberth, V. Gonzalez, J. Goupil, L.J. Harkness-Brennan, H. Hess, D.S. Judson, A. Jungclaus, W. Korten, M. Labiche, L. Alexis, R. Menegazzo, D. Mengoni, J. Nyberg, R.M. Perez-Vidal, Zs. Podolyak, A. Pullia, F. Recchia, P. Reiter, F. Saillant,

M.D. Salsac, E. Sanchis, O. Stezowski, C. Theisen, J.J. Valiente-Dobon, J.D. Holt, J. Menendez, A. Schwenk, J. Simonis. *Testing ab initio nuclear structure in neutron-rich nuclei: Lifetime measurements of second 2^+ state in ^{16}C and ^{20}O.* Phys. Rev. C**101**, 021303(2020).

M. Ciemała, S. Ziliani, F. Crespi, S. Leoni, B. Fornal, A. Maj, P. Bednarczyk, G. Benzoni, A. Bracco, C. Boiano, S. Bottoni, S. Brambilla, M. Bast, M. Beckers, T. Braunroth, F. Camera, N. Cieplicka-Oryńczak, E. Clement, O. Dorvaux, S. Erturk, G. de France, C. Fransen, A. Goldkuhle, J. Grębosz, M.N. Harakeh, L.W. Iskra, B. Jacquot, A. Karpov, M. Kicińska-Habior, Y. Kim, M. Kmiecik, A. Lemasson, S.M. Lenzi, M. Lewitowicz, H. Li, I. Matea, K. Mazurek, C. Michelagnoli, M. Matejska-Minda, B. Million, C. Mueller-Gatermann, V. Nanal, P. Napiorkowski, D.R. Napoli, R. Palit, M. Rejmund, Ch. Schmitt, M. Stanoiu, I. Stefan, E. Vardaci, B. Wasilewska, O. Wieland, M. Zielińska, M. Ziębliński and AGATA Collaboration and PARIS Collaboration and VAMOS Collaboration. *Short-range Lifetime Measurements for Deep-inelastic Reaction Products: the ^{19}O Test Case.* Acta Phys. Pol. B **51**, 699(2020).

A.A. Ciemny, W. Dominik, T. Ginter, R. Grzywacz, Z. Janas, M. Kuich, C. Mazzocchi, M. Pfutzner, M. Pomorski, D. Bazin, T. Baumann, A. Bezbakh, B.P. Crider, M. Cwiok, S. Go, G. Kamiński, K. Kolos, A. Korgul, E. Kwan, S. Liddick, K. Miernik, V.S. Paulauskas, J. Pereira, T. Roginski, K. Rykaczewski, C. Sumithtatachchi, Y. Xiao, H. Schatz, P. Sarriguren. *First identification of ^{58}Zn β-delayed proton emission.* Phys. Rev. C **101**,034305(2020).

G. Di Giorgio, F. Consoli, R. de Angelis, P. Andreoli, M. Cipriani, G. Cristofari, A. Bonasera, M. Salvadori, J. Sura. *Development of advanced Thomson spectrometers for nuclear fusion experiments initiated by laser* J. Instrum. **15**, C10013(2020).

P.C.F. Di Stefano, N. Brewer, A.Fijałkowska, Z. Gai, K.C. Goetz, R. Grzywacz, D. Hamm, P. Lechner, Y. Liu, E. Lukosi, M. Mancuso, C. Melcher, J. Ninkovic, F. Petricca, A.C. Rasco, C. Rouleau, K.P. Rykaczewski, P. Squillari, L. Stand, D. Stracener, M. Stukel, M. Wolińska-Cichocka, I. Yavin. *The KDK (potassium decay) experiment.* J. Phys.: Conf. Ser. **1342**, 012062(2020).

J. Diaz-Cortes, J. Benlliure, J.L. Rodriguez-Sanchez, H. Alvarez-Pol, T. Aumann, C.A. Bertulani, B. Blank, E. Casarejos, D. Cortina-Gil, D. Dragosavac, V. Fohr, A. Gargano, M. Gascon, W. Gawlikowicz, A. Heinz, K. Helariutta, A. Kelic-Heil, S. Lukic, F. Montes, D. Perez-Loureiro, L. Pieńkowski, K-H. Schmidt, M. Staniou, K. Subotic, K. Summerer, J. Taieb, A. Trzcińska. *Systematic reduction of the proton-removal cross section in neutron-rich medium-mass nuclei.* Phys. Lett. B **811**, 135962(2020).

A. Ertoprak, C. Qi, B. Cederwall, M. Doncel, U. Jakobsson, B.M. Nyako, G. Jaworski, P. Davies, G. de France, I. Kuti, D.R. Napoli, R. Wadsworth, S.S. Ghugre, R. Raut, B. Akkus, H. Al Azri, A. Algora, G. de Angelis, A. Atac, T. Back, A. Boso, E. Clement, D.M. Debenham, Zs. Dombradi, S. Erturk, A. Gadea, F. Ghazi Moradi, A. Gottardo, T. Huyuk, E. Ideguchi, H. Li, C. Michelagnoli, V. Modamio, J. Nyberg, M. Palacz, C.M. Petrache, F. Recchia, M. Sandzelius, M. Siciliano, D. Sohler, J. Timar, J.J. Valiente-Dobon, Z.G. Xiao. *Lifetimes of core-excited states in semi-magic ^{95}Rh.* Eur. Phys. J. A **56**, 291(2020)

M. Fiedorowicz, I.M. Khan, D. Strzemecki, J. Orzel, M. Welniak-Kaminska, A. Sobiborowicz, M. Wieteska, Z. Rogulski, L. Cheda, W. Wargocka-Matuszewska, K. Kilian, C. Szczylik, A.M. Czarnecka. *Renal carcinoma CD105-/CD44-cells display stem-like properties in vitro and form aggressive tumors in vivo.* Sci. Rep. **10**, 5379(2020).

C. Frosin, S. Barlini, G. Poggi, G. Casini, M. Bini, A.A. Stefanini, S. Valdre, D. Gruyer, M. Ciemała, A. Maj, M. Ziębliński, B. Sowicki, K. Mazurek, N. Cieplicka-Oryńczak, M. Matejska-Minda, E. Bonnet, B. Borderie, R. Bougault, M. Bruno, A. Buccola, A. Camaiani, A. Chibhi, M. Cinausero, M. Cicerchia, J. Duenas, D. Fabris, J. Frankland, F. Gramegna, M. Henri, A. Kordyasz, T. Kozik, N. Le Neindre, I. Lombardo, O. Lopez, G. Mantovani, T. Marchi, A. Olmi, P. Ottanelli, M. Parlog, S. Piantelli, G. Pasquali, S. Upadhyahya, G. Verde, E. Vient. *Energy response and identification efficiency of CsI(Tl) crystals irradiated with energetic protons.* Nucl. Instrum. Methods Phys. Res. A**951**, 163018(2020).

C. Frosin, S. Barlini, G. Poggi, G. Casini, M. Bini, A.A. Stefanini, S. Valdre, D. Gruyer, M. Ciemała, A. Maj, M. Ziebliński, B. Sowicki, K. Mazurek, N. Cieplicka-Oryńczak, M. Matejska-Minda, E. Bonnet, B. Borderie, R. Bougault, M. Bruno, A. Buccola, A. Camaiani, A. Chibhi, M. Cinausero, M. Cicerchia, J. Dues, D. Fabris, J. Frankland, F. Gramegna, M. Henri, A. Kordyasz, N. Le Neindre, I. Lombardo, O. Lopez, G. Mantovani, T. Marchi, A. Olmi, P. Ottanelli, M. Parlog, S. Piantelli, G. Pasquali, S. Upadhyahya, G. Verde, E. Vient. *Energy response and identification efficiency of CsI(Tl) crystals irradiated with energetic protons.* J. Phys.: Conf. Ser. **1561**, 012010(2020).

E.M. Gazeeva, A.A. Bezbakh, V.Z. Goldberg, M.S. Golovkov, B. Zalewski, Z.K. Kurmanaliyev, D.K. Nauruzbayev, A.K. Nurmukhanbetova, A. Serikov. *An Effective Way of Measuring the Excitation Function for (a, n) Reactions at Low Energies.* Bull. Russ. Acad. Sci.: Phys. **84**, 420(2020).

S. Guo, C.M. Petrache, D. Mengoni, Y.X. Liu, Q.B. Chen, Y.H. Qiang, A. Astier, E. Dupont, K.K. Zheng, J.G. Wang, B. Ding, B.F. Lv, M.L. Liu, Y.D. Fang, X.H. Zhou, D. Bazzacco, A. Boso, A. Goasduff, F. Recchia, D. Testov, F. Galtarossa, G. Jaworski, D.R. Napoli, S. Riccetto, M. Siciliano, J.J. Valiente-Dobon, C. Andreoiu, F.H. Garcia, K. Ortner, K. Whitmore, B. Cederwall, E.A. Lawrie, I. Kuti, D. Sohler, T. Marchlewski, J. Srebrny, A. Tucholski. *Pseudospin partner bands in ^{130}Ba.* Phys. Rev. C **102**, 044320(2020).

S. Guo, C.M. Petrache, D. Mengoni, Y.H. Qiang, Y.P. Wang, Y.Y. Wang, J. Meng, Y.K. Wang, S.Q. Zhang, P.W. Zhao, A. Astier, J.G. Wang, H.L. Fan, E. Dupont, B.F. Lv, D. Bazzacco, A. Boso, A. Goasduff, F. Recchia, D. Testov, F. Galtarossa, G. Jaworski, D.R. Napoli, S. Riccetto, M. Siciliano, J.J. Valiente-Dobon, M.L. Liu, G.S. Li, X.H. Zhou, Y.H. Zhang, C. Andreoiu, F.H. Garcia, K. Ortner, K. Whitmore, A. Atac-Nyberg, T. Back, B. Cederwall, E.A. Lawrie, I. Kuti, D. Sohler, T. Marchlewski, J. Srebrny, A. Tucholski. *Evidence for pseudospin-chiral quartet bands in the presence of octupole correlations.* Phys. Lett. B **807**, 135572(2020).

J. Jastrzębski, N. Zandi, J. Choiński, M. Sitarz, A. Stolarz, A. Trzcińska, M. Vagheian. *Investigation of the Production of the Auger Electron Emitter* ^{135}La *Using Medical Cyclotrons.* Acta Phys. Pol. B **51**, 861(2020).

S. Jazrawi, D.T. Doherty, J.M. Allmond, P.H. Regan, R.V.F. Janssens, W. Korten, S. Zhu, M. Zielińska, D. Radford, S. Ansari, K. Auranen, B. Bucher, M.P. Carpenter, W.N. Catford, K. Hadyńska-Klęk, J. Henderson, M. Hendricks, M. Komorowska, F.G. Kondev, T. Lauritsen, J. Li, G. Lotay, P.J. Napiorkowski, E. Padilla-Rodal, R.C. Pardo, B.C. Rasco, W. Reviol, D.G. Sarantites, D. Seweryniak, D. Santiago-Gonzalez, G. Savard, P. Singh, S.M. Stolze, R. Vondrasek, G. Wilson, C.Y. Wu, J. Wu. *A High-Resolution Study of the ^{110}Tc ightarrow ^{110}Ru ightarrow ^{110}Rh ightarrow ^{110}Pd Decay Chain with the GRETINA Array.* J. Phys.: Conf. Ser. **1643**, 012140(2020).

G. Kamiński, B. Zalewski, S.G. Belogurov, A.A. Bezbakh, D. Biare, V. Chudoba, A.S. Fomichev, E.M. Gazeeva, M.S. Golovkov, A.V. Gorshkov, L.V. Grigorenko, D.A. Kostyleva, S.A. Krupko, I.A. Muzalevsky, E.Yu. Nikolskii, Yu.L. Parfenova, P. Plucinski, A.M. Quynh, A. Serikov, S.I. Sidorchuk, R.S. Slepnev, P.G. Sharov, P. Szymkiewicz, A. Swiercz, S.V. Stepantsov, G.M. Ter-Akopian, R. Wolski. *Status of the new fragment separator ACCULINNA-2 and first experiments.* Nucl. Instrum. Methods Phys. Res. B **463**, 504(2020).

N. Keeley, K.W. Kemper, K. Rusek. *Important Influence of Entrance Channel Reorientation Coupling on Proton Stripping.* Eur. Phys. J. A **56**, 263(2020).

N. Keeley, K.W. Kemper, K. Rusek. *Multistep processes in heavy-ion-induced single-nucleon transfer reactions.* Phys. Rev. C **102**, 014617(2020).

A.R.L. Kennington, G. Lotay, D.T. Doherty, D. Seweryniak, C. Andreoiu, K. Auranen, M.P. Carpenter, W.N. Catford, C.M. Deibel, K. Hadyńska-Klęk, S.Hallam, D.E.M. Hoff, T. Huang, R.V.F. Janssens, S. Jazrawi, J. Jose, F.G. Kondev, T. Lauritsen, J. Li, A.M. Rogers, J. Saiz, G. Savard, S. Stolze, G.L. Wilson, S. Zhu. *Search for Nova Presolar Grains: γ-Ray Spectroscopy of ^{34}Ar and its Relevance for the Astrophysical ^{33}Cl(p,γ) Reaction.* Phys. Rev. Lett. **124**, 252702(2020).

K. Krutul, P.J. Napiorkowski, K. Hadyńska-Klęk, K. Wrzosek-Lipska, M. Komorowska, M. Paluch-Ferszt, Z. Szefliński, P. Horodek, A. Olejniczak, V.A. Skuratov. *Radiation Hardness Studies of PIN-diode Detectors Irradiated with Heavy Ions.* Acta Phys. Pol. B Proc. Suppl. **13**, 861(2020).

H.M. Maridi. *Energy Dependence and Surface Contribution of the Nucleon-Nucleus Optical Potential.* Bull. Russ. Acad. Sci.: Phys. **84**, 473(2020).

I. Martel, N. Keeley, K.W. Kemper, K. Rusek. *Multi-neutron transfer in He-8-induced reactions near the Coulomb barrier.* Phys. Rev. C **102**, 034609(2020).

M. Matejska-Minda, P.J. Napiorkowski, R. Kumar, M. Saxena, S. Dutt, A. Agarwal, I. Ahmed, S. Bhattacharya, A. Jhingan, J. Kaur, M. Kicińska-Habior, M. Kumar, S. Kumar, D. Kumar, V. Nanal, R. Palit, N.K. Rai, M. Shuaib, A. Sood, A. Stolarz, T. Trivedi, A.K. Tyagi, R.K. Bhowmik, H.J. Wollersheim. *Revised Lifetime Of The 11/2(-) State in ^{45}Sc via Coulomb Excitation.* Acta Phys. Pol. B **51**, 829(2020).

M. Mazzocco, N. Keeley, A. Boiano, C. Boiano, M.L. Commara, A. Lagni, C. Manea, C. Parascandolo, D. Pierroutsakou, C. Signorini, E. Strano, D. Torresi, H. Yamaguchi, D. Kahl, L. Acosta, D. Meo, J.P. Fernandez-Garcia, T. Glodariu, J. Grębosz, A. Guglielmetti, Y. Hirayama, N. Imai, H. Ishiyama, N. Iwasa, S.C. Jeong, H.M. Jia,

Y.H. Kim, S. Kimura, S. Kubono, G.L. Rana, C.J. Lin, P. Lotti, G. Marquínez-Duran, I. Martel, H. Miyatake, M. Mukai, T. Nakao, M. Nicoletto, A. Pakou, K. Rusek, Y. Sakaguchi, A.M. Sánchez-Benítez, T. Sava, O. Sgouros, V. Soukeras, F. Soramel, E. Stiliaris, L. Stroe, T. Teranishi, N. Toniolo, Y. Wakabayashi, Y.X. Watanabe, L. Yang, Y.Y. Yang, H.Q. Zhang. *Direct processes for the systems ^{7}Be,^{8}B + ^{208}Pb at Coulomb barrier energies.* J. Phys.: Conf. Ser. **1643**, 012096(2020).

S. Yu. Mezhevych, A.T. Rudchik, A.A. Rudchik, K.W. Kemper, K. Rusek, O.A. Ponkratenko, I.E. Koshchy, S.B. Sakuta. *$^{13}C(^{11}B,\ ^{12}C)^{12}B$ Reaction at 45 MeV, ^{12}C + ^{12}B Interaction Versus that of ^{12}C + $^{10,11}B$.* Acta Phys. Pol. B **51**, 1949(2020).

S.Yu. Mezhevych, A.T. Rudchik, K. Rusek, K.W. Kemper, A.A. Rudchik, O.A. Ponkratenko, S.B. Sakuta. *$^{13}C(^{11}B,\ ^{12}C)^{12}B$ Reaction Mechanism at 45 MeV and Interaction of ^{12}C.* Nucl. Phys. At. Energy (Iader. Fiz. Enerh.) **21**, 21(2020).

S.Yu. Mezhevych, A.T. Rudchik, K. Rusek, K.W. Kemper, A.A. Rudchik, O.A. Ponkratenko, S.B. Sakuta. *Mechanisms of 14C(11B,10B)15C reaction at energy 45 MeV for ground and excited states of ^{10}B and ^{15}C nuclei.* Nucl. Phys. At. Energy (Iader. Fiz. Enerh.) **21**, 231(2020).

G. Montagnoli, A.M. Stefanini, C.L. Jiang, G. Colucci, A. Goasduff, D. Brugnara, M. Mazzocco, M. Siciliano, F. Scarlassara, L. Corradi, E. Fioretto, F. Galtarossa, M. Heine, T.V. Patten, S. Szilner, P. Cólović, T. Mijatović, S. Bottoni, G. Jaworski, I. Zanon. *Study of fusion hindrance in the system ^{12}C+^{24}Mg.* J. Phys.: Conf. Ser. **1643**, 012098(2020).

L. Morrison, K. Hadyńska-Klęk, Zs. Podolyak, D.T. Doherty, L.P. Gaffney, L. Kaya, L. Próchniak, J. Samorajczyk-Pyśk, J. Srebrny, T. Berry, A. Boukhari, M. Brunet, R. Canavan, R. Catherall, S. J. Colosimo, J.G. Cubiss, H. De Witte, Ch. Fransen, E. Giannopoulos, H. Hess, T. Kroell, N. Lalovic, B. Marsh, Y. Martinez Palenzuela, P.J. Napiorkowski, G. O'Neill, J. Pakarinen, J.P. Ramos, P. Reiter, J.A. Rodriguez, D. Rosiak, S. Rothe, M. Rudigier, M. Siciliano, J. Snall, P. Spagnoletti, S. Thiel, N. Warr, F. Wenander, R. Zidarova, M. Zielińska. *Quadrupole deformation of ^{130}Xe measured in a Coulomb-excitation experiment.* Phys. Rev. C **102**, 054304(2020).

L. Morrison, K. Hadyńska-Klęk, Z. Podolyák, L.P. Gaffney, L. Kaya, T. Berry, A. Boukhari, M. Brunet, R. Canavan, R. Catherall, S.J. Colosimo, J.G. Cubiss, H.D. Witte, D.T. Doherty, C. Fransen, E. Giannopoulos, H. Grawe, H. Hess, T. Kröll, N. Lalović, B. Marsh, Y. Martinez Palenzuela, G. O'Neill, J. Pakarinen, J.P. Ramos, P. Reiter, J.A. Rodriguez, D. Rosiak, S. Rothe, M. Rudigier, M. Siciliano, E.C. Simpson, P. Spagnoletti, S. Thiel, N. Warr, F. Wenander, R. Zidarova, M. Zielińska. *Dealing with contaminants in Coulomb excitation of radioactive beams.* J. Phys.: Conf. Ser. **1643**, 012146(2020).

D. Muir, L. Próchniak, A. Pastore, J. Dobaczewski. *Structure of Krypton Isotopes using the Generalised Bohr Hamiltonian Method.* J. Phys.: Conf. Ser. **1643**, 012147(2020).

I.A. Muzalevskii, V. Chudoba, S.G. Belogurov, A.A. Bezbakh, D. Biare, A.S. Fomichev, S.A. Krupko, E.M. Gazeeva, M.S. Golovkov, A.V. Gorshkov, L.V. Grigorenko, G. Kamiński, O. Kiselev, D.A. Kostyleva, M.Y. Kozlov, B. Mauyey, I. Mukha, E.Y. Nikolskii, Y.L. Parfenova, W. Piątek, A.M. Quynh, V.N. Schetinin, A. Serikov,

S.I. Sidorchuk, P.G. Sharov, R.S. Slepnev, S.V. Stepantsov, A. Swiercz, P. Szymkiewicz, G.M. Ter-Akopian, R. Wolski, B. Zalewski. *Detection of the Low Energy Recoil ^{3}He in the Reaction $^{2}H(^{8}He,^{3}He)^{7}H$.* Bull. Russ. Acad. Sci.: Phys. **84**, 500(2020).

A. Nannini, M. Rocchini, K. Hadyńska-Klęk, N. Marchini, D.T. Doherty, M. Zielińska, M. Siciliano, A. Illana, M. Saxena, D. Bazzacco, G. Benzoni, F. Camera, M. Chiari, P.R. John, A. Goasduff, M. Komorowska, M. Matejska-Minda, D. Mengoni, P. Napiorkowski, D.R. Napoli, M. Ottanelli, A. Perego, F. Recchia, P. Sona, D. Testov, J.J. Valiente-Dobon. *Coulomb excitation studies at LNL with the SPIDER-GALILEO set-up.* Phys. Scr. **95**, 024005(2020).

J.D. Ovejas, A. Knyazev, I. Martel, O. Tengblad, M.J.G. Borge, J. Cederkall, N. Keeley, K. Rusek, C. Garcia-Ramos, L.A. Acosta, A.A. Arokiaraj, M. Babo, T. Cap, N. Ceylan, G. de Angelis, A. Di Pietro, J.P. Fernandez, P. Figuera, L. Fraile, H. Fynbo, D. Galaviz, J.H. Jensen, B. Jonson, R. Kotak, T. Kurtukian, M. Madurga, G. Marquinez-Duran, M. Munch, A.K. Orduz, R. Honorio, A. Pakou, T. Perez, L. Peralta, A. Perea, R. Raabe, M. Renaud, K. Riisager, A.M. Sanchez-Benitez, J. Sanchez-Segovia, O. Sgouros, V. Soukeras, P. Teubig, S. Vinals, M. Wolińska-Cichocka, R. Wolski, J. Yang. *Halo Effects in the Low-energy Scattering of ^{15}C with Heavy Targets.* Acta Phys. Pol. B **51**, 731(2020).

J.D. Ovejas, A. Knyazev, I. Martel, O. Tengblad, M.J.G. Borge, J. Cederkall, N. Keeley, K. Rusek, C. Garciá-Ramos, T. Pérez, L.A. Acosta, A.A. Arokiaraj, M. Babo, T. Cap, N. Ceylan, G.D. Angelis, A.D. Pietro, J.P. Fernández, P. Figuera, L. Fraile, H. Fynbo, D. Galaviz, J.H. Jensen, B. Jonson, R. Kotak, T. Kurtukian, M. Madurga, G. Marquínez-Durán, M. Munch, A.K. Orduz, R. Honório, A. Pakou, L. Peralta, A. Perea, R. Raabe, M. Renaud, K. Riisager, A.M. Sánchez-Benítez, J. Sánchez-Segovia, O. Sgouros, V. Soukeras, P. Teubig, S. Vinals, M. Wolińska-Cichocka, R. Wolski, J. Yang. *Study of the scattering of ^{15}C at energies around the Coulomb barrier.* J. Phys.: Conf. Ser. **1643**, 012095(2020).

A. Pagano, E. De Filippo, E. Geraci, E.V. Pagano, P. Russotto, K. Siwek-Wilczyńska, L. Acosta, L. Auditore, T. Cap, G. Cardella, M.B. Chatterjee, M. Colonna, B. Gnoffo, F. Favela, G. Lanzalone, C. Maiolino, N.S. Martorana, M. Papa, S. Pirrone, G. Politi, E. Piasecki, L. Quattrocchi, F. Rizzo, A. Trifiro, M. Trimarchi. *Nuclear neck-density determination at Fermi energy with CHIMERA detector.* Eur. Phys. J. A **56**, 102(2020).

A. Pakou, L. Acosta, P.D. O'Malley, S. Aguilar, E.F. Aguilera, M. Baines, D. Bardayan, F.D. Becchetti, Ch. Boomershine, M. Brodeur, F. Cappuzzello, S. Carmichael, L. Caves, E. Chavez, C. Flores-Vazquez, A. Gula, J.J. Kolata, B. Liu, D.J. Marin-Lambarri, F.F. Morales, K. Rusek, A.M. Sanchez-Benitez, O. Sgouros, V.R. Sharma, V. Soukeras, G. Souliotis. *Dominance of direct reaction channels at deep sub-barrier energies for weakly bound nuclei on heavy targets: The case ^{8}B + ^{208}Pb.* Phys. Rev. C **102**, 031601(2020).

A. Pakou, O. Sgouros, V. Soukeras, F. Cappuzzello, L. Acosta, C. Agodi, A. Boiano, S. Calabrese, D. Carbone, M. Cavallaro, N.N. Deshmukh, A. Foti, A. Hacisalihoglu, N. Keeley, M. La Commara, I. Martel, M. Mazzocco, A. Muoio, C. Parascandolo, D. Pierroutsakou, K. Rusek, A.M. Sanchez-Benitez, G. Santagati, G. Souliotis, A. Spatafora, E. Strano, D. Torresi, A. Trzcińska. *^{9}Be + p breakup at 5.67A MeV in a full kinematics approach.* Phys. Rev. C **101**, 024602(2020).

A. Pakou, O. Sgouros, V. Soukeras, F. Cappuzzello, L. Acosta, C. Agodi, A. Boiano, S. Calabrese, D. Carbone, M. Cavallaro, N.N. Deshmukh, A. Foti, A. Hacisalihoglou, N. Keeley, M.L. Commara, I. Martel, M. Mazzocco, A. Muoio, C. Parascandolo, D. Pierroutsakou, K. Rusek, A.M. Sanchez-Benítez, G. Santagati, G. Souliotis, A. Spatafora, E. Strano, D. Torresi, A. Trzcińska. *A clear signature of the breakup modes for ^{9}Be on a proton target at 5.6 MeV/nucleon.* J. Phys.: Conf. Ser. **1643**, 012102(2020).

M. Paluch-Ferszt, B. Kozłowska, M. Dybek *Comparison of dose distributions in target areas and organs at risk in conformal and VMAT techniques and dose verifications with the use of thermoluminescence dosimetry.* Nukleonika **65**, 217(2020).

C.M. Petrache, B. . Lv, Q.B. Chen, J. Meng, A. Astier, E. Dupont, K.K. Zheng, P.T. Greenlees, H. Badran, T. Calverley, D.M. Cox, T. Grahn, J. Hilton, R. Julin, S. Juutinen, J. Konki, J. Pakarinen, P. Papadakis, J. Partanen, P. Rahkila, P. Ruotsalainen, M. Sandzelius, J. Saren, C. Scholey, J. Sorri, S. Stolze, J. Uusitalo, B. Cederwall, A. Ertoprak, H. Liu, S. Guo, J.G. Wang, X.H. Zhou, I. Kuti, J. Timar, A. Tucholski, J. Srebrny, C. Andreoiu. *Multiple chiral bands in ^{137}Nd.* Eur. Phys. J. A **56**, 208(2020).

C.M. Petrache, N. Minkov, T. Nakatsukasa, B.F. Lv, A. Astier, E. Dupont, K.K. Zheng, P.T. Greenlees, H. Badran, T. Calverley, D.M. Cox, T. Grahn, J. Hilton, R. Julin, S. Juutinen, J. Konki, J. Pakarinen, P. Papadakis, J. Partanen, P. Rahkila, P. Ruotsalainen, M. Sandzelius, J. Saren, C. Scholey, J. Sorri, S. Stolze, J. Uusitalo, B. Cederwall, A. Ertoprak, H. Liu, S. Guo, M.L. Liu, J.G. Wang, X.H. Zhou, I. Kuti, J. Timar, A. Tucholski, J. Srebrny, C. Andreoiu. *Signatures of enhanced octupole correlations at high spin in ^{136}Nd.* Phys. Rev. C **102**, 014311(2020).

S. Piantelli, G. Casini, A. Ono, G. Poggi, G. Pastore, S. Barlini, A. Boiano, E. Bonnet, B. Borderie, R. Bougault, M. Bruno, A. Buccola, A. Camaiani, A. Chbihi, M. Cicerchia, M. Cinausero, M. Agostino, M. Degerlier, J.A. Duenas, Q. Fable, D. Fabris, J.D. Frankland, C. Frosin, F. Gramegna, D. Gruyer, M. Henri, A. Kordyasz, T. Kozik, N. Le Neindre, I. Lombardo, O. Lopez, G. Mantovani, T. Marchi, L. Morelli, A. Olmi, P. Ottanelli, M. Parlog, G. Pasquali, A.A. Stefanini, G. Tortone, S. Upadhyaya, S. Valdre, G. Verde, E. Vient, M. Vigilante, R. Alba, C. Maiolino. *Dynamical fission of the quasiprojectile and isospin equilibration for the system ^{80}Kr+^{48}Ca at 35 MeV/nucleon.* Phys. Rev. C **101**, 034613(2020).

L.Próchniak *On collective octupole degrees of freedom – next pieces of the formal background.* Acta Phys. Pol. B Proc. Suppl **13**, 481(2020).

M. Rocchini, K. Hadyńska-Klęk, A. Nannini, J.J. Valiente-Dobon, A. Goasduff, D. Testov, D. Mengoni, P.R. John, M. Siciliano, B. Melon, P. Sona, M. Ottanelli, A. Perego, M. Chiari, M. Zielińska, D. Bazzacco, G. Benzoni, S. Bettarini, M. Brianzi, F. Camera, P. Cocconi, C. Czelusniak, D.T. Doherty, M. Komorowska, N. Marchini, M. Matejska-Minda, P.J. Napiorkowski, E. Pasquali, L. Ramina, M. Rampazzo, F. Recchia, D. Rosso, L. Sottili, A. Tredici. *SPIDER: A Silicon PIe DEtectoR for low-energy Coulomb-excitation measurements.* Nucl. Instrum. Methods Phys. Res. A **971**, 164030(2020).

A.T. Rudchik, A.A. Rudchik, O.O. Chepurnov, K. Rusek, K.W. Kemper, I.E. Koshchy, S.Yu. Mezhevych, Val.M. Pirnak, A. Ponkratenko, A. Stolarz, R. Siudak, A.P. Ilyin,

V.B. Mishchenko, Yu.M. Stepanenko, V.V. Uleshchenko, Yu.O. Shyrma. *Elastic and inelastic scattering of ^{10}B ions by ^{6}Li nuclei at energy 51 MeV.* Nucl. Phys. At. Energy (Iader. Fiz. Enerh.) **21**, 29(2020).

A.T. Rudchik, A.A. Rudchik, O.E. Kutsyk, K. Rusek, K.W. Kemper, E. Piasecki, A. Stolarz, A. Trzcińska, V.M. Pirnak, O.A. Ponkratenko, I. Strojek, I.E. Koshchiy, R. Siudak, S.B. Sakuta, V.A. Plujko, A.P. Ilyin, Yu.M. Stepanenko, V.V. Uleshchenko, Yu.O. Shyrma, V.V. Kheilo. *$^{12}C(^{15}N, ^{14}C)^{13}N$ reaction at 81 MeV. Competition between one and two particle transfers.* Nucl. Phys. At. Energy (Iader. Fiz. Enerh.) **21**, 295(2020).

P. Russotto, E. De Filippo, E.V. Pagano, L. Acosta, L. Auditore, T. Cap, G. Cardella, S. De Luca, E. Geraci, B. Gnoffo, G. Lanzalone, I. Lombardo, C. Maiolino, N.S. Martorana, T. Minniti, S. Norella, A. Pagano, M. Papa, E. Piasecki, S. Pirrone, G. Politi, F. Porto, L. Quattrocchi, F. Rizzo, E. Rosato, K. Siwek-Wilczyńska, A. Trifiro, M. Trimarchi, Verde, J. Wilczyński. *Dynamical versus statistical production of Intermediate Mass Fragments at Fermi Energies.* Eur. Phys. J. A **56**, 12(2020).

A. Sentkowska, S. Piwowarczyk, K. Pyrzyńska. *Simultaneous determination of vitamin B6 and catechins in dietary supplements by ZIC-HILIC chromatography and their antioxidant interactions.* Eur. Food Res. Technol. **246**, 1609(2020).

A. Sentkowska, K. Pyrzyńska. *Determination of selenium species in beetroot juices.* Heliyon **6**, e04194(2020).

A. Sentkowska and K. Pyrzyńska *Comparative Study of Chlorogenic Acid Extraction from Different Plants.* Int. J. of Res. in Engineering and Science (IJRES) **8**, 13(2020).

O. Sgouros, V. Soukeras, A. Pakou, F. Cappuzzello, L. Acosta, C. Agodi, N. Alamanos, S. Calabrese, D. Carbone, M. Cavallaro, A. Foti, N. Keeley, I. Martel, K. Rusek, D. Torresi. *Study of the $^{6}\mathrm{Li} + p$ and $^{7}\mathrm{Li} + p$ Systems in the Continuum Discretized Coupled Channels Approach.* Acta Phys. Pol. B **51**, 737(2020).

M. Siciliano, I. Zanon, A. Goasduff, P.R. John, T.R. Rodriguez, S. Peru, I. Deloncle, J. Libert, M. Zielińska, D. Ashad, D. Bazzacco, G. Benzoni, B. Birkenbach, A. Boso, T. Braunroth, M. Cicerchia, N. Cieplicka-Oryńczak, G. Colucci, F. Davide, G. de Angelis, B. de Canditiis, A. Gadea, L.P. Gaffney, F. Galtarossa, A. Gozzelino, K. Hadyńska-Klęk, G. Jaworski, P. Koseoglou, S.M. Lenzi, B. Melon, R. Menegazzo, D. Mengoni, A. Nannini, D.R. Napoli, J. Pakarinen, D. Quero, P. Rath, F. Recchia, M. Rocchini, D. Testov, J.J. Valiente-Dobon, A. Vogt, J. Wiederhold, W. Witt. *Shape coexistence in neutron-deficient ^{188}Hg investigated via lifetime measurements.* Phys. Rev. C **102**, 014318(2020).

M. Sitarz, J.P. Cussonneau, T. Matulewicz, F. Haddad. *Radionuclide candidates for beta plus gamma coincidence PET: An overview.* Appl. Radiat. Isot. **155**, UNSP 108898(2020).

A. Slabuszewska-Jozwiak, M. Wlodarczyk, K. Kilian, Z. Rogulski, M. Ciebiera, J. Szymańska-Majchrzak, K. Zareba, J.K Szymański, D. Raczkiewicz, G. Nowicka, G. Jakiel. *Does the Caesarean Section Impact on 11β HSD2 and Fetal Cortisol?.* Int. J. Environ. Res. Public Health **17**, 5566(2020).

A.M. Stefanini, G. Montagnoli, M.D. Fabbro, G. Colucci, P. Čolović, L. Corradi, E. Fioretto, F. Galtarossa, A. Goasduff, J. Grębosz, M. Heine, G. Jaworski, M. Mazzocco, T. Mijatovic, S. Szilner, M. Bajzek, D. Brugnara, M. Siciliano, I. Zanon. *Fusion Hindrance and Pauli Blocking in ^{58}Ni + ^{64}Ni.* J. Phys.: Conf. Ser. **1643**, 012105(2020).

M. Stryjczyk, B. Andel, A.N. Andreyev, J. Cubiss, J. Pakarinen, K. Rezynkina, P. Van Duppen, S. Antalic, T. Berry, M.J.G. Borge, C. Clisu, D.M. Cox, H. De Witte, L.M. Fraile, H.O.U. Fynbo, L.P. Gaffney, L.J. Harkness-Brennan, M. Huyse, A. Illana, D.S. Judson, J. Konki, J. Kurcewicz, I. Lazarus, R. Lica, M. Madurga, N. Marginean, R. Marginean, C. Mihai, P. Mosat, E. Nacher, A. Negret, J. Ojala, J.D. Ovejas, R.D. Page, P. Papadakis, S. Pascu, A. Perea, Zs. Podolyak, V. Pucknell, E. Rapisarda, F. Rotaru, C. Sotty, O. Tengblad, V. Vedia, S. Vinals, R. Wadsworth, N. Warr, K. Wrzosek-Lipska and IDS Collaboration. *Decay studies of the long-lived states in ^{186}Tl.* Phys. Rev. C **102**, 024322(2020).

A. Trzcińska, E. Piasecki, G. Cardella, D. Dell'Aquila, E. De Filippo, S. De Luca, B. Gnoffo, M. Kowalczyk, G. Lanzalone, I. Lombardo, C. Maiolino, N.S. Martorana, A. Pagano, V.E. Pagano, S. Pirrone, G. Politi, L. Quattrocchi, F. Rizzo, P. Russotto, A. Trifiro, M. Trimarchi, M. Vigilante. *Barrier distributions of the ^{24}Mg + ^{90}Zr,^{92}Zr systems: Influence of energy dissipation.* Phys. Rev. C **102**, 034617(2020).

V.V. Uleshchenko, K. Kemper, I.E. Koshchi, S.M. Lukyanov, O.A. Ponkratenko, A.A. Rudchik, A.T. Rudchik, Yu.M. Stepanenko, Yu.O. Shyrma. *Energy dependence of the elastic 1 divided by 28 MeV deuteron scattering on beryllium isotopes.* Nucl. Phys. At. Energy (Iader. Fiz. Enerh.) **21**, 137(2020).

S. Valdre, S. Barlini, M. Bini, A. Boiano, E. Bonnet, B. Borderie, R. Bougault, M. Bruno, A. Buccola, A. Camaiani, G. Casini, A. Chbihi, C. Ciampi, M. Cicerchia, M. Cinasusero, J.A. Duenas, D. Fabris, J.D. Frankland, C. Frosin, E. Galichet, F. Gramegna, D. Gruyer, M. Henri, A. Kordyasz, T. Kozik, J. Lemarie, N. le Neindre, I. Lombardo, O. Lopez, G. Mantovani, T. Marchi, L. Morelli, S. Nam, A. Olmi, A. Ordine, P. Ottanelli, M. Parlog, G. Pasquali, G. Pastore, S. Piantelli, G. Poggi, J. Quicray, A.A. Stefanini, G. Tortone, S. Upadhyaya, G. Verde, E. Vient, M. Vigilante and FAZIA Collaboration. *Charged particle identification using time of flight with FAZIA.* Nuovo Cimento C **43**, 10(2020).

B. Wasilewska, M. Kmiecik, M. Ciemała, A. Maj, J. Lukasik, P. Pawlowski, B. Sowicki, M. Zięblíński, J. Grębosz, F.C.L. Crespi, P. Bednarczyk, A. Bracco, S. Brambilla, I. Ciepal, N. Cieplicka-Oryńczak, B. Fornal, K. Gugula, M.N. Harakeh, M. Jezabek, M. Kicińska-Habior, M. Krzysiek, P. Kulessa, M. Lewitowicz, M. Matejska-Minda, K. Mazurek, P. Napiorkowski, Ch. Schmitt, Y. Sobolev. *Measurement of the γ Decay from the Energy Region of the Pygmy Dipole States Excited in the $^{208}Pb(p,p'\gamma)$ Reaction at CCB.* Acta Phys. Pol. B **51**, 677(2020).

K. Wrzosek-Lipska, L. Próchniak, P.E. Garrett, S.W. Yates, J.L. Wood, P.J. Napiorkowski, T. Abraham, J.M. Allmond, F.L. Bello Garrote, H. Bidaman, V. Bildstein, C. Burbadge, M. Chiari, A. Diaz Varela, D.T. Doherty, S. Dutt, K. Hadyńska-Klęk, M. Hlebowicz, J. Iwanicki, B. Jigmeddorj, M. Kisieliński, M. Komorowska, M. Kowalczyk, R. Kumar, T. Marchlewski, M. Matejska-Minda, B. Olaizola, F. Oleszczuk, M. Palacz, E. Pasquali,

E.E. Peters, M. Rocchini, E. Sahin, M. Saxena, J. Srebrny, A. Tucholski. *Quadrupole Deformation of ^{110}Cd Studied with Coulomb Excitation.* Acta Phys. Pol. B **51**, 789(2020).

C.J. Zachary, N.T. Brewer, J.C. Batchelder, E. Wang, J.H. Hamilton, J.M. Eldridge, B.M. Musangu, V.A. Ramayya, C.J. Gross, K.P. Rykaczewski, R. Grzywacz, A.C. Dai, E.R. Xu, Y.X. Liu, Y. Sun, M. Madurga, D. Miller, D.W. Stracener, C. Jost, E.F. Zganjar, J.A. Winger, M. Karny, V.S. Paulauskas, S.H. Liu, M. Wolińska-Cichocka, S.W. Padgett, A.J. Mendez, K. Miernik, A. Fijałkowska, V.S. Ilyushkin. *Identification of new transitions and levels in ^{Gd}from β-decay studies.* hys. Rev. C **101**, 054312(2020).

C.J. Zachary, E. Wang, N.T. Brewer, J.C. Batchelder, J.H. Hamilton, J.M. Eldridge, B.M. Musangu, V.A. Ramayya, C.J. Gross, K.P. Rykaczewski, R. Grzywacz, A.C. Dai, F.R. Xu, M. Madurga, D. Miller, D.W. Stracener, C. Jost, E.F. Zganjar, J.A. Winger, M. Karny, V.S. Paulauskas, S.H. Liu, M. Wolińska-Cichocka, S.W. Padgett, A.J. Mendez, K. Miernik, A. Fijałkowska, V.S. Ilyushkin. *New transitions and levels for ^{163}Tb obtained from β-decay studies.* Phys. Rev. C **102**, 044302(2020).

S. Ziliani, M. Ciemała, F.C.L. Crespi, S. Leoni, B. Fornal, A. Maj, P. Bednarczyk, G. Benzoni, A. Bracco, C. Boiano, S. Bottoni, S. Brambilla, M. Bast, M. Beckers, T. Braunroth, F. Camera, N. Cieplicka-Oryńczak, E. Clément, S. Coelli, O. Dorvaux, S. Erturk, G. de France, C. Fransen, A. Goldkuhle, J. Grębosz, M.N. Harakeh, Ł.W. Iskra, B. Jacquot, A. Karpov, M. Kicińska-Habior, Y. Kim, M. Kmiecik, A. Lemasson, S.M. Lenzi, M. Lewitowicz, H. Li, I. Matea, K. Mazurek, C. Michelagnoli, M. Matejska-Minda, B. Million, C. Müller-Gatermann, V. Nanal, P. Napiorkowski, D.R. Napoli, R. Palit, M. Rejmund, Ch. Schmitt, M. Stanoiu, I. Stefan, E. Vardaci, B. Wasilewska, O. Wieland, M. Zięblíński, M. Zielińska and AGATA Collaboration and PARIS Collaboration and VAMOS Collaboration. *Spectroscopy of Neutron-rich Nitrogen Isotopes with AGATA+PARIS+VAMOS.* Acta Phys. Pol. B **51**, 709(2020).

E.4 Seminars

E.4.1 Seminars co-organised by HIL

Nuclear Physics Seminars

Seminars organised jointly by the divisions of Nuclear Physics and Nuclear Structure Theory of the Faculty of Physics, University of Warsaw and the Heavy Ion Laboratory, University of Warsaw

V. Guadilla — Institute of Experimental Physics, University of Warsaw, Warszawa, Poland — 16 January 2020
Beta-decay measurements with Total Absorption gamma-ray Spectroscopy at IGISOL

A. Syntfeld-Każuch — National Centre for Nuclear Research — 23 January 2020
Udział wolnych składowych scyntylacji w mierzonej energetycznej zdolności rozdzielczej detektora
The influence of the slow scintillation component on detector energy resolution.

G. Wlazłowski — Faculty of Physics, Warsaw University of Technology, Warszawa, Poland — 27 February 2020
Nuclear density functional theory as a source of microscopic input for pulsar glitch models

T. Cap — National Centre for Nuclear Research — 5 March 2020
Reakcje wielonukleonowego transferu i fragmentacji w zderzeniach niefuzyjnych układów jądrowych
Multi-nucleon transfer and fragmentation reactions in collisions of non-fusing nuclear systems

N. Keeley — National Centre for Nuclear Research — 16 April 2020
The Curious Incident of the Dog in the Night-Time: The Enigma of ^{8}B

A. Goasduff — Faculty of Physics, University of Warsaw, Warszawa, Poland — 23 April 2020
Gamma Spectroscopy at LNL, present and future

A. Gawlik — Faculty of Physics and Applied Computer Science, University of Lodz, Łódź, Poland — 30 April 2020
Radiative neutron capture cross section measurement of germanium isotopes at the n_TOF CERN facility and its relevance for stellar nucleosynthesis

A. Kalinowski — Institute of Experimental Physics, University of Warsaw, Warszawa, Poland — 7 May 2020
Uczenie maszynowe w fizyce subatomowej
Machine learning in subatomic physics

P. Magierski — Faculty of Physics, Warsaw University of Technology, Warszawa, Poland — 14 May 2020

Reakcje nadciekłych jąder atomowych w świetle teorii funkcjonału gęstości

Reactions of superfluid atomic nuclei in the light of the density functional theory

A. Maj — The H. Niewodniczański Institute of Nuclear Physics PAN, Kraków, Poland — 21 May 2020

PARIS calorimeter - idea, status and first experiments

K. Pomorski — Inst. of Physics, Maria Curie-Sklodowska Univ., Lublin, Poland — 28 May 2020

Shape isomers and possible shape coexistence in Pt, Hg and Pb isotopes with $N \leq 126$

J. Sharpey-Schafer — iThemba Lab. for Accelerator Based Sciences, Faure, South Africa — 4 June 2020

Nuclear Collective Excitations and Realistic Models

G. Colucci — Heavy Ion Laboratory, University of Warsaw, Warszawa, Poland — 15 October 2020

A fast ionization chamber for the detection of fusion-evaporation residues produced by the exotic beams of SPES: design, tests and first experiment

E. Masha — INFN. Sezione di Milano, Milano, Italy — 22 October 2020

Underground nuclear astrophysics and the study of the $^{22}Ne(\alpha;\gamma)^{26}Mg$ and $^{20}Ne\ (p;\gamma)^{21}Na$ reaction at LUNA

S. Puławski — Institute of Physics, University of Silesia, Katowice, Poland — 5 November 2020

Badanie relatywistycznych zderzeń hadronów i jonów przy wykorzystaniu detektora NA61/SHINE działającego przy akceleratorze SPS w CERN

Study of relativistic collisions of hadrons and ions using the NA61/SHINE detector operating at the SPS accelerator at CERN

A. Trzcińska — Heavy Ion Laboratory, University of Warsaw, Warszawa, Poland — 19 November 2020

Rozkład wysokości barier na fuzję w systemach $^{24}Mg + {}^{90,92}Zr$ – wpływ dyssypacji

Fusion barrier distributions in $^{24}Mg + {}^{90,92}Zr$ systems – the impact of dissipation

C. Petrache — Institute de Physique Nucléaire, CNRS/IN2P3, Université Paris-Sud, Université Paris-Saclay, Orsay, France — 26 November 2020

Chirality and wobbling in nuclei: new achievements and perspectives

S. Go — Kyushu University, Fukuoka, Japan 3 December 2020
Mapping of fragmented $\nu f5/2 \rightarrow \pi 7/2$ transitions in neutron-rich Co isotopes

N. Piotrowska, K. Tudyka — Silesian University of Technology, Gliwice, Poland 10 December 2020
Izotopowe skale czasu dla zdarzeń z historii Ziemi i człowieka
Isotopic timescales for events in Earth and human history

K. Miernik — Faculty of Physics, University of Warsaw, Warszawa, Poland 17 December 2020
Narzędzia do analizy dużych zestawów danych
Tools for analyzing large data sets

E.4.2 External seminars given by the HIL staff

P.J. Napiorkowski 16–17 January 2020
Nuclear deformation in excited states
COPIGAL Mini-Workshop, Polish Academy of Sciences. Scientific Center in Paris, France

P.J. Napiorkowski 10–14 February 2020
Progress report on experimental projects at HIL
ENSAR2 Town Meeting 2, Athens, Greece

A. Sentkowska 5-6 March 2020
Potencjał chromatografii oddziaływań hydrofilowych w analizie specjacyjnej selenu
Potential of hydrophilic interaction chromatography in the speciation analysis of selenium
XIII Konferencja Analiza Specjacyjna – Możliwości i Kierunku Rozwoju, Poznań, Poland

K. Wrzosek-Lipska 10 August 2020
Shape coexistence studied with Coulomb excitation in the $N \sim 104$ and $N \sim 50$ regions
UK Lockdown & Distancing Nuclear Seminars

E.4.3 Poster presentations

M. Pęgier, K. Kilian, K. Pyrzyńska 30 June – 1 July 2020
Zastosowanie techniki ekstrakcji do fazy stałej do wydzielania i zatężania jonów skandu
Application of solid phase extraction for separation and preconcentration of scandium ions
Wirtualna Konferencja Naukowa Kampusu Ochota

J. Choiński, K. Kilian, P.J. Napiorkowski, M. Pęgier, A. Sentkowska, A. Stolarz, A. Trzcińska 16–18 October 2020
Ośrodek produkcji i badań radiofarmaceutyków w Środowiskowym Laboratorium Ciężkich Jonów – stan aktualny i perspektywy
Radiopharmaceutical Production and Research Center at the Heavy Ion Laboratory University of Warsaw

46th Extraordinary Congress of Polish Physicists

G. Jaworski 16–18 October 2020
Filtr krotności neutronów NEDA
The Neutron multiplicity filter NEDA
46th Extraordinary Congress of Polish Physicists

P.J. Napiorkowski, K. Hadyńska-Klęk, M. Komorowska, L. Próchniak,
K. Wrzosek-Lipska, J. Srebrny, M. Kicińska-Habior 16–18 October 2020
Badania struktury jąder atomowych prowadzone przez Warszawską Grupę Wzbudzeń Kulombowskich
Nuclear structure studies performed by the Warsaw Coulomb Excitation Group
46th Extraordinary Congress of Polish Physicists

M. Palacz, J. Samorajczyk-Pyśk, J. Kownacki, J. Srebrny
on behalf of the EAGLE Collaboration 16–18 October 2020
EAGLE — wielodetektorowy spektrometr promieniowania gamma w ŚLCJ UW
EAGLE — a multidetector γ-ray spectrometer at HIL UW
46th Extraordinary Congress of Polish Physicists

M. Paluch-Ferszt, U. Kazimierczak, Z. Szefliński 16–18 October 2020
Dawka lokalna i jej rola w biologicznej odpowiedzi linii komórkowej ssaków in vitro
Local dose and its role in the biological response of mammalian cell lines in vitro
46th Extraordinary Congress of Polish Physicists

K. Rusek, J. Choiński, P.J. Napiorkowski 16–18 October 2020
Środowiskowe Laboratorium Ciężkich Jonów
The Heavy Ion Laboratory
46th Extraordinary Congress of Polish Physicists

E.4.4 Lectures for students and student laboratories

Z. Szefliński summer semester of the academic year 2019/2020, 30 hours
Techniki jądrowe w diagnostyce i terapii medycznej
Nuclear Techniques in Medical Diagnostics and Therapy
Faculty of Physics, University of Warsaw, Warszawa, Poland

K. Kilian summer semester of the academic year 2019/2020, 15 hours
Radiofarmaceutyki synteza, wytwarzanie i zastosowania
Radiopharmaceutical synthesis, production and applications
Faculty of Chemistry, University of Warsaw, Warszawa, Poland

K. Kilian summer semester of the academic year 2019/2020, 60 hours
Pracownia radiofarmaceutyków
Laboratory of Radiopharmaceuticals
Faculty of Physics, University of Warsaw, Warszawa, Poland

K. Kilian winter semester of the academic year 2020/2021, 30 hours
Metody izotopowe i chemia radiofarmaceutyków
Radiochemistry and radiopharmaceuticals
Faculty of Physics, University of Warsaw, Warszawa, Poland

E.4.5 Science popularization lectures

A. Sentkowska „Noc Bibliotek - zdrowy klimat na czytanie" – online lecture

Czy więcej znaczy lepiej? (2x60 min)
Does more means better?

E.5 Honours and Awards

The Rector of the University of Warsaw awards

In 2020 the following employees of the Heavy Ion Laboratory received the Rector of the University of Warsaw award:
Eliza Balcerowska, Tomasz Bracha, Marek Budziszewski, Jarosław Choiński, Przemysław Gmaj, Wiesław Kalisiewicz, Marian Kopka, Wojciech Kozaczka, Jolanta Matuszczak, Paweł Napiorkowski, Łukasz Standyło, Anna Stolarz, Lidia Strzelczyk, Lech Szeląg, Łukasz Świątek, Roman Tańczyk, Agnieszka Trzcińska, Marzena Wolińska-Cichocka.

E.6 Laboratory staff

Director: Krzysztof Rusek
Deputy director: Paweł Napiorkowski
Director's Proxy for technical issues: Jarosław Choiński
Financial executive: Eliza Balcerowska

Senior scientists:

Krzysztof Kilian, Andrzej Kordyasz[a], Marcin Palacz, Ernest Piasecki[a], Leszek Próchniak, Krzysztof Rusek, Anna Stolarz, Zygmunt Szefliński[a]

Scientific staff and engineers:

Tomasz Abraham, Andrzej Bednarek, Jarosław Choiński, Lucia De Dominicis[b], Przemysław Gmaj, Katarzyna Hadyńska-Klęk[c], Grzegorz Jaworski, Grzegorz Kamiński[d], Urszula Kaźmierczak, Marian Kopka, Michał Kowalczyk, Katarzyna Krutule[e], Ireneusz Mazur, Jan Miszczak, Paweł Napiorkowski, Wojciech Okliński[a], Monika Paluch-Ferszt, Mateusz Pęgier, Wojciech Piątek[d], Bogdan Radomyski, Olga Saeed Mohamed Nassar, Justyna Samorajczyk-Pyśk, Aleksandra Sentkowska, Julian Srebrny[a], Łukasz Standyło, Roman Tańczyk, Agnieszka Trzcińska, Andrzej Tucholski, Marzena Wolińska-Cichocka, Katarzyna Wrzosek-Lipska, Bogumił Zalewski[d],

Doctoral candidates:

Mateusz Filipek[b], Michalina Komorowska,

Technicians:

Mariusz Antczak, Tomasz Bracha, Piotr Jasiński, Bartosz Kalisiewicz, Wiesław Kalisiewicz, Robert Kopik, Wojciech Kozaczka, Zbigniew Kruszyński, Piotr Krysiak, Krzysztof Łabęda, Kamil Makowski, Mariusz Matuszewski Bogusław Paprzycki, Krzysztof Pietrzak, Łukasz Świątek

Administration and support:

Eliza Balcerowska, Anna Błaszczyk-Duda, Marek Budziszewski, Barbara Kowalska[a], Joanna Kowalska, Jolanta Matuszczak, Anna Odziemczyk, Jolanta Ormaniec, Anna Ratyńska, Ewa Sobańska, Lidia Strzelczyk, Lech Szeląg, Andrzej Wiechowski, Katarzyna Włodarczyk[a], Magdalena Zawal,

Voluntary scientists:

Jędrzej Iwanicki, Maciej Kisieliński, Jan Kownacki, Piotr Pluciński, Andrzej Wojtasiewicz, Irena Żejmo

[a] part time
[b] until 30 September
[c] on maternity leave
[d] on leave
[e] since 10 August

E.7 Laboratory Council

1. Prof. dr hab. Józef Andrzejewski
Nuclear Physics Division
University of Łódź, Łódź

2. Prof. dr hab. Janusz Braziewicz
Institute of Physics
Jan Kochanowski University, Kielce

3. Prof. dr hab. Mieczysław Budzyński
Institute of Physics
Maria Curie-Skłodowska University, Lublin

4. Prof. dr hab. Ewa Bulska
Biological and Chemical Research Centre
University of Warsaw, Warszawa

5. Prof. dr hab. Katarzyna Chałasińska-Macukow
Faculty of Physics
University of Warsaw, Warszawa

6. Dr Jarosław Choiński
Heavy Ion Laboratory
University of Warsaw, Warszawa

7. Prof. dr hab. inż. Andrzej Chmielewski
Institute of Nuclear Chemistry and Technology, Warszawa

8. Przemysław Gmaj
(representative of the HIL staff)
Heavy Ion Laboratory
University of Warsaw, Warszawa

9. Prof. dr hab. Marta Kicińska-Habior
(**Chairman of the Council**)
Faculty of Physics
University of Warsaw, Warszawa

10. Prof. dr hab. Stanisław Kistryn
M. Smoluchowski Institute of Physics
Jagiellonian University, Kraków

11. Prof. dr hab. Franciszek Krok
Department of Physics
Warsaw University of Technology, Warszawa

12. Prof. dr hab. Leszek Królicki
Department of Nuclear Medicine
Medical University of Warsaw, Warszawa

13. Prof. dr hab. inż. Krzysztof Kurek
The National Centre for Nuclear Research
Świerk k/Warszawy

14. Prof. dr hab. Adam Maj
The Henryk Niewodniczański
Institute of Nuclear Physics
Polish Academy of Sciences, Kraków

15. Prof. dr hab. Tomasz Matulewicz
Faculty of Physics
University of Warsaw, Warszawa

16. Dr Paweł Napiorkowski
Heavy Ion Laboratory
University of Warsaw, Warszawa

17. Prof. dr hab. Wojciech Nawrocik
Faculty of Physics
Adam Mickiewicz University, Poznań

18. Prof. dr hab. Paweł Olko
The Henryk Niewodniczański
Institute of Nuclear Physics
Polish Academy of Sciences, Kraków

19. Dr hab. Leszek Próchniak
Heavy Ion Laboratory
University of Warsaw, Warszawa

20. Prof. dr hab. Krzysztof Rusek
(Director of HIL)
Heavy Ion Laboratory
University of Warsaw, Warszawa

21. Dr hab. Elżbieta Stephan, prof. UŚ
Institute of Physics
University of Silesia, Katowice

E.8 Programme Advisory Committee

PAC members

- Konrad Czerski (Institute of Physics, University of Szczecin, Szczecin, Poland)
- Gilles de France (GANIL, Caen, France)
- Nicholas Keeley (National Centre for Nuclear Research, Otwock, Poland)
- Maria Kmiecik (The H. Niewodniczański Institute of Nuclear Physics PAN, Kraków, Poland)
- Andrzej Magiera (M. Smoluchowski Institute of Physics, Jagiellonian University, Kraków, Poland)
- Chiara Mazzocchi (Faculty of Physics, University of Warsaw, Warszawa, Poland)
- Marco Mazzocco (Padova University, Padova, Italy)
- Leszek Próchniak (Heavy Ion Laboratory, University of Warsaw, Warszawa, Poland)
- Siergiej Sidorczuk (Joint Institute for Nuclear Research, Dubna, Russia)
- Władysław Trzaska (Department of Physics, University of Jyväskylä, Finland)

The international Programme Advisory Committee of the Heavy Ion Laboratory usually meets twice a year, in spring and autumn. The deadline for submitting proposals is three weeks before a PAC meeting. PAC approved experiments are scheduled at the meetings of the Users' Committee, which also serves as a link between cyclotron users and the Laboratory. The Users' Committee is chaired by Jarosław Perkowski (the University of Łódź).

E.9 HIL external users

In 2020 there were **18** external users and visitors from **10** scientific institutions, including 4 people from 4 scientific institutes in Poland, 4 people from 3 scientific institutions in the European Union and associated countries and 10 people from 3 scientific institutes in other countries.

HIL external users and visitors were from:

Poland

- Faculty of Physics, University of Warsaw, Warszawa, Poland
- Faculty of Chemistry, University of Warsaw, Warszawa, Poland
- National Centre for Nuclear Research, Otwock, Poland
- Poznań University of Technology, Poznań, Poland

European Union and associated countries

- INFN, Laboratori Nazionali di Legnaro, Legnaro, Italy
- INFN Sezione di Padova, Padova, Italy
- INFN Sezione di Pavia, Pavia, Italy

Other countries

- Institute for Nuclear Research, The National Academy of Sciences of Ukraine, Kyiv, Ukraine
- National Research Center "Kurchatov Institute", Moscow, Russia
- Cyclotron Institute, Texas A&M University, College Station, USA

List of Authors